TOLUENE DISPROPORTIONATION AND TRANSALKYLATION WITH C_9 AROMATICS OVER ZSM-5 ZEOLITES

A THESIS
SUBMITTED TO THE
UNIVERSITY OF POONA

FOR THE DEGREE OF
DOCTOR OF PHILOSOPHY
IN CHEMISTRY

BY
NAMDEO RAMJI MESHRAM
M. Sc.

PHYSICAL CHEMISTRY DIVISION
NATIONAL CHEMICAL LABORATORY
PUNE - 411008 (INDIA)

MAY - 1984

C E R T I F I C A T E

Certified that the work incorporated in the thesis Toluene Disproportionation and Transalkylation with C_9 Aromatics over ZSM-5 Zeolites was carried out by the candidate under my supervision. Such material, as has been taken from other sources, has been duly acknowledged.

S. B. Kulkarni

(S. B. Kulkarni)
Supervisor

Poona-8,
May, 1984.

A C K N O W L E D G E M E N T

The author would like to express his gratitude to the following people and organizations for their contribution to this work.

Dr.(Miss) S.B.Kulkarni : for guidance and constant encouragement throughout the course of this investigation.

Dr. P. Ratnasamy : for giving him an opportunity to work in the field of catalysis and many valuable suggestions at every stage of this investigation.

Dr. S. G. Hegde and Mr. I. Balkrishnan : for their help in the experimental work.

Dr. M. K. Dongre, Mr. S. B. Dake and all his colleagues-for their cooperation.

Mr. S. M. Kulkarni : for typing this thesis.

Director, National Chemical Laboratory Pune - for allowing him to submit this work in the form of a thesis.

The CSIR New Delhi : for the award of fellowship.

N. R. MESHRAM

NCL Pune,
May, 1984.

CONTENTS

CHAPTER - III

Toluene Disproportic-nation

CHAPTER-IV

Transalkylation of toluene with C_9 aromatic hydrocarbons on HZSli-5 and dealuminated mordenites

-----0000----

CHAPTER - I

INTRODUCTION

1.1. INTRODUCTION

Toluene is mainly obtained from crude naptha during petroleum reforming process by distillation of BTX (benzene, toluene and xylenes). However, toluene gets over produced and is relatively cheaper than benzene and xylenes. This is because its derivatives are not in competition with the natural products. Benzene and xylene derivatives, on the other hand, are in great demand for synthetic fibres and plastics which have many advantages over natural materials like cotton, wool and silk. Due to rapid expansion of these polymeric material producing industries, the demand for benzene and xylenes, especially para-xylene, has increased. The major source of production of para-xylene is the isomerization of C_8 aromatics cut from naptha reformate stream. However, the process is bit tedious in respect to the separation of ethylbenzene from para-xylene and is commercially less attractive. On the other hand, the conversion of relatively cheaper toluene into benzene and xylenes which is free from ethylbenzene via disproportionation, dealkylation, alkylation and transalkylation is an attractive route to fulfil the demand for para-xylene.

The commercial value of C_9 aromatic hydrocarbons is considerably lower than C_8 aromatic hydrocarbons. These C_9 aromatics especially trimethylbenzenes are the side reaction

products in the toluene disproportionation reaction (produced by the disproportionation of xylenes) and can be utilized to upgrade the C_8 aromatics yield either by recycling the formed C_9 aromatics in toluene disproportionation or by mixing them in the toluene stream and converted by dealkylation/transalkylation routes.

Toluene disproportionation and alkylation have been extensively studied using variety of alkylating agents and variety of Friedel-Crafts catalysts and traced out a clear cut idea about the behaviour of the methylbenzene towards these catalysts[1-4]. An excellent review published by Nightgle[5] also demonstrates their action on methylbenzenes. However, the Friedel-Crafts technology based on aluminium chloride and haloacids inherits some undesirable features in their use, for example, corrosiveness of the acid and disposal of the waste catalyst which creates pollution.

The other classes of catalysts are silica-alumina[6-10] and crystalline zeolites[11-15]. The activity of the catalysts based on silica-alumina is low necessitating the use of higher temperatures. At higher temperatures, however, due to predominance of dealkylation and cracking reactions, most of the toluene degrade into gaseous products and results in a fast deactivation of the

catalysts. However, the catalysts based on zeolite classes, Linde X or Y[10] and mordenites[16-18] give improved yield of benzene and xylenes in the disproportionation/transalkylation reactions. Tatsuaki et al[19] reported 45% xylene yield by transalkylation of toluene with trimethylbenzene isomers over H mordenite, CeY and Hy catalyst. The catalysts exchanged with multivalent cation showed no activity for transalkylation. The exchanged cations stick out of the mordenite channel wall, thus hindering the diffusion of reactant into the channel and to the active sites. The trimethylbenzene isomers were reactive in the order,1,2,4 > 1,2,3 > 1,3,5 on H mordenite catalyst.

Aneke et al[10] investigated the toluene disprotionation on a composite catalyst material consisting of 72% wt. % HY, 18 wt.% β-AlF_3 and 10 wt.% Cu and compared its activity with silica-alumina HY and H mordenite. The result showed that the HY and H mordenite had high initial activity. However, the activity dropped down rapidly due to coke formation on the active surface. In contrast, the composite catalyst showed improvement in selectivity and stability. Shopov et al[20] reported the toluene disproportionation over nickel modified CaY catalysts. The catalyst obtained by ion exchange with nickel showed high toluene disproportionation activity and attributed it to

the presence of 50% of total nickel which remained unreduced and acted as a main source of proton acidity.

Benesi[11] showed that mordenite is more active than Y faujasite in the toluene disproportionation reaction. He studied the toluene disproportionation reaction as a function of the temperature for decomposition of NH_4 form of Y faujasite and mordenite and showed that at all stages of zeolite decomposition, the mordenite possessed higher activity.

Recent invention of ZSM-5[21] (Zeolite Socony Mobil) zeolite, a new variety of pentasil zeolites, has made a revolution in the petrochemical industry. The ZSM-5 zeolite with high selectivity and specificity in converting methanol to gasoline was first disclosed by Mobil Oil Company in 1976 in the so called a Mobil Methanol Process[22]. Thereafter, the ZSM-5 based catalysts have stimulated much interest in many industrial processes (listed in Table 1.1). Especially for toluene disproportionation, the enclosed channel system in ZSM-5 zeolite with pore opening, 0.58 nm which matches with the size of benzene, toluene and para-xylene molecules offers high performance[24,25]. Using an acidic ZSM-5 catalyst, Mobil Oil Co. developed a low temperature toluene disproportionation process (LTD). The high efficiency (activity and

TABLE - 1.1

Industrial processes based on shape selective zeolites[23]

Process	Objective	Major chemical/process characteristics
Selecto-forming	Octane number increase in gasoline; LPG production.	Selective n-paraffin cracking.
M-Forming	High yield; octane number increase in gasoline.	Cracking depending on degree of branching; aromatics alkylation by cracked fragments.
Dewaxing	Light fuel from heavy fuel oil; lube oils with low temperature pour point.	Cracking of high molecular weight n- and mono-methyl paraffins.
Xylene isomerization	High yield para-xylene production.	High throughput, long cycle life; suppression of side reactions
Ethyl benzene	High yield ethyl benzene production eliminate $AlCl_3$ handling	
Toluene dis-proportionation	Benzene and xylenes from toluene	
Methanol-to-gasoline	Methanol (from coal or natural gas) conversion to high grade gasoline	Synthesis of hydro-carbons only, restricted to gasoline range (C_4 to C_{10}) including aromatics.

selectivity) of ZSM-5 zeolite catalyst for this reaction stem out from a variety of features[26]:

(a) a high acidity leading to high activity for this reaction;

(b) a pore dimension that greatly favours the diffusion of para-xylene (the diffusivity of para-xylene is at least three orders of magnitude higher than that of ortho- or meta-xylenes) and exclude molecules with critical dimensions higher than that of 1,3,5-trimethylbenzenes[27];

(c) restriction in the nature of transition state thereby preventing further conversion of the xylenes. The relative values for the isomerization (K_i) and disproportionation (K_d) rate constant measured for a variety of zeolite catalysts show (Table 1.2) the absence of disproportionation of xylene which prevent the loss of C_8 aromatic compounds by secondary reactions, including coking.

TABLE - 1.2

Isomerization vs disproportionation of the xylenes[24]

Catalyst	K_i/K_d
Faujasite, Y	10-20
Mordenite	70
ZSM-5	1000

Kaeding et al[28] and Chu[29-32] reported the synthesis of p-xylene in high yield by disproportionation/alkylation of toluene using ZSM-5 based catalyst modified with variety of accessible inorganic compounds which can sit in the channel and reduce the available space. Chen et al[33] also reported very high yield of para-xylene ~ 90% (as illustrated in Fig. 1.1) by alkylation/disproportionation of toluene when the diffusional constraints are increased either geometrically (by using larger crystals which provides longer path) or chemically by modification with P and Mg.

1.2. STRUCTURE AND CHARACTERISTICS OF ZSM-5 ZEOLITE

(A) Structure of ZSM-5

The structure of ZSM-5 zeolite was reported by Kokotalio et al[34] and is shown in Fig. 1.2. The framework of ZSM-5 contains a linked tetrahedra as shown in Fig. 1.2a and consists of 8 five membered rings. These building units then join through edges to form a chain as shown in Fig. 1.2b. The chains are connected to form a sheet and the linking of the sheet leads to a three dimensional framework structure. The chains extended along the Z axis and the sheets parallel to (010) and (100) are shown in Fig. 1.2.c and 1.2.d. The ZSM-5 framework can be generated

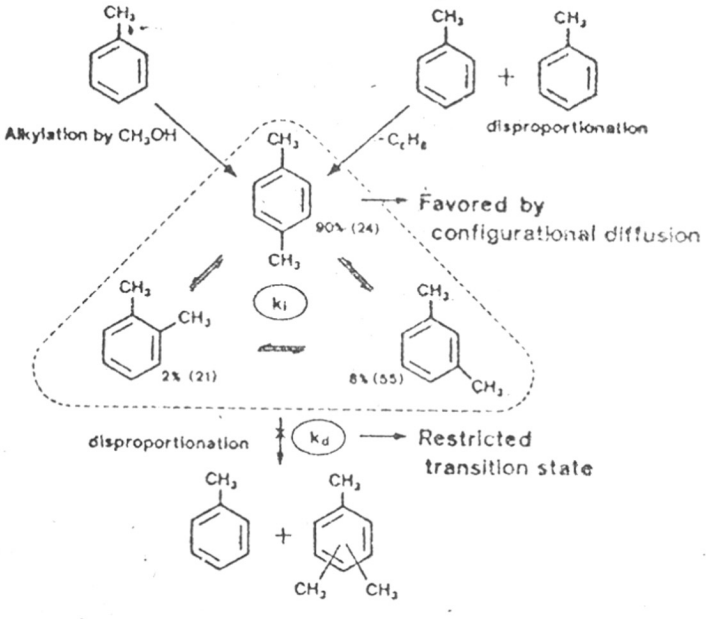

FIG.1.1. PRODUCTION OF PARA-XYLENE [26]

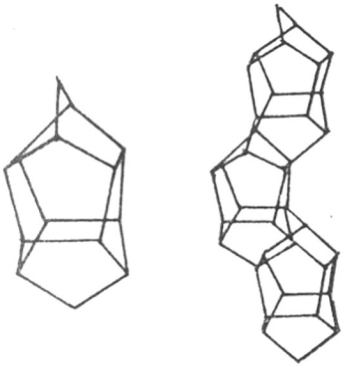

a b

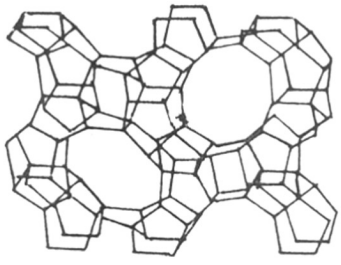

c

a) CHARACTERISTIC CONFIGURATION OF ZSM-5
b) LINKAGE OF ZSM-5

c) SKELETAL DIAGRAM OF 010 FACE

d) SKELETAL DIAGRAM OF 100 FACE

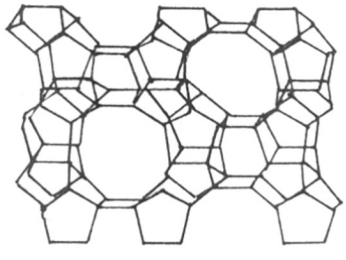

d

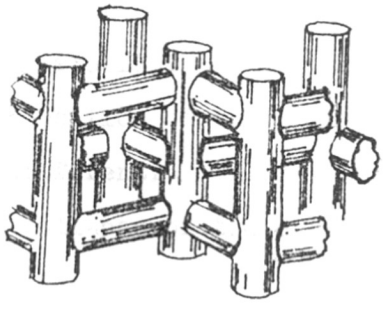

e

e) CHANNEL STRUCTURE OF ZSM-5 ZEOLITE

FIG. 12: STRUCTURE OF ZSM-5 ZEOLITE.

by linking the sheets (Fig. 2.1c) across mirror plane forming four and six membered rings.

The framework of ZSM-5 is made of the two intersecting channel systems (Fig. 2.1e), One Sinusoidal running parallel to (001). The elliptical 10 ring is having opening 0.58 x 0.51 nm and straight one has 0.56 0.54 nm opening.

Flanigen et al[35] reported a zeolite which is devoid of alumina and encloses the same structure as described for ZSM-5 called the end member of the ZSM family and named silicalite. The silicalite is highly hydrophobic and adsorb selectively the organic molecules over water.

(B) Thermal stability

The resistance to structure collapse at elevated temperature is known as the thermal stability of the zeolites. The thermal stability of the zeolites is usually determined from the position of the high temperature exothermic peak in differential thermal analysis (DTA) because the thermal collapse of the crystal structure is accompanied by a liberation of heat[36]. It has been also determined by measuring the loss in crystallinity, by the decrease in the X-ray diffraction peak heights, of a sample

heated at the predetermined temperatures, for a fix time as compared to the original peak height for the unheated sample.

McDanieal and Maher[36] reported that the thermal stability of the X and Y zeolites increases with increasing Si/Al ratio. This may be because of the predominance of the more stable Si-O-Si bonds than Si-O-Al bonds in the silica-rich zeolites. Barrer et al[37] reported that the thermal stability of the alkalimetal and ammonium cation exchanged forms of chabazite increases with increasing the size of the exchange cation in the alkali metal series and attributed this relation to the relative ability of the various cations to fill the voids in the crystal after dehydration.

ZSM-5 zeolites are characterized by high Si/Al ratio and hence possess very high thermal stability. Flanigen et al[35] reported that the silicalite which is devoid of the alumina in the framework (the end member of ZSM series) is stable in air upto 1373 K and is converted slowly to amorphous silica at 1573 K.

(C) Sorption and Diffusion

Sorption and diffusion plays a role of paramount importance in molecular shape selective catalysis[23,26]. The screening of the molecules of different size and shapes

determines the reactants and products selectivity. The molecules with high diffusivity will react preferentially and selectively while molecules which are excluded from zeolite interior will only react on the external non-selective surface of the zeolite. Products with high diffusivity will be preferentially desorbed while the bulkier molecules will be converted and equilibriated to smaller molecules which will diffuse out, or eventually to larger species which will block the pores.

The diffusion and sorption properties of ZSM-5 zeolite have been evaluated systematically by many workers. Mobil researchers[22,38] have qualitatively reported the relative intracrystalline mobility of hydrocarbons in the ZSM-5 channel system. n-Paraffins and monomethyl substituted paraffins diffuse more rapidly than dimethyl substituted paraffins. Among the monocyclic hydrocarbons the relative diffusion coefficient (RDC) from vapour phase adsorption is as follows :

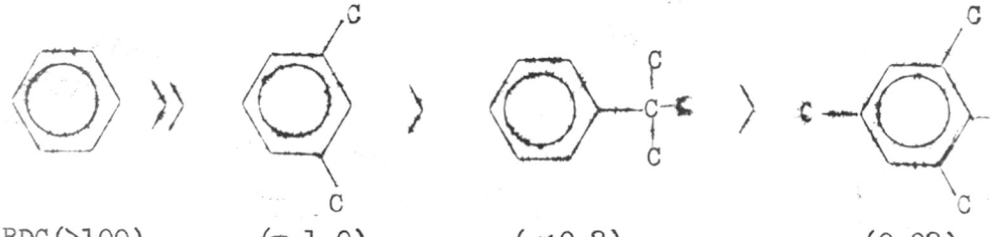

RDC (>100) (~1-0) (~0.2) (0.02)

Derouane and Gabelica[39] evaluated the channel length occupied per unit cell by the adsorbates from the amount adsorbed, using molecular dimensions and assuming an end to end configuration of adsorbed molecule. They have shown that linear paraffins (upto C_6) fill whole pore while 3-methyl pentane, para-xylene and toluene are adsorbed exclusively in the linear and elliptical channels. They have made the following generalizations:

(1) Linear aliphatics diffuse rather freely in the HZSM-5 framework and can be adsorbed in both the channel system.

(2) Isoaliphatic compound experience steric hindrance effects which may restrict their diffusion in the sinusoidal channel system.

(3) Aromatic compounds and methyl substituted aliphatics have strong preference for diffusion or adsorption in the linear and elliptical channels.

Anderson et al[40] reported the sorption of hydrocarbons in H-ZSM-5, silicalite and NaZSM-5 at 293 K and $P/P_o = 0.5$. They have classified the sorbate/sorbent systems into two (fast and slow) categories. In the fast category > 95% of equilibrium sorption was reached in < 10 minutes and in slow the uptake was continuously increasing with time after several minutes. 3-Methylpentane, toluene and para-xylene which fell into fast category with HZSM-5

and silicalite, but into slow category with NaZSM-5. The critical value for effective molecular size separating fast and slow hydrocarbons is > 0.58 and < 0.61 nm for HZSM-5 and silicalite while for NaZSM-5 is > 0.43 and < 0.56. From the above study they have concluded that the pore volume and channel size are similar for HZSM-5 and silicalite while the presence of Na ions in NaZSM-5 influence the apparent free channel size.

Flanigen et al[35] demonstrated the sorption properties of silicalite in terms of its surface selectivity rather than pore size effect. They have shown the organophillic and hydrophobic selectivity of the silicalite surface by competative adsorption of n-hexane and water. In case of n-hexane the pore filling is essentially complete at a relative pressure, 0.03. In contrast, water does not fill the pore at any relative pressure. The adsorbed water volume at a relative pressure near one is about 25% of the saturation pore volume for n-hexane. This hydrophobic selectivity of silicalite is attributed to the absence of the water adsorption sites in silicalite.

(D) Surface Acidity

It is well known that the zeolites contain both Brönsted and Lewis types of acid sites. The isomorphous substitution of trivalent aluminium for the tetravalent

silicon in the lattice creates the acid sites. Since the trivalent aluminium atom is forced to assume a tetravalent position and nett unit negative charge is created at this point on the solid surface which requires neutralization by a cation such as proton (Brönsted sites). In the absence of compensating cation, the aluminium atom would tend to acquire a pair of electrons to fill its p-orbital (Lewis acid sites). The acid sites in zeolites are created by following treatments[41]:

(1) By exchange with ammonium ions followed by thermal decomposition

$$MZ \xrightarrow{NH_4^+} NH_4Z \xrightarrow{\text{heat}} HZ.$$

(2) By treatment with dilute acid

$$MZ \xrightarrow{HA} HMZ$$

(3) By treatment with organic ammonium salt followed by thermal decomposition

$$MZ \xrightarrow{TMA} TMAMZ \xrightarrow{\text{heat}} HMZ$$

(4) By exchange with multivalent cations

$$MZ \xrightarrow{M_1^{2+}} (M_1OH)^+ HZ$$

$$MZ \xrightarrow{M_1^{3+}} (M_1OH)^{2+} HZ$$

$$(M_1OH)^{2+} HZ \longrightarrow [M_1(OH)_2^+]H_2Z$$

(5) By washing with water

$$MZ \xrightarrow{H_2O} HMZ$$

Many techniques have been used to evaluate the distribution and the number of these sites. Most commonly used techniques are : Infrared spectroscopy[41,42], Microcalorimetry[43] and Temperature Programmed Desorption (TPD)[40,44,45] of NH_3. Auroux et al[43] extensively studied the surface acidity of ZSM-5 zeolite by using microcalorimetry and infrared spectroscopy as a function of various parameters that affect the distribution and number of acid sites such as calcination temperature, silica to alumina ratio and modification by incorporation of phosphorous or coking. They have shown that the number of acid sites decreases with increasing calcination temperature (from 655 to 1075 K), increasing SiO_2/Al_2O_3 ratio and incorporation of phosphorous or coke. They also suggested the non-uniform distribution of acid sites in HZSM-5 zeolite protonated by HCl treatment. The HZSM-5 zeolites, protonated samples prepared either by acid treatment or by calcination of NH_4-ZSM-5 samples were compared by studying their affinity to ammonia at 416 K. The results indicate that the site filling is normal in protonated sample prepared from the ammonium form and that consequently the acid sites are uniformly distributed in this sample. Therefore, the heteregeneous distribution of acid sites observed in the acidified H-ZSM-5 is not the consequence of non-uniform distribution of aluminium ions in the freshly synthesized sodium form but was created by HCl acidification treatment. Hydrochloric acid can remove both sodium and aluminium ion from the lattice.

Topsøe et al[44] showed the existence of three types of acid sites on the protonated H-ZSM-5 zeolite by temperature programmed desorption of ammonia and designated these sites as α, β and γ sites. The desorption activation energies for α, β and γ sites are :20.2, 23.1 and 38.8 K cal mol^{-1} respectively. From the IR spectroscopy of H-ZSM-5 they have shown three types of IR absorption bands at 3720, 3740 and 3600 cm^{-1}. The bands at 3720 - 3740 cm^{-1} were assigned to weakly bound surface hydroxyl groups which adsorb NH_3 in less energetic β state (23.1 K $\frac{cal}{mol^{-1}}$) or α state (20.2 K cal mol^{-1}) whereas the band at 3600 cm^{-1} was assigned to strong Brönsted sites which are responsible for the adsorption of NH_3 in highly energetic γ state (38.8 K cal mol^{-1} NH_3 desorption activation energy) which are located at the channel intersections.

(E) Shape Selective Properties

The shape selective properties of ZSM-5 result from the conjunction of four different, although structurally interrelated, features:

(1) A channel (or pore) opening consisting of 10 membered oxygen rings which is intermediate between that of classical shape selective zeolites (such as erionite or zeolite A) and that of large pore zeolites (such as faujasites and mordenite).

(2) The presence of channel intersections (or intersecting elements) which offers a free space of larger dimensions (about 0.9 nm), the latter may play distinct role in the ordering of simple molecules[46] and could be the locus for the catalytic activity[47].

(3) The absence of cages along the channels, such cages which offer a large available space are the preferential locus for the formation of carbonaceous residues.

(4) The occurrence of slightly differentiated channel net works. Aromatics and branched paraffins were indeed found to be preferentially adsorbed in the linear channels which are elliptical. This may lead to preferential diffusion paths and eventually prevent major counter diffusion effects[39].

Reactions such as cracking and hydrocracking[27,48,49] distillate dewaxing[50] and upgrading of Fischer-Tropsch synthesis mixtures[51]; methanol to hydrocarbon[52] and isomerization of xylenes explain product selectivity. Restricted transition state selectivity is related to the high resistance to coking of ZSM-5 zeolites[53] and high selectivity in isomerization of xylene.

(F) Aging

The deposition of carbonaceous residues usually occurs during catalytic reaction and conversion of alkylaromatics (by cyclisation, dehydrogenation, further alkylation) eventually leading to polyalkylaromatic, the

coke precursors. The coke deposits lower the catalyst activity by site coverage and/or by pore blocking which prevent the access of the reactant to the active sites. Rollman and Walsh[53] had demonstrated that the intracrystalline coking of zeolites is a shape-selective process which largely depends on the size and architecture of their channels. The zeolites which provide enough space for the synthesis of polyalkylaromatics would therefore deactivate fast. Dajcifve et al[54] explained the location of coke in the three zeolites namely mordenite, offretite and ZSM-5 zeolites which differ in the channels system by acidity measurement. The acidity measurements were performed by ammonia adsorption on fresh and deactivated catalysts after 20 minutes on stream in methanol reaction. The strong acid sites present in the mordenite totally disappeared in coked catalysts indicating that the psuedounidimensional channels of mordenite had been blocked by coke. In case of offretite although the strong acid sites are decreased, treatment at increasing temperature partially regenerated the acid sites indicating that coke was mainly deposited in cages and larger channels. In contrast with the aging of either mordenite or offretite, the range of acid strength in HZSM-5 remain unchanged. However, the reduction of total ammonia adsorption capacity was attributed to the inhibition by deposited coke on the external surface and it was concluded that the coke in HZSM-5

was mainly deposited on the external surface. This point was also proved by Walsh and Rollmann[53] and they suggested that due to the restriction of the transition state, the polyalkylaromatics were not formed in the channels.

(G) Ion Exchange

It is well established that the ion exchange capacity of classical zeolite is equivalent to the tetrahedral aluminium content of the zeolite structure. Olson et al[55] reported the caesium ion-exchange capacity of series of ZSM-5 zeolites. Caesium ion exchange into a series of hydrogen form of ZSM-5 samples with SiO_2/Al_2O_3 ratio ranging from 89 to 8666 showed a very good stoichiometric correlation indicating that the relation of framework aluminium to ion-exchange capacity observed for the classical zeol ites holds also for the highly siliceous zeolite even at low level of aluminium. The ratio of Cs/Al was found to be slightly lower than unity.

1.3. OBJECTIVE OF THE PRESENT WORK

The literature survey indicates that ZSM-5 zeolite offers high performance over other zeolite and non-zeolite based catalysts, so far used for the disproportionation of toluene. The researchers working in the toluene reactions over ZSM-5 zeolite based catalysts, however, concentrated their efforts only on the synthesis

of para-xylene either by disproportionation or alkylation with methanol and put in much effort in the development of the para-selective catalysts. They modified the ZSM-5 catalysts by using a variety of inorganic modifiers like phosphorous, boron, magnesium and tin, which sit in the channels, block partially and enhance the selectivity for para-xylene. These modifiers, however, react strongly with the acid sites in the ZSM-5 channels and strongly reduce the total acidity which, in turn, decreases the toluene conversion to about 10-20% mole as against 60% mole equilibrium conversion.

A detailed study of disproportionation of toluene over ZSM-5 based catalysts has therefore been undertaken to achieve higher (near equilibrium) conversion of toluene and to improve the yield of xylenes by transalkylation with C_9 aromatic hydrocarbons. The present work contemplates a process of toluene disproportionation to obtain high selectivity to benzene and xylenes and a stable activity of the HZSM-5 catalysts modified with transition metals.

The present investigation was undertaken with the following objectives:

1. To prepare a series of ZSM-5 zeolites of varying SiO_2/Al_2O_3 mole ratios and vary the surface acidity of the catalysts by calcination at different temperatures or by incorporation of inorganic modifiers like phosphorous, boron, magnesium and nickel, etc.

2. To study the surface acidity of the modified ZSM-5 catalysts by the temperature programmed desorption (TPD) of ammonia and thermogravimetry and to correlate this data with the activity of the samples for toluene disproportionation and transalkylation reactions.

3. To study the influence of pressure, reaction temperature, space velocity on the selectivity and catalyst stability in toluene disproportionation and transalkylation reactions using modified ZSM-5 zeolite catalysts of different SiO_2/Al_2O_3 mole ratios.

4. To investigate the sorption and diffusion properties of the ZSM-5 catalysts using probe molecules of varying sizes and shapes e.g. (a) benzene, toluene, para-xylene, (b) cyclohexane, ortho-xylene and 1,3,5 and 1,2,4 trimethylbenzenes.

5. To study the transalkylation of C_7, C_9 aromatic hydrocarbons over HZSM-5 zeolite blended with dealuminated hydrogen mordenite of varying SiO_2/Al_2O_3 ratios in different proportions.

———•••———

CHAPTER II
SYNTHESIS, MODIFICATION AND CHARACTERIZATION

2.1. SYNTHESIS

ZSM-5 zeolite is a member of pentasil family of zeolites. This was first reported by Argauer and Landolt[21]. Because of its wide applications, especially in the petrochemical industry, several processes for its synthesis using a variety of organic cations as templates and different sources of SiO_2 and Al_2O_3 have been explored[56-59].

In the present work, ZSM-5 zeolites of varying SiO_2/Al_2O_3 ratios were prepared by mixing solutions of sodiumsilicate, aluminium sulphate, sulphuric acid and triethyl-n-propyl ammonium bromide according to a procedure described elsewhere[58]. The synthesis runs were carried out at 453 K in a stainless steel autoclave (capacity 75 ml) at autogenous pressure. The reactant materials used had the following compositions : sodium silicate (SiO_2 = 27.2, Na_2O = 8.4, H_2O = 64.4 % wt.), aluminium sulphate ($Al_2(SO_4)_3$, $18H_2O$, Merck), sulphuric acid, (BDH Analar grade 98%) and triethyl-n-propyl ammonium bromide TEPABr, (synthesized in the laboratory). Appropriate amounts of aluminium sulphate and sulphuric acid were mixed in distilled water to yield solution A. Calculated quantity of a quaternary salt (TEPABr) was added to sodium silicate solution to yield solution B. The two solutions A and B were then mixed in a stainless steel reaction vessel with continuous stirring to form a

free flowing gel. The vessel was then closed and heated to the desired temperature and left at this temperature for sufficient time usually about 10 to 100 hours depending on the SiO_2/Al_2O_3 ratios of the gel mix. After completion of the reaction, the reactor was cooled in cold water. The solid mass was then filtered and washed with hot distilled water till it was free from sulphate and bromide ions. The resulting sample was dried in a static air oven at 393 K for 12 hours. The sample was then characterized by x-ray diffraction and ir spectroscopy. Finally, the sample was calcined at 823 K for 8 hours in flowing air in a muffle furnace to decompose the organic base. The sodium form of the ZSM-5 zeolite (NaZSM-5) was obtained in this way.

2.2. MODIFICATION

The NH_4ZSM-5 samples were prepared by ammonium exchange of the NaZSM-5 using a 5M NH_4Cl solution. The exchanges were performed at 368 K on a waterbath. It was repeated three times to replace the sodium ions by ammonium ions. The NH_4ZSM-5 zeolites were dried at 393 K and calcined at 823 K to get hydrogen form of the zeolites. The samples were analysed by flame photometry and wet chemical analysis. The unit cell compositions of the samples are given in Table 2.1. These were calculated on the assumption that the total number of Si + Al tetrahedra per unit cell is equal to 96.

TABLE - 2.1

Chemical composition of zeolite samples

Sample	Chemical Formulae	SiO_2/Al_2O_3 molar ratio
HZSM-5	$Na_{0.02}(SiO_2)_{90.98}(AlO_2)_{5.02}15H_2O$	36
HZSM-5	$Na_{0.03}(SiO_2)_{93.72}(AlO_2)_{2.28}21H_2O$	86
HZSM-5	$Na_{0.08}(SiO_2)_{94.69}(AlO_2)_{1.31}18H_2O$	144
HZSM-5	$Na_{0.07}(SiO_2)_{94.90}(AlO_2)_{1.09}18H_2O$	165
HZSM-5	$Na_{0.07}(SiO_2)_{95.40}(AlO_2)_{0.60}10H_2O$	320
NiHZSM-5	$Na_{0.02}Ni_{0.53}(SiO_2)_{90.98}(AlO_2)_{5.02}15H_2O$	36
NiHZSM-5	$Na_{0.02}Ni_{1.08}(SiO_2)_{90.98}(AlO_2)_{5.02}15H_2O$	36
NiHZSM-5	$Na_{0.02}Ni_{2.14}(SiO_2)_{90.98}(AlO_2)_{5.02}15H_2O$	36
NiHZSM-5	$Na_{0.02}Ni_{5.44}(SiO_2)_{90.98}(AlO_2)_{5.02}15H_2O$	36
NiPtH-ZSM-5	$Na_{0.02}Ni_{0.53}Pt_{0.06}(SiO_2)_{90.98}(AlO_2)_{5.02}15H_2O$	36
PMgHZSM-5	$Na_{0.02}P_{3.68}Mg_{11.73}(SiO_2)_{90.98}(AlO_2)_{5.02}15H_2O$	36
PMgHZSM-5	$Na_{0.02}P_{7.37}Mg_{7.04}(SiO_2)_{90.98}(AlO_2)_{5.02}15H_2O$	36
PHZSM-5	$Na_{0.02}P_{14.73}(SiO_2)_{90.98}(AlO_2)_{5.02}15H_2O$	36
BHZSM-5	$Na_{0.02}B_{15.82}(SiO_2)_{90.98}(AlO_2)_{5.02}15H_2O$	36

The nickel and boron modified forms of the zeolite (NiHZSM-5) and BHZSM-5, with different amounts of nickel and boron were prepared by impregnation with $Ni(NO_3)$ and H_3BO_3 solutions respectively. Appropriate quantities of the solutions were added to the zeolite samples. The well homogenized slurry was slowly dried with intermittant stirring at 333 K until the slurry was dry. The powdered samples were further dried in air oven at 393 K overnight and then calcined at static air in the muffle furnace at 823 K for about 5 hours.

The phosphorous (PHZSM-5) and phosphorous and magnesium (PMgHZSM-5) modified forms of the zeolites were prepared according to the procedure described earlier[60]. A solution of diammonium hydrogen phosphate was added to HZSM-5 zeolite. The resulting mixture was allowed to stand overnight and evaporated at 333 K with constant stirring. It was then dried for 8 hours at 393 K and then calcined in static air at 773 K. The calcined PHZSM-5 was used for magnesium impregnation. The composition of the zeolites thus prepared are given in Table 2.1.

The ZSM-5 zeolites used for toluene disproportionation and transalkylation reactions at atmospheric pressure were in the form of 10-20 mesh particles. These were obtained by crushing the zeolite pellets followed by sieving. The pellets were obtained by applying a pressure of 4-5 tons/cm^2 in a hydraulic press.

For high pressure reactions the zeolites were used in the form of extrudates, which were prepared by mixing the zeolite with bentonite (10%)and Kaolinite (5%) binders before extrusion.

2.3. CHARACTERIZATION

(A) X-ray Diffraction (XRD)

XRD is one of the most powerful tool among the various techniques so far used for characterization of the zeolites. It has been widely used to study crystallinity, phase transformation during crystallization[58,61] and structural changes during various treatments like calcination and ion exchange[62,63]. Bibby et al[64] used XRD for the non-destructive determination of Al content in the ZSM-5 zeolite. In the XRD powder pattern of the ZSM-5 they found that the spacing, Δ, between the two peaks between 45.0 and 46° 2θ (CuKα radiation) decreases as the Al content in the zeolite increases. The intensity of the two peaks falls and the peaks broaden considerably as the Al content increases.

The x-ray diffractograms were recorded using Philips PW 1700 X-ray diffractor with nickel filtered, CuKα radiation (λ = 1.5405 Å).

The interplanar distances 'd' for NaZSM-5 (SiO_2/Al_2O_3 = 36) are presented in Table 2.2 along with published 'd' values for ZSM-5[21]. The values obtained are consistent with those reported in the literature. The x-ray diffraction patterns of all the zeolite samples with different SiO_2/Al_2O_3 ratio and metal impregnation are similar (Fig. 2.1 and 2.3). Thus, the samples synthesized are crystalline and they belong to the ZSM-5 type. The most intense lines occurring at 2θ 7.9 ± 0.1, 8.8 ± 0.1 and 23 ± 0.22 are the characteristic peaks of the ZSM-5 type zeolite. The intensity of the above peaks is found to increase when the zeolite as synthesized is calcined (Fig. 2.2). The increase in the intensity, when a synthesized form is calcined, is due to the decomposition of the occluded organic cations which are present in the channels of ZSM-5[62]. Increase in the SiO_2/Al_2O_3 ratio is associated with changes in position and intensities of the peaks. The prominent changes are : (1) the intensity increases with increasing SiO_2/Al_2O_3 ratio (Fig. 2.3), (2) appearance of a doublet (at 2θ, 24.2 and 24.32) in place of a singlet (24.25) in the case of sample having SiO_2/Al_2O_3 of 320.

Nakamato and Takahashi[63] have reported, that when SiO_2/Al_2O_3 ratio was higher than about 170, the crystal structure of ZSM-5 changes from orthorhombic to

TABLE - 2.2

Lattice spacings ('d' values) of synthesised NaZSM-5, SiO_2/Al_2O_3 = 36

Interplanar spacings 'd' Å (observed)	Interplanar spacings 'd' Å (reported)*	Interplanar spacings 'd' Å (observed)	Interplanar spacings 'd' Å (reported)
11.13	11.25	3.98	4.01
9.99	9.92	3.83	3.84
9.71	9.70	3.75	3.75
9.01	8.92	3.67	3.64
7.43	7.46	3.44	3.45
7.07	7.00	3.39	3.34
6.60	6.70	3.13	3.16
6.47	6.36	3.05	3.04
5.95	5.98	2.93	2.94
5.78	5.71	2.70	2.72
5.57	5.56	2.65	2.60
5.15	4.97	2.54	2.50
4.77	4.59	2.46	2.47
4.37	4.34	-	2.39
4.13	4.24	-	-

* Ref. 21

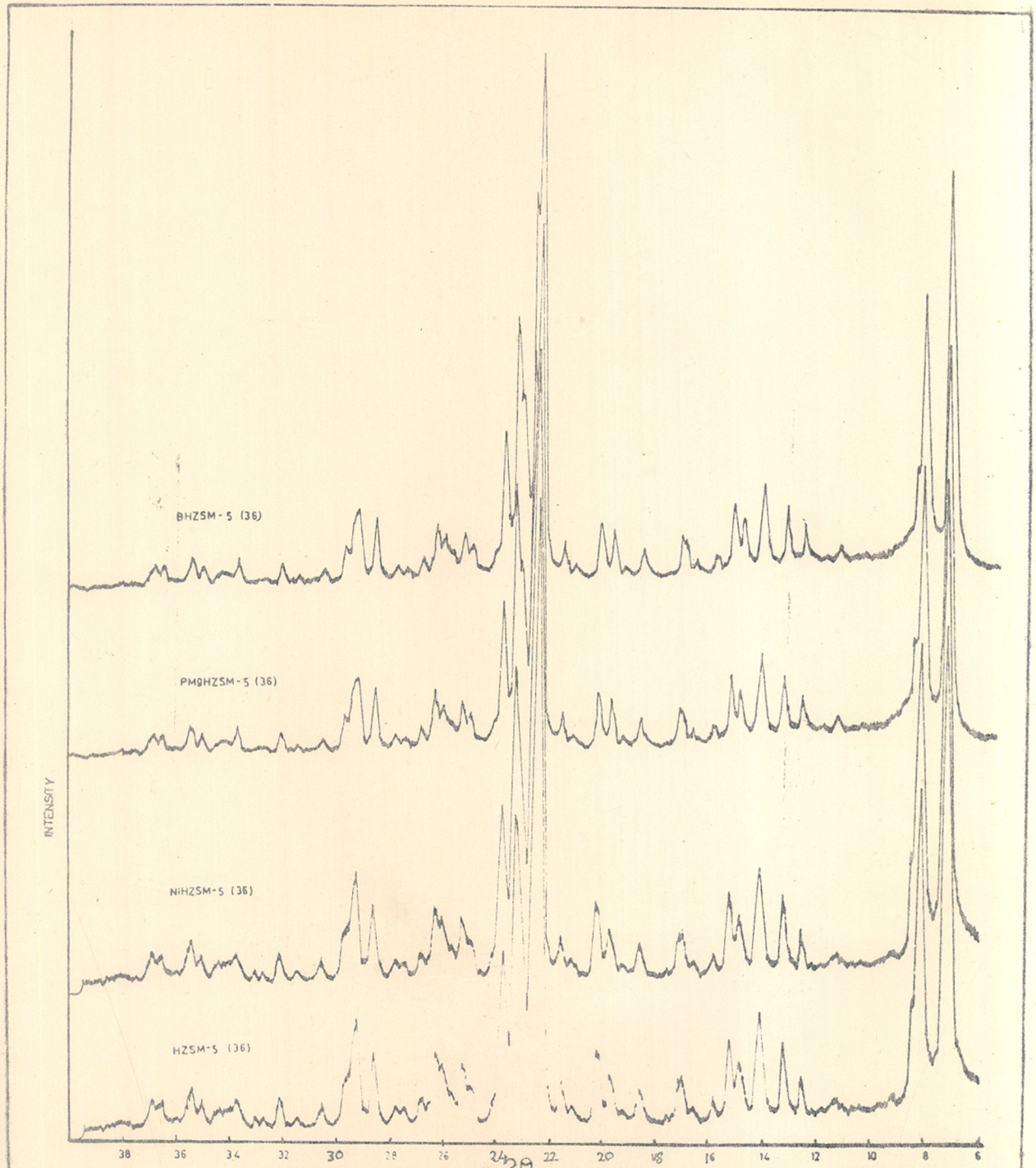

FIG.2.1 X-RAY DIFFRACTOGRAMS OF HZSM-5 AND MODIFIED HZSM-5 ZEOLITES. THE NOS. IN BRACKETS REFER TO SiO_2/Al_2O_3 RATIO.

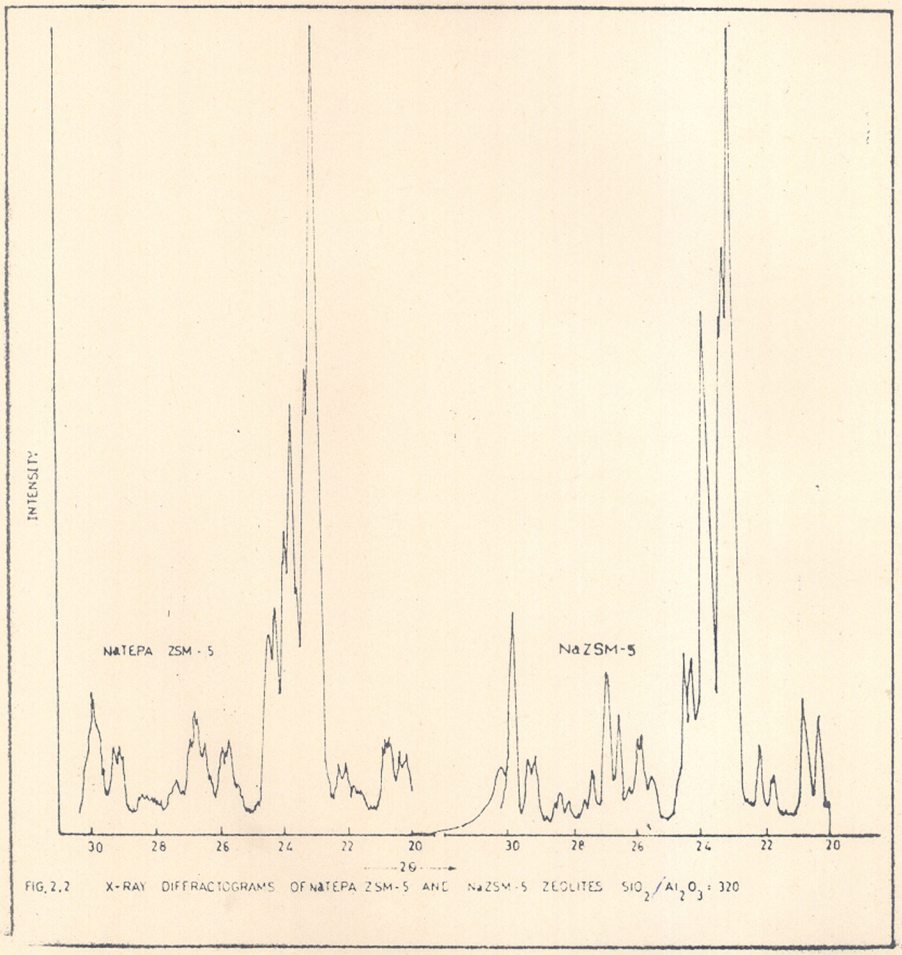

FIG. 2.2 X-RAY DIFFRACTOGRAMS OF NaTEPA ZSM-5 AND NaZSM-5 ZEOLITES SiO_2/Al_2O_3 = 320

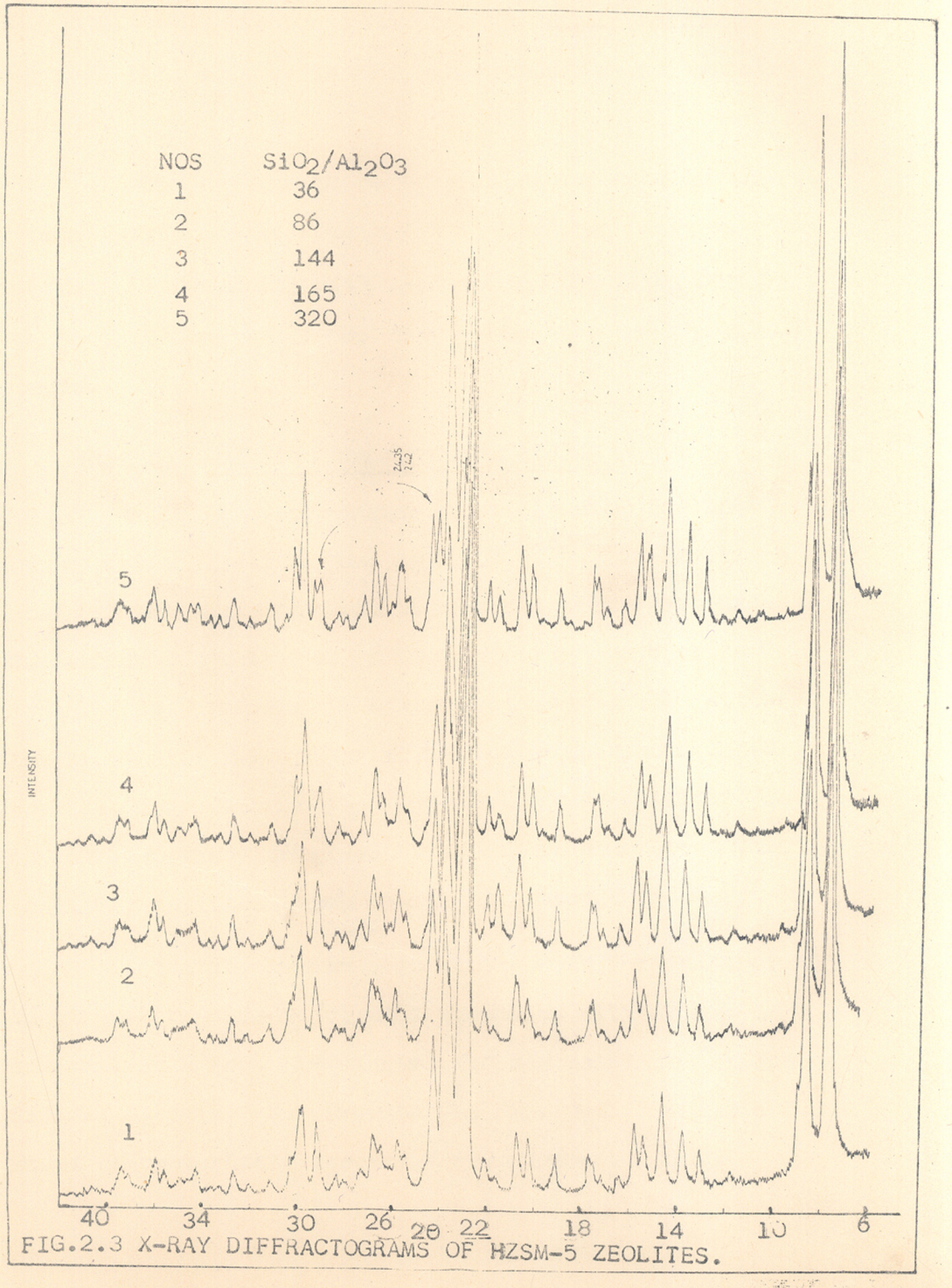

FIG.2.3 X-RAY DIFFRACTOGRAMS OF HZSM-5 ZEOLITES.

to monoclinic symmetry by mere calcination and remains unchanged after NH_4 ion exchange. Wu et al[62] also reported that changes in SiO_2/Al_2O_3 ratio cause symmetry changes.

The changes in peak position observed in the present study may be attributed to symmetry changes. The increase in intensity with increasing SiO_2/Al_2O_3 may be due to the increase in the crystallite size of the ZSM-5 sample.

(B) Infrared spectroscopy (IR)

The IR spectroscopy is widely used for the structural analysis of the zeolites[65-67]. It is also used for the characterization of surface hydroxyl groups. The infrared spectra of pyridine adsorbed on zeolite revealed the presence of Brönsted and Lewis acid sites[44]. Jacobs et al[68] have reported the x-ray amorphous ZSM-5 zeolite. They demonstrated that ir is very sensitive for the characterization of zeolites and it can detect very small crystallites which cannot be detected by x-ray.

The ir spectra were recorded on Perkin-Elmer 221 spectrometer using Nujol mull technique with KCN as an internal standard. IR spectra for the sample of different SiO_2/Al_2O_3 ratio are given in the Fig. 2.4. The Table 2.3 shows characteristic stretching frequencies.

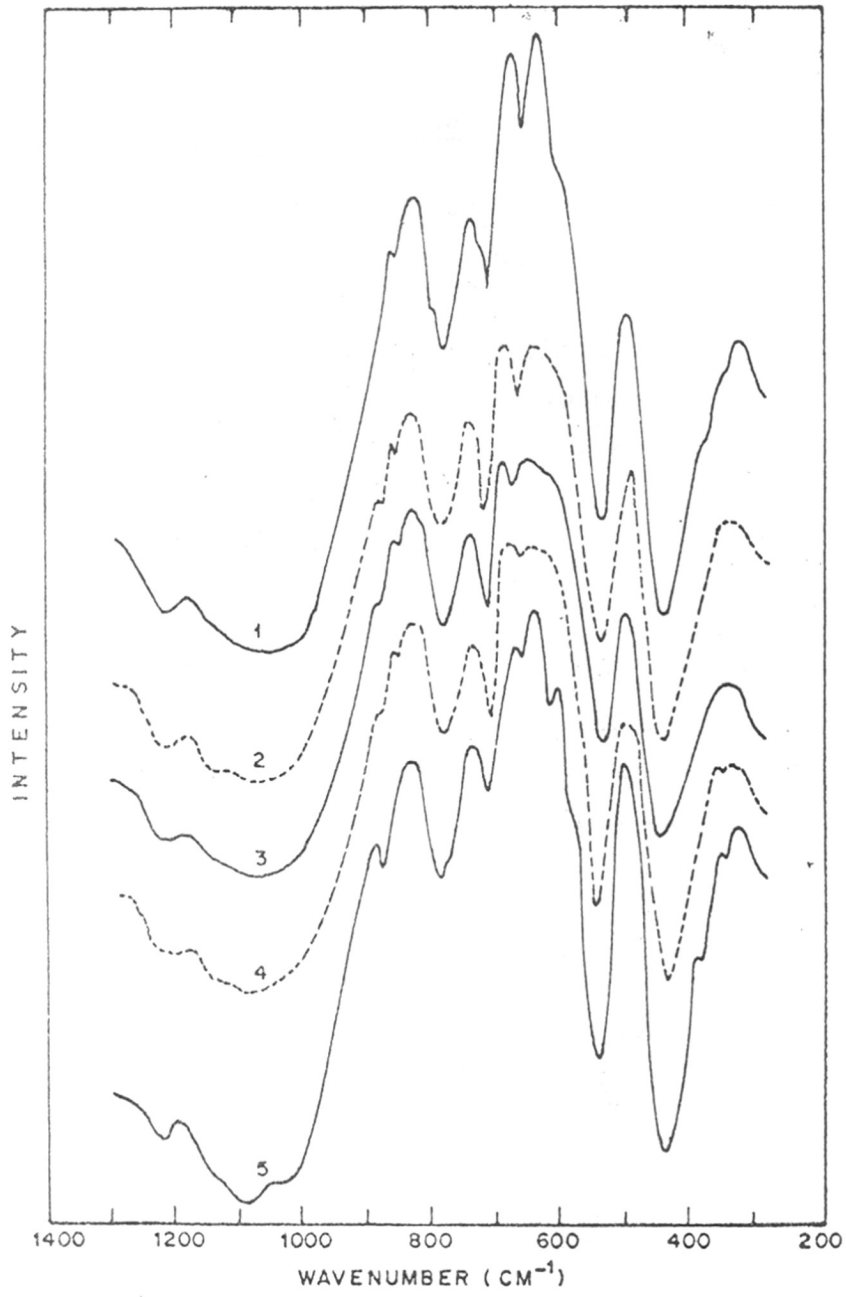

FIG. 2.4. IR SPECTRA OF HZSM-5 ZEOLITES. NUMBERS 1-5 REFER TO SiO_2 / Al_2O_3 RATIOS, 36, 86, 144, 165 AND 320 RESPECTIVELY.

TABLE - 2.3

Framework vibration frequencies for NaZSM-5

SiO_2/Al_2O_3 = 86

Wave number (cm^{-1})	Assignment*
450	Si-O bending
540	Distorted double 5 rings
590	ELC5
620	ELC5
720	TISS
790	ELSS
840	ELSS
1075	ITAS
1020	Si-O asymmetric stretch

---

* ELC5 = External link complex 5 membered ring.

ITSS = Internal tetrahedral symmetric stretch.

ELSS = External link symmetric stretch.

ITAS = Internal tetrahedral symmetric stretch.

The absorption band at 550 cm^{-1} is assigned to highly distorted double five membered ring which is characteristic of ZSM-5 type of zeolite[69]. The frequencies observed for samples 1-5 (Fig. 2.4) are in good agreement with the reported values. Thus, the ir data further confirm that the samples synthesized belong to the pentasil family of ZSM-5 zeolites.

Flanigen[65] reported a linear decrease for the position of main assymetric stretch band near 980 to 1100 cm^{-1} with increasing atom fraction of Al in the tetrahedral sites. The decrease in the frequency with increasing Al concentration was attributed to change in the bond length and bond order. The larger bond length of Al-O and decreased electronegativity of Al results in a decrease of forge constant. The present samples of different alumina content also show a decrease in frequency as expected.

(C) Scanning Electron Microscopy (SEM)

The crystalline phases were analysed for morphology of the crystals using SEM (Sterioscan Model 150,Cambridge, U.K.). The sample was dusted on aluminium pegs and coated with an Au-Pd evaporated film. The SEM photographs of crystalline samples of different SiO_2/Al_2O_3 ratios are shown in Fig. 2.5A. The crystals show similar morphology to

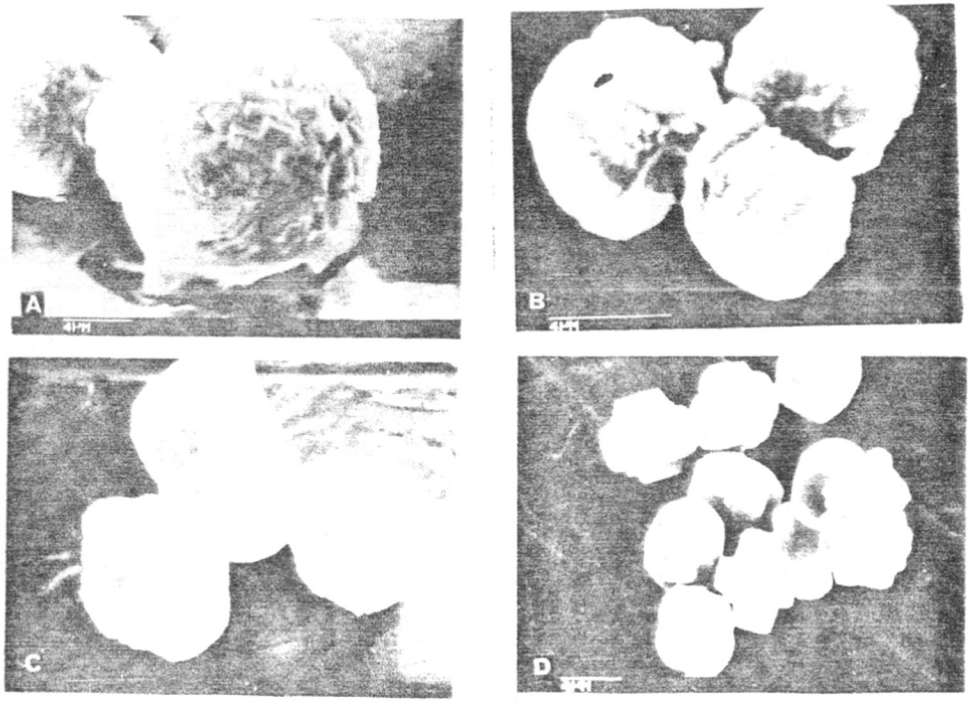

FIG.2.5A. SEM PHOTOGRAPH OF ZSM-5 ZEOLITE OF SiO_2/Al_2O_3 RATIOS [(A)86,(B)144,(C)165,(D)320]

those reported[57]. The crystallite size of the samples is about 2-6 micron. The ZSM-5 samples show that with increasing SiO_2/Al_2O_3 ratio, the crystallite size also increases.

(D) Thermal Analysis

The thermal analysis was performed using automatic Hungarian derivatograph (MOM 102 Budapest). The thermograms were recorded under the following conditions:

(i) Sample weight - 70 mg
(ii) Heating rate - 10 k/min.
(iii) Sensitivity
  (a) DTA 1/5
  (b) DTG 1/5
  (c) TGA 70 milligram
(iv) Atmosphere: air suction.

Preheated and finely powdered α alumina was used as an internal standard.

A typical thermogram of the synthesized ZSM-5 (TEPA-ZSM-5) is shown in the Fig. 2.5B. The TG thermograms show two successive stages of weight loss. The 1st stage from 298 to 473 K is due to the loss of water which is present in the zeolite channels and second is associated with the decomposition of organic cations (TEPA). It was found that pure TEPABr decomposes in the range 353 to 473 K. However, decomposition of the TEPA occluded

FIG·2·58. DTA AND TG THERMOGRAMS OF TEPA ZSM-5 ZEOLITE., SiO_2/Al_2O_3 = 86

in the channels of the ZSM-5 (TEPA-ZSM-5) takes place between 593 and 873 K. Hence, there must exist a strong bonding between TEPA molecules and the framework atoms of the ZSM-5 zeolite. The TEPA molecules lost per unit cell in the above temperature (593 to 873 K) range is 3.5 i.e. close to the theoretical value of 4. This indicates that one TEPA molecule is occluded per channel intersection, because the unit cell is conveniently divided into four equivalent intersecting elements which comprise the channel intersection[70]. The presence of two exotherms (in DTA) corresponding to 665 to 670 K and 750 to 755 K respectively shows that there may exist two types of TEPA species in the ZSM-5 channel. The weight loss estimated from the TG data at 750-873 K (the second stage) corresponds to 1.8 TEPA molecules per unit cell which is nearly equal to the number of Al atoms per unit cell. The high temperature required for decomposition of these molecules of TEPA may be attributed to their strong interaction and binding to the framework Al atoms located at the channel intersection. The present results are consistent with the results reported by Parker et al[101]. They showed that tetraalkylammonium ions in the ZSM-5 precursors are occluded at two sites, (i) where they are associated with acid sites and act as counter ions, and (ii) the others which are not associated with the acid sites. The Al free silicalite contains only latter form

of the tetraalkylammonium ions, which decompose by the Hofmann reaction and form olefins and trialkylamines.

The TG curves of the HZSM-5 of different SiO_2/Al_2O_3 ratios prepared by the decomposition of NH_4ZSM-5 are given in Fig. 2.6. The weight loss between 298 to 673 K in TG is due to the loss of zeolitic water present in the channels of the zeolite. The weight loss determined by thermogravimetric and gravimetric technique (using McBain spring balance at 673 K and 10^{-6} torr) show good agreement (Table 2.4). The weight loss above 673K is attributed to the dehydroxylation of surface hydroxyl groups.

The number of surface hydroxyl groups has been estimated by assuming that the weight loss from 673 to 1273 K occurs from the dehydroxylation of OH groups. The number of hydroxyl groups, thus estimated, for samples containing different SiO_2/Al_2O_3 ratios is shown in Table 2.4. This number decreases with increasing SiO_2/Al_2O_3 ratio, as there is a decrease in the framework aluminium atoms with which they are bound. An estimate of the number of OH groups can also be made from measurements on chemisorption of ammonia on zeolites. The two estimated values are nearly same (Table 2.7).

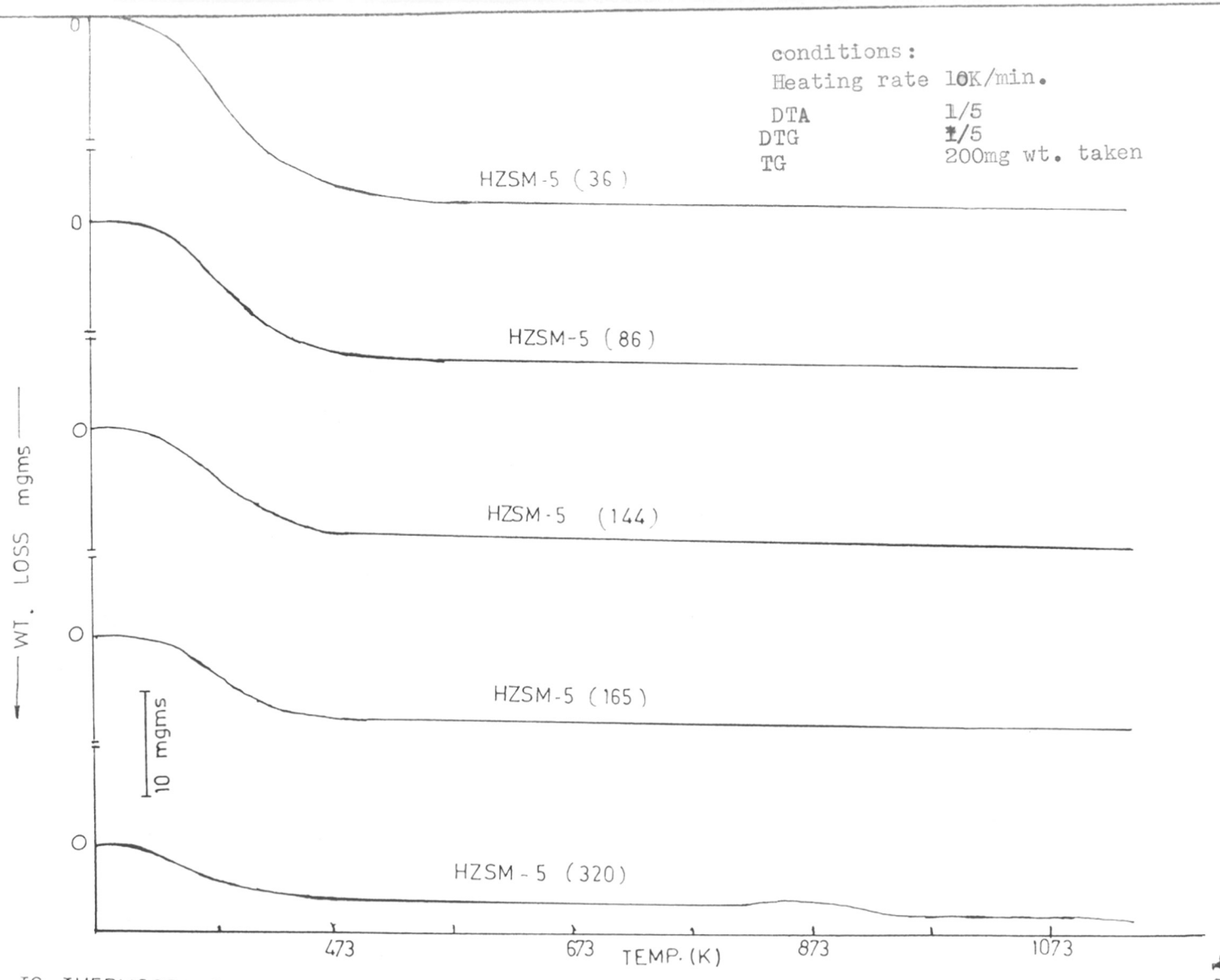

FIG. 2.6. TG THERMOGRAMS OF HZSM-5 ZEOLITES. THE NUMBER IN BRACKET REFERS TO SiO_2 / Al_2O_3 RATIO

TABLE - 2.4

Thermogravimetric analysis of HZSM-5 samples

Sample	Al/UC	% Wt.loss[a]	% Wt.loss[b]	No. of OH group/ unit cell[c]
HZSM-5 (36)	5.02	9.40	9.72	11.31
HZSM-5 (86)	2.28	7.20	7.60	8.93
HZSM-5 (144)	1.31	5.50	5.59	8.90
HZSM-5 (165)	1.09	4.50	5.29	6.16
HZSM-5 (320)	0.64	3.00	3.12	3.46

a = Thermogravimetric wt. loss calculated in the temperature range 298 to 673 K.

b = Weight loss calculated at 673 K under vacuum (10^{-6} torr) using McBain spring balance.

c = Number of hydroxyl groups on the surface estimated from weight loss in the range 673 to 1273 K.

The numbers in bracket refer to SiO_2/Al_2O_3 ratios.

(E) Sorption of argon

ZSM-5 zeolite is a highly porous material with a large internal surface area where the active centres are located. The external surface area represents only 5% of its total surface area[71].

The argon sorption was used for the estimation of the surface area and the micropore volume. The sorption was measured on 'Accusorb Unit' (Micromeritics Model2100 E) volumetrically at liquid nitrogen temperature (77 K). The surface occupied by argon molecule was taken to be 13.8 $Å^2$[72]. The surface area was calculated using the BET[73] equation :

$$\frac{P}{V(P_o-P)} = \frac{1}{V_m C} + \frac{C-1}{V_m C} \cdot \frac{P}{P_o}$$

where P = adsorbate pressure,

P_o = saturation pressure,

V_m = monolayer capacity,

C = constant, characteristic of adsorbate-adsorbent interaction.

A typical BET plot is made in Fig. 2.7. Surface area of the sample is evaluated from the slope of the straight line and given in Table 2.5 for the various samples.

The adsorption isotherms constructed for the samples of different SiO_2/Al_2O_3 ratios are shown in

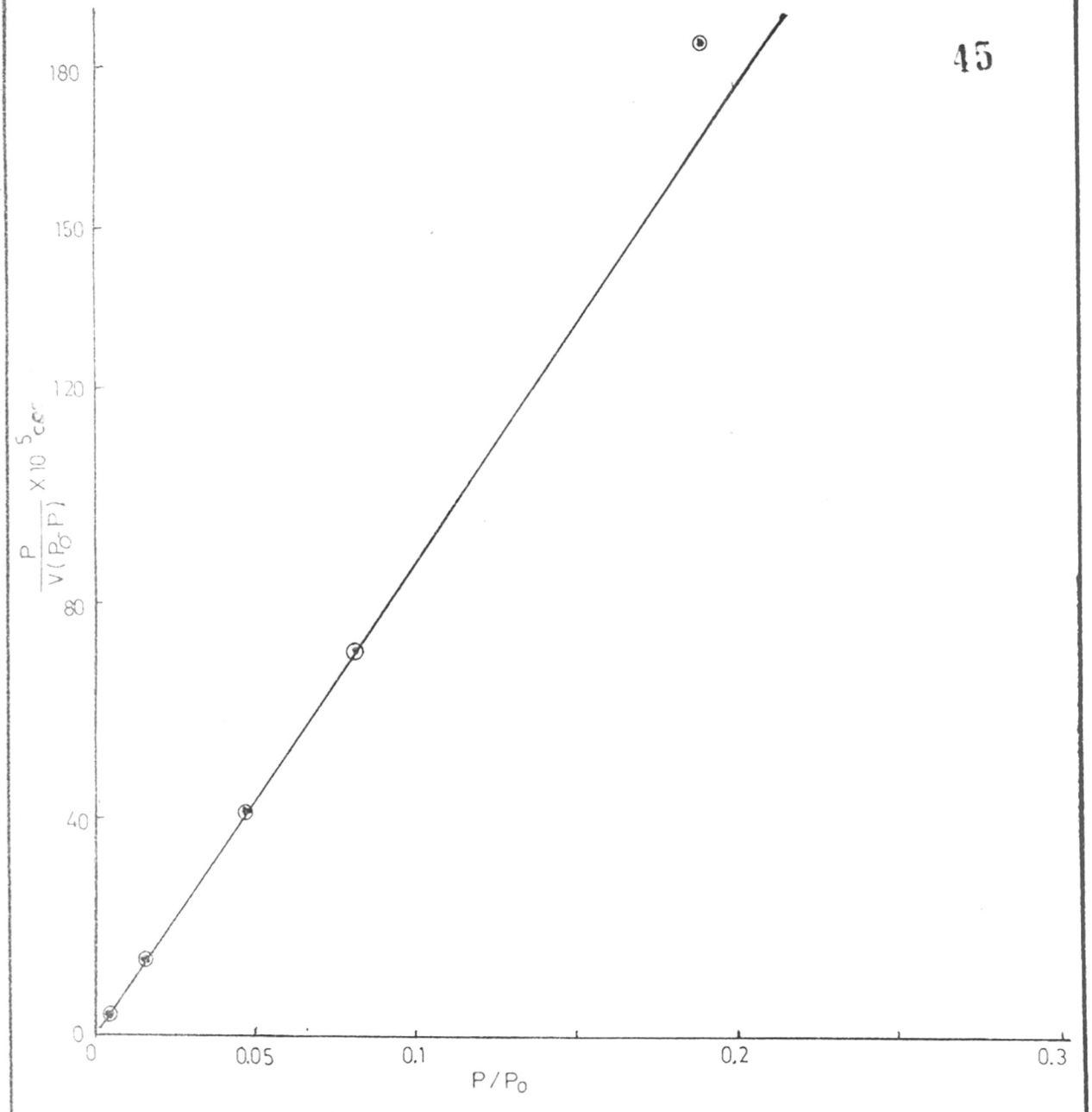

FIG. 2.7. BET PLOT FOR HZSM-5 ZEOLITE, $SiO_2 / Al_2O_3 = 36$.

TABLE - 2.5

BET surface area and pore volume of HZSM-5 and modified HZSM-5 zeolites

Sample	Surface area m^2/gm	Pore volume cc/gm	SiO_2/Al_2O_3 molar ratio
1. HZSM -5	427.85	0.167	36
2. HZSM-5	438.22	0.164	86
3. HZSM-5	421.37	0.158	144
4. HZSM-5	415.12	0.157	165
5. HZSM-5	412.00	0.159	320
6. NiHZSM-5 (0.55)	423.78	0.158	36
7. NiHZSM-5 (1.10)	415.00	0.145	36
8. NiHZSM-5 (2.22)	402.59	0.315	36
9. NiHZSM-5 (5.6)	390.12	0.130	36
10. NiPtHZSM -5 (0.55 Ni, 0.2 Pt)	430.20	0.158	36
11. PMgHZSM-5 (5 Mg and 2 P)	329.60	0.122	36
12. PMgHZSM-5 (3 Mg and 4 P)	320.50	0.118	36
13. PHZSM-5 (8)	236.0	0.09	36
14. BHZSM-5 (3)	300.5	0.112	36

Note : The number in bracket refers to the % wt. of the added element in H-ZSM-5 zeolites.

Fig. 2.8. The micropore volume which can be derived from type I adsorption isotherm was calculated using Dubinin equation[74] :

$$\log_{10}V_a = \log_{10}V_o - D\ (\log P/P_o)^2$$

where V_a is the volume adsorbed per unit mass of the adsorbent, V_o is the volume of adsorbed phase or the pore volume, P/P_o is the relative pressure, D is a constant, varying with temperature and the adsorbate-adsorbent interaction. A plot of $\log_{10}V_a$ against $(\log P/P_o)^2$ should, therefore, be a straight line (Fig. 2.9). The intercept which is equal to $\log_{10}V_o$ can be obtained and would lead to the micropore volume V_o

$$V_a = V_o\ (Q_g/Q_l)$$

where Q_g and Q_l being the density of the adsorbate in the gas and liquid phase respectively.

It can be seen that increase in the SiO_2/Al_2O_3 ratio decreases surface area and micropore volume (Table 2.5 , samples 1-5). This decrease may be due to a partial shrinking of the unit cell at higher SiO_2/Al_2O_3 ratio. A decrease in the surface area and micropore volume is also observed when boron, phosphorous and magnesium are incorporated in the ZSM-5. It has been suggested that compounds of these elements occupy portion in the channels thus effectively reducing their volume.[33]

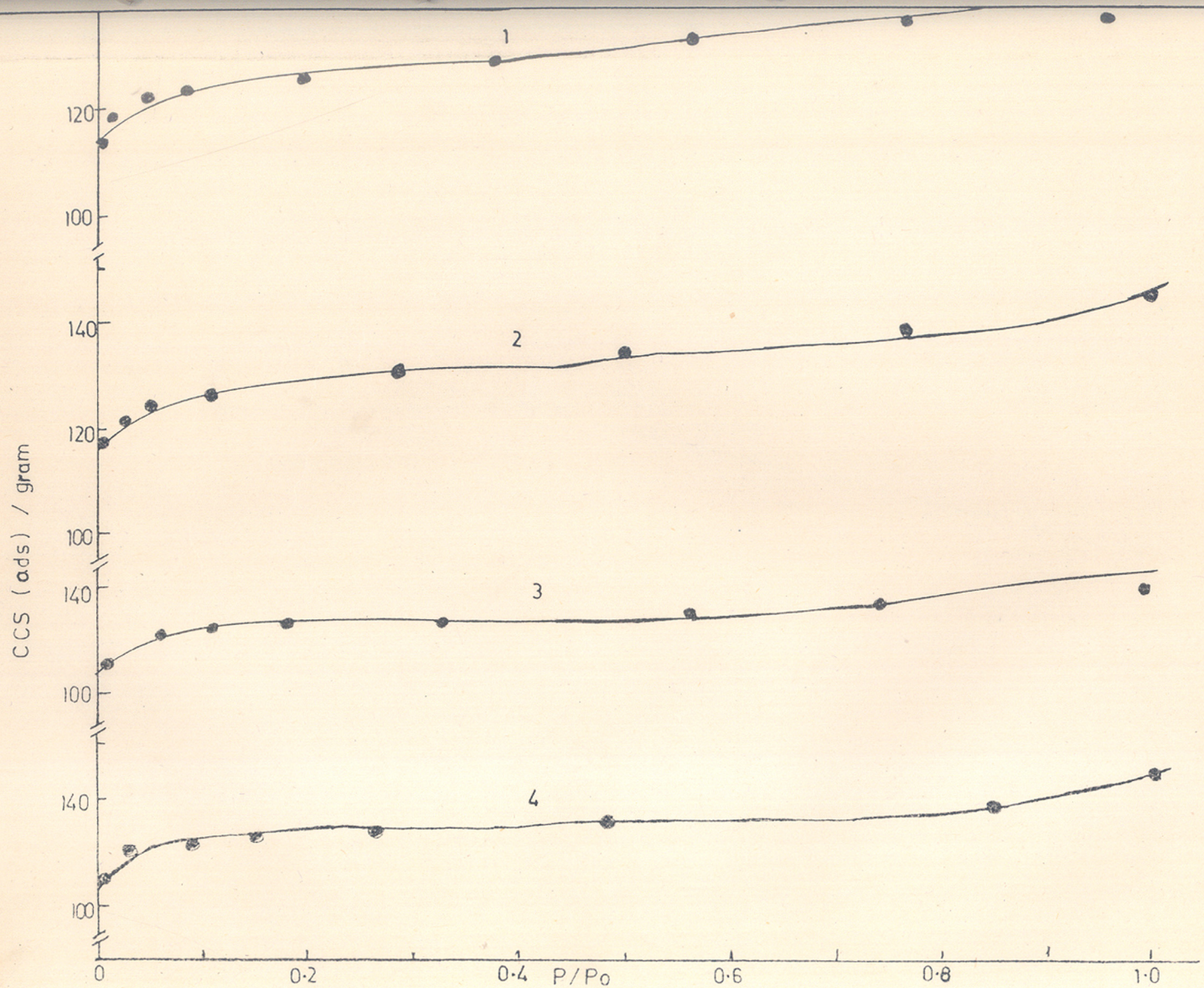

FIG. 2·8· ARGON ADSORPTION ISOTHERMS ON HZSM 5 ZEOLITES OF DIFFERENT SiO_2/Al_2O_3 RATIOS AT 77 K. NOS. 1-4 REFER TO SiO_2/Al_2O_3 RATIO 36, 86, 144 AND 320 RESPECTIVELY.

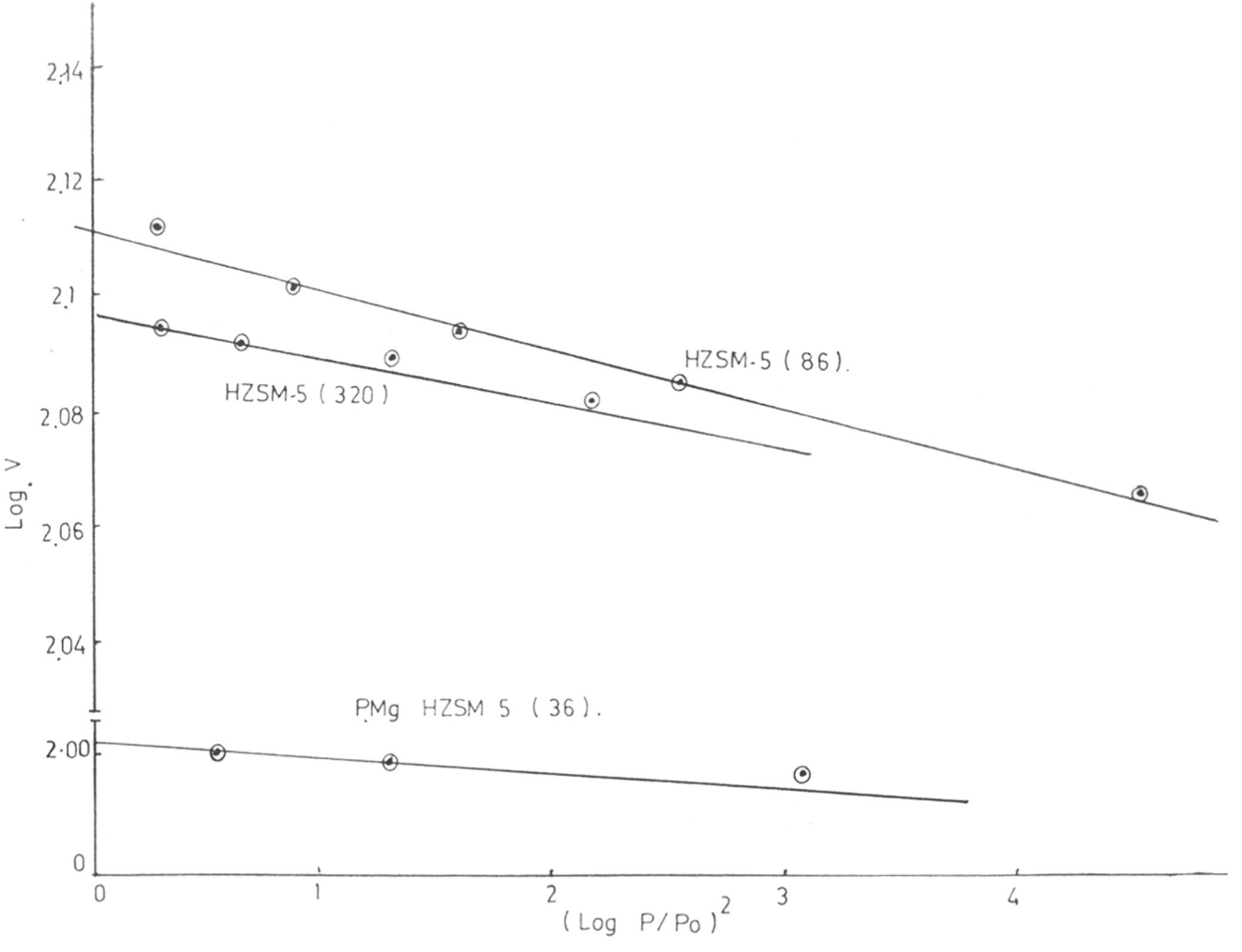

FIG . 2.8 DUBININ PLOT FOR HZSM-5 ZEOLITE AND PHOSPHOROUS AND MAGNESIUM MODIFIED HZSM-5. THE NOS. IN BRACKET REFER TO SiO_2/Al_2O_3 RATIO

(F) Sorption of Water and Hydrocarbons

The sorption measurements have been suggested as powerful tool to determine the effective shape selectivity of ZSM-type zeolites[26] and feasibility of occurrance of a particular reaction. As described in Chapter 1, the structure of ZSM-5 consists of three dimensional channel system, one of which is straight and the other sinusoidal. The dimensions of straight channel is 0.54 x 0.56 nm and sinusoidal, 0.51 x 0.55 nm. By measuring the diffusivity of molecules of different sizes and shapes, one can get information on the accessibility of different reactants to the active sites which lie burried in the intracrystalline voids and probable product distribution during reaction. The sorption of polar molecules like water, on the other hand, can be used to determine approximately the number of active species[55,75,76] (Al^{3+} ions).

The sorption measurements of the hydrocarbons benzene, toluene, cyclohexane, p-xylene, o-xylene and 1,2,4 trimethylbenzene which represent major products formed in the toluene disproportionation and C_7,C_9 transalkylation reactions, were carried out under the following experimental conditions using McBain silica spring balance (Fig. 2.10).

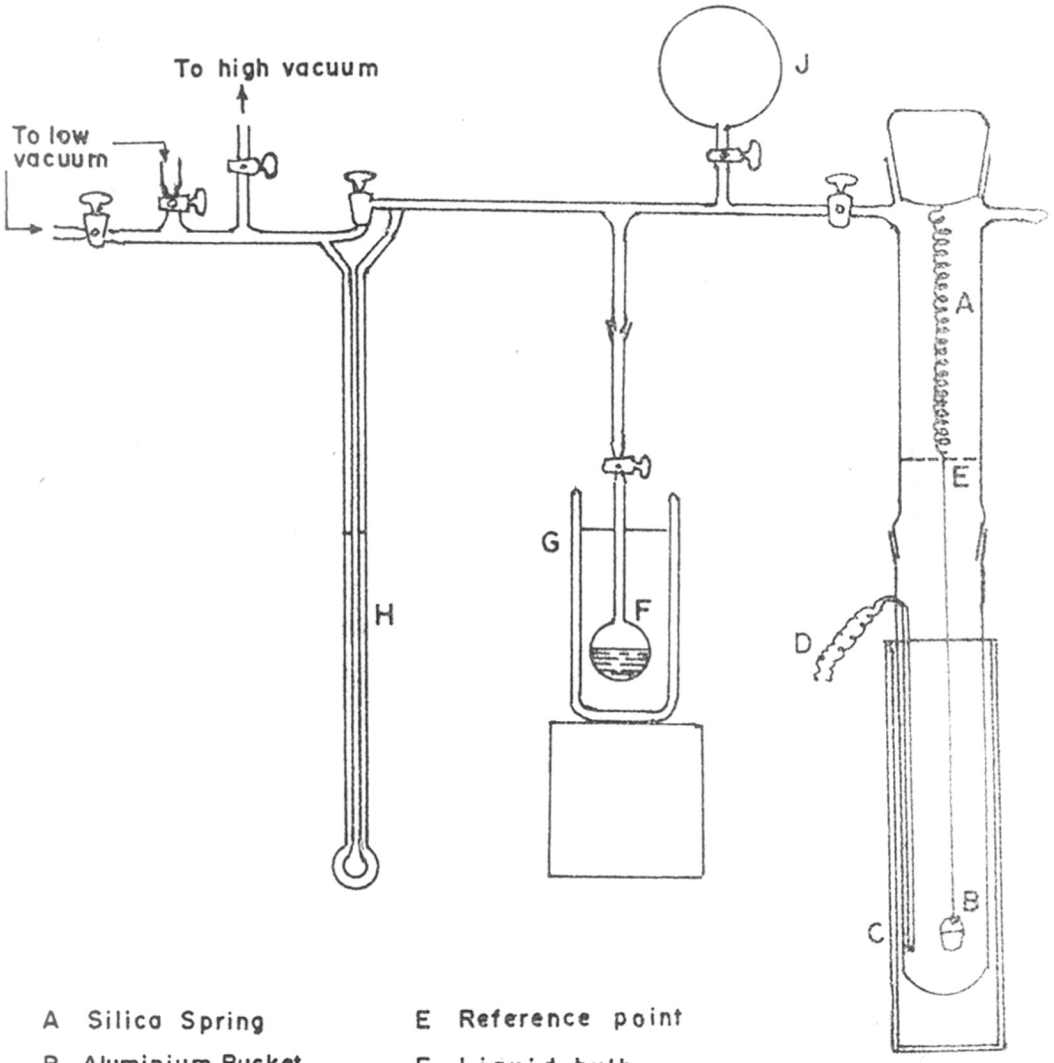

A Silica Spring
B Aluminium Bucket
C Furnace or Thermostat
D Thermocouple
E Reference point
F Liquid bulb
G Thermostat
H Manometer
J Gas Reservoir

FIG. 2.10 GRAVIMETRIC ADSORPTION UNIT

A sensitive silica spring was used for the measurement of weight changes. The zeolite sample, about 200 mgs was pressed into a pellet and weighed into an aluminium bucket which was attached to the silica spring. The assembly was evacuated by means of a two stage rotary pump and mercury diffusion pump to a vacuum of 10^{-6} torr. The sample was activated at 673 K by continuous pumping till a constant weight was obtained. After the zeolite sample had reached a constant weight, the temperature of the sample was lowered to the desired value. To study the equilibrium sorption, the sorbate was admitted to the sample at constant temperature and pressure and sorption was calculated, using a cathetometer to measure the extension of the spring (accuracy $\pm$ 0.01 mm) as a function of time.

The amount adsorbed vs time plots for different hydrocarbons are shown in Fig. 2.11 wherein two groups of curves can be recognized. For the first type, equilibrium adsorption is attained within 10-20 minutes, and for the second, there is a steady, though slow, increase in the amount adsorbed with time. Benzene, tolumne and p-xylene belong to the first group. For the others, even after a lapse of two hours, the equilibrium had not been attained because their critical diameters are larger than pore size. Anderson et al[40] showed that the effective molecular size separating fast and slow sorption was > 0.58 < 0.61 nm, which is larger than the free channel dimension. The present results confirm their findings.

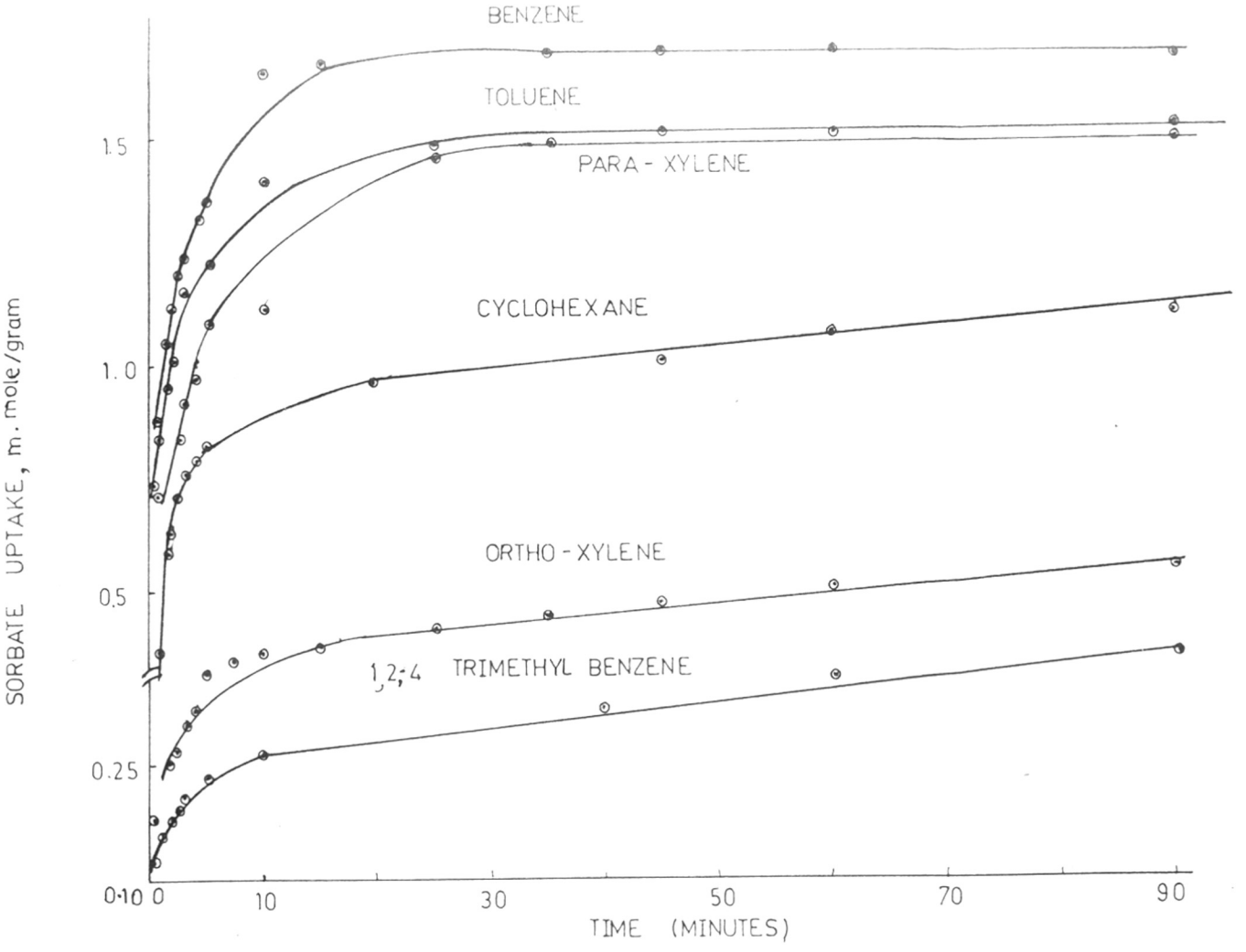

FIG - 2.11 COMPARATIVE SORPTION OF HYDROCARBONS OVER HZSM - 5, $SiO_2/Al_2O_3 = 36$

The sorption data for hydrocarbons are presented in Table 2.6. It can be seen that the number of molecules adsorbed per unit cell 'n' is about 10 for benzene which is in fair agreement with the value (8.7) reported for pure silicalite[35]. The corresponding values for toluene and p-xylene are 8.7 and 9.2 respectively. A progressive increase in the incorporation of nickel in HZSM-5 (NiHZSM-5 samples 6-9, Table 2.6) results in a decrease in the value of 'n'. The uptake vs time curves for the NiHZSM-5 and HZSM-5 for cyclohexane are illustrated in Fig. 2.12. It is seen that 80% of total sorption takes place in 10 minutes in the case of HZSM-5 whereas only 68% is sorbed in 10 minutes in the case of NiHZSM-(Ni^{++} 2.2%). Hence it may be inferred that the entry of cyclohexane molecules in NiHZSM-5 pores is restricted as compared to that in HZSM-5. This may be due to the fact that nickel ions stick to the walls of the ZSM-5 channels and this results in an increase in the diffusional resistance of ZSM-5 zeolite. The impregnation of boron, phosphorous and magnesium (BHZSM-5, MgPHZSM-5) (Table 2.6) also reduces the value of 'n', since these species are known to penetrate into the channels of the ZSM-5 and block the pores partially. Fig. 2.12 also compares the adsorption of cyclohexane in the PMgHZSM-5 and HZSM-5. This blocking effect is more pronounced with BHZSM-5 (sample 12, Table 2.6) in which the adsorption is very small. The present results

TABLE - 2.6

Hydrocarbon and water sorption in zeolites

Sample	n ≐ Sorbate uptake molecules/unit cell						
	B	T	PX	CH	OX	TMB	Water
1. HZSM-5 (36)	10.18	9.1	9.48	6.80	2.56	2.10	40.75
2. HZSM-5 (86)	11.38	9.99	10.51	5.23	1.97	0.78	33.20
3. HZSM-5 (144)	9.40	8.50	8.78	3.37	1.40	0.71	21.50
4. HZSM-5 (165)	10.06	8.66	9.20	2.85	1.34	0.65	21.20
5. HZSM-5 (320)	9.67	8.67	9.34	1.68	0.87	0.52	10.24
6. NiHZSM-5 (36)	9.78	8.76	9.17	6.43	2.57	-	-
7. NiHZSM-5 (36)	9.44	8.45	8.69	5.95	2.62	-	-
8. NiHZSM-5 (36)	9.00	8.23	8.50	5.89	2.48	-	-
9. NiHZSM-5 (36)	8.85	7.91	8.28	4.95	1.93	-	-
10. PMgHZSM-5 (36)	7.40	-	6.53	1.68	-	-	-
11. PHZSM-5 (36)	0.022	0.01	-	-	-	-	-
12. BHZSM-5 (36)	0.019	0.016	0.018	0.008	-	-	-

Note : The number in bracket refers to the SiO_2/Al_2O_3 molar ratio.

Abbreviations : B = benzene; T = toluene; PX = para-xylene; CH = cyclohexane; OX = ortho-xylene; TMB = 1,2,4 trimethylbenzene.

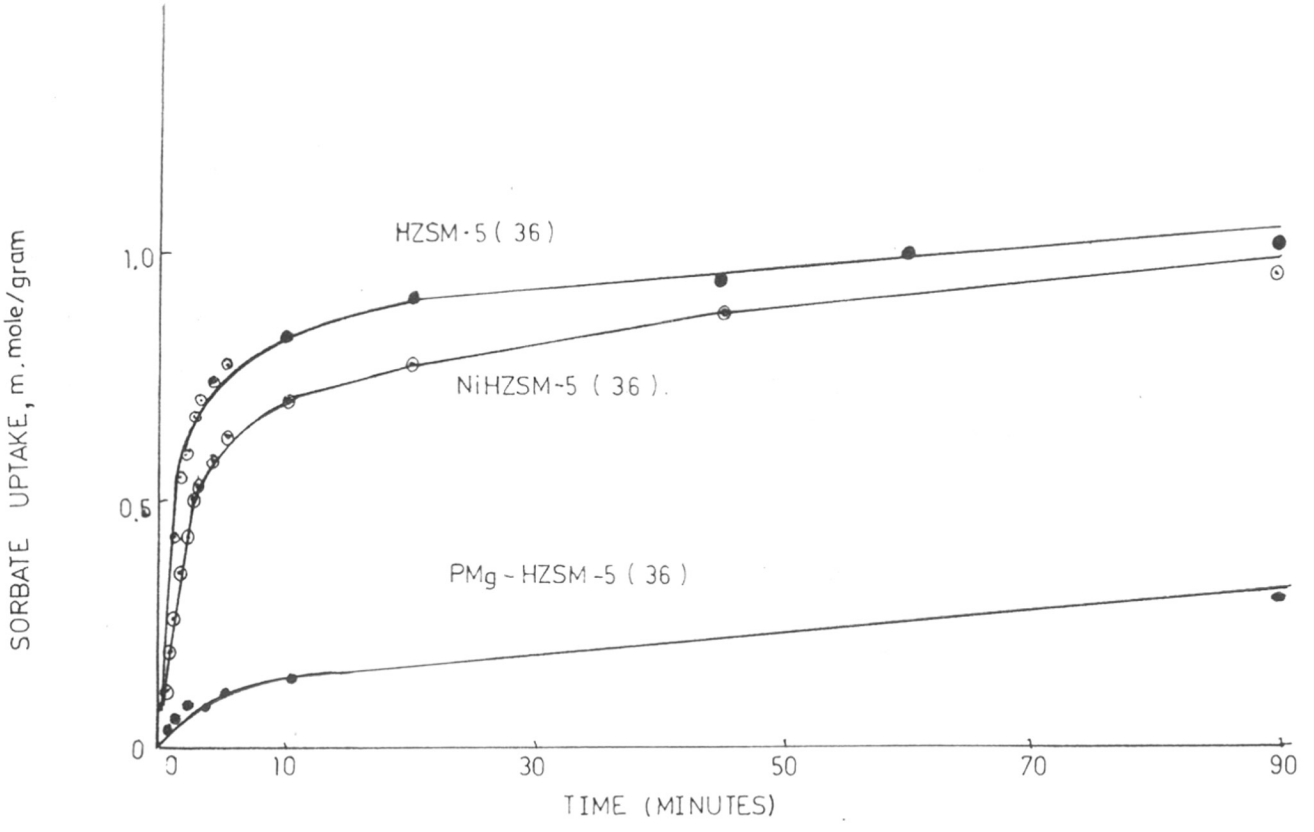

FIG .2.12. SORPTION OF CYCLOHEXANE OVER MODIFIED HZSM-5 ZEOLITES. THE NUMBER IN BRACKET REFERS TO SiO_2/Al_2O_3 RATIO .

are consistent with the high para-xylene selectivity of boron, phosphorous and magnesium modified ZSM-5 zeolites in the toluene disproportionation[28] reaction and high olefins selectivity in the conversion of methanol to hydrocarbons[77,78]. These catalysts restrict the diffusion of ortho- and meta-xylenes in the first reaction and the formation of larger molecules ($>C_4$) in the second.

Fig. 2.13 represents the adsorption of hydrocarbons in ZSM-5 zeolites of varying SiO_2/Al_2O_3 ratios. It is observed that the value of 'n' remains constant (Fig. 2.13, curves 2-4) irrespective of SiO_2/Al_2O_3 ratio in the case of benzene, toluene and para-xylene adsorbates. On the other hand, adsorption of cyclohexane, ortho-xylene and 1,2,4 trimethylbenzene is found to decrease with increasing SiO_2/Al_2O_3 ratio of the HZSM-5. The reduced adsorption in these cases as compared to that of benzene, toluene and para-xylene can be attributed to the larger molecular diameter of these compounds. A further decrease with increase in SiO_2/Al_2O_3 may be due to a partial shrinking of the unit cell with increasing SiO_2/Al_2O_3 ratio. This shrinking effect is especially reflected in cyclohexane, ortho-xylene and 1,2,4 trimethylbenzene adsorption. The uptake of cyclohexane and o-xylene in HZSM-5 samples of SiO_2/Al_2O_3 ratio 36 and 320 are illustrated in Fig. 2.14.

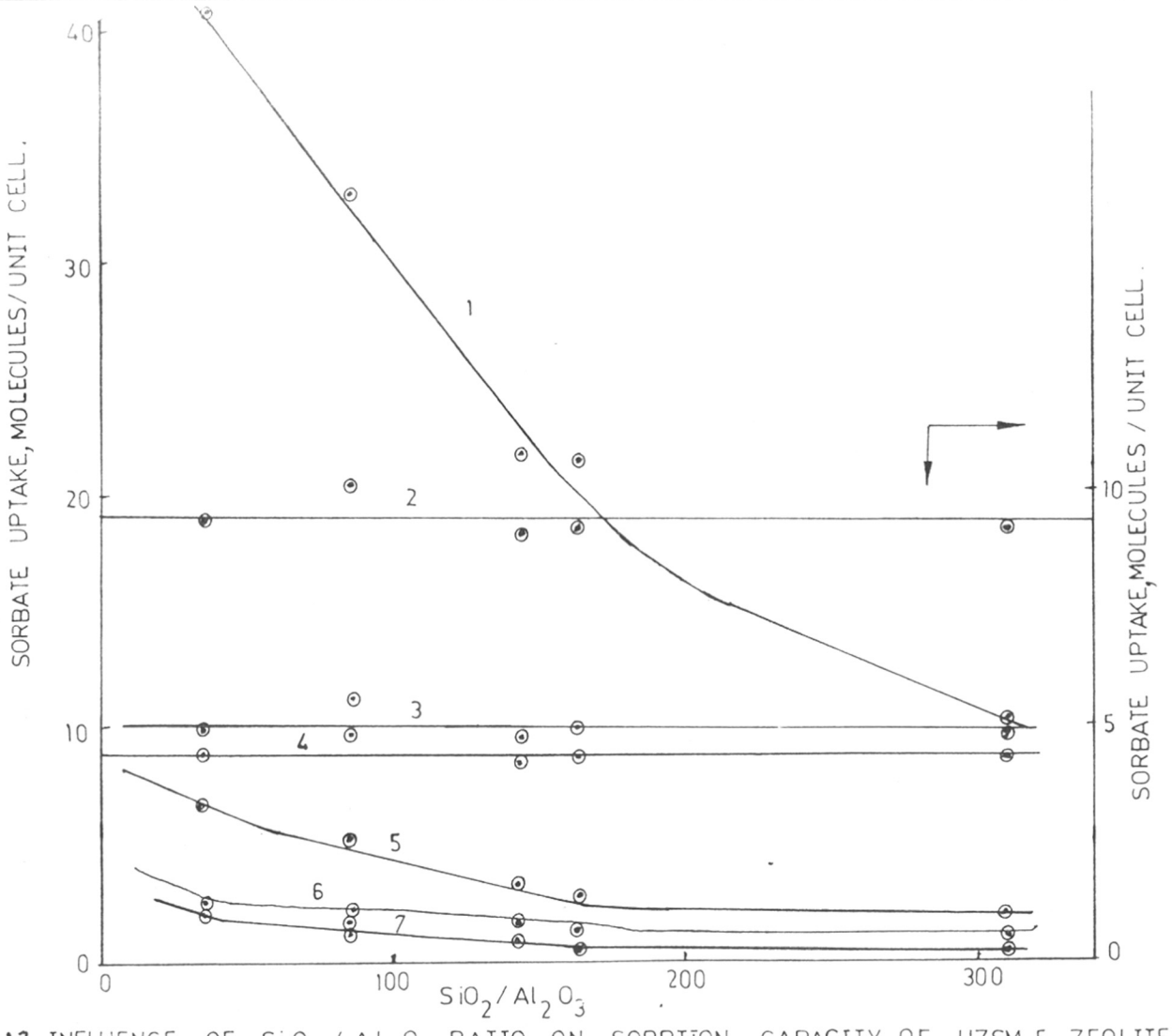

FIG . 2.13. INFLUENCE OF SiO_2/Al_2O_3 RATIO ON SORPTION CAPACITY OF HZSM-5 ZEOLITES AT 298K. CURVES NUMBER 1—7 REFER WATER, PARA-XYLENE, BENZENE, TOLUENE, CYCLOHEXANE, ORTHO XYLENE AND 1,2,4 TRIMETHYLBENZENE.

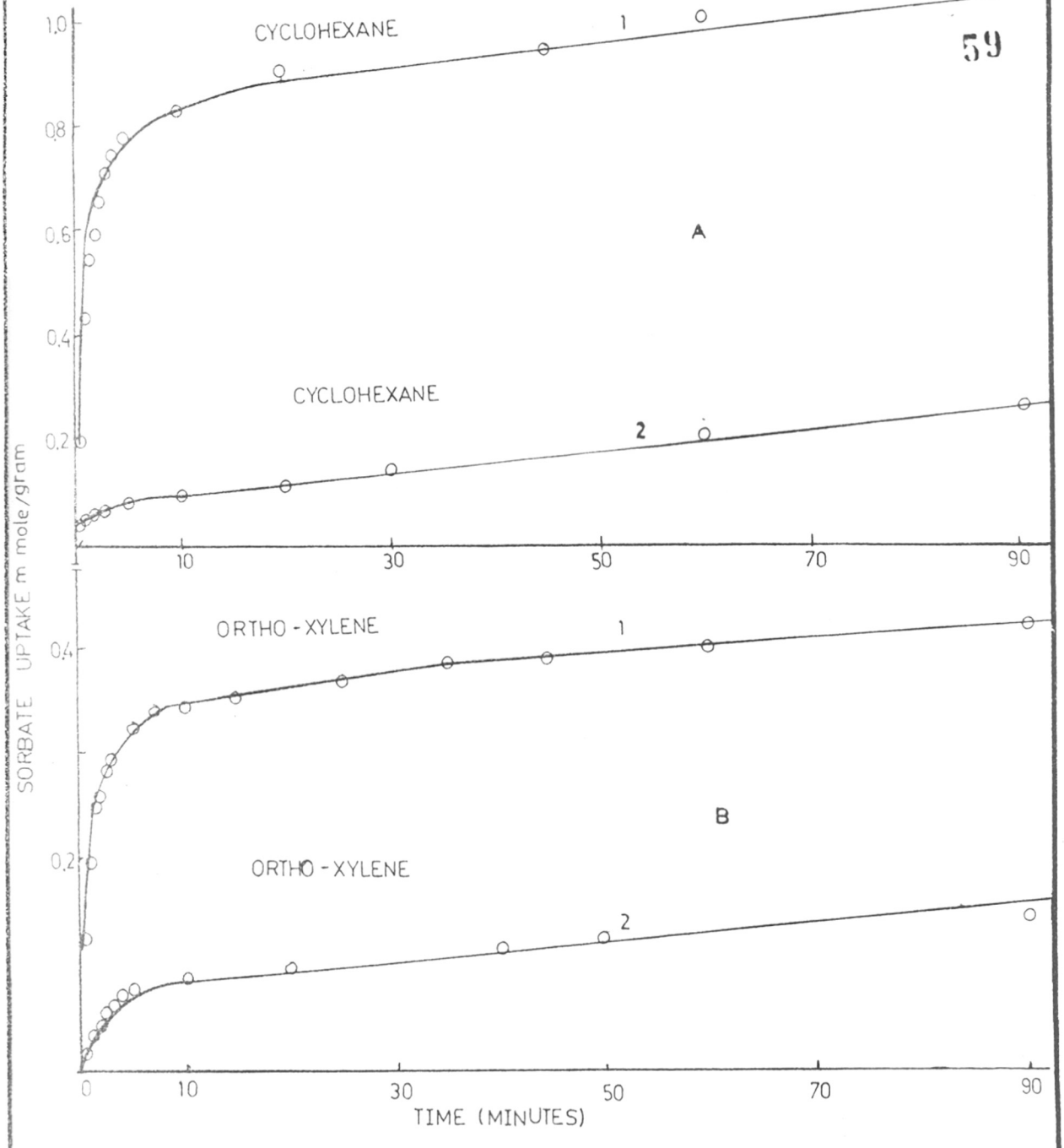

FIG. 2.14 A&B SORPTION OF CYCLOHEXANE (A) AND ORTHO-XYLENE (B) OVER HZSM-5 ZEOLITES. CURVE NOS. 1 AND 2 ARE FOR SAMPLE HAVING SiO_2/Al_2O_3 RATIO 36 & 320 RESPECTIVELY.

Flanigen et al[35] reported the hydrophobic selectivity of silicalite, which is aluminium free ZSM-5 zeolite, as well as graphon, dehydrated 'Hisil' carbon molecular sieve, and suggested that in the absence of surface sites which are hydrophilic or the sites for hydrogen bonding, polar, or acid-base interactions, the surface becomes non-specific, homogeneous and hydrophobic. This hydrophobicity of the silicalite was attributed to the absence of aluminium in the lattice position. The fall in the adsorption of water (Fig. 2.13) with increasing SiO_2/Al_2O_3 ratio is consistent with increasing hydrophobicity of the ZSM-5 zeolite. Mao et al[79a] also reported similar results in terms of 'relative affinity index' (RAI) defined as the ratio of sorbed n-hexane to water.

(G) Diffusion

Crank[102] formulated the following expression for concentration independent diffusion in spherical particles of radius 'a'

$$\frac{Q_t - Q_o}{Q_\infty - Q_o} = 1 - \frac{6}{\pi^2} \sum_{n=1}^{n=\infty} \frac{1}{n^2} e^{-Dn^2\pi^2 t/a^2} \quad \ldots (1)$$

where Q_o, Q_t, Q_∞ represent total amount adsorbed by a spherical particle at time, zero, t and ∞ respectively, D is the effective diffusivity, 'a' is the microsphere radius, n is the number of microspheres per unit macro-

sphere volume. For small values of t, however, a simple equation has been derived

$$\frac{Q_t - Q_o}{Q_\infty - Q_o} = 6\left(\frac{D}{\pi a^2}\right)^{1/2}\sqrt{t} \qquad \ldots (2)$$

Thus, by plotting the LHS against $\sqrt{t}$, the diffusivity can be evaluated from the slope of the linear plot.

From the adsorption data the plots were made by using equation (2) and from the slope the diffusivity of the hydrocarbons was determined.

The typical plots are illustrated in Fig. 2.15. It can be seen that (Table 2.7) the diffusivities of toluene and p-xylene are constant irrespective of SiO_2/Al_2O_3 ratio and the diffusivity of o-xylene is decreased with increasing SiO_2/Al_2O_3 ratio as expected. In case of ZSM-5 zeolite modified with phosphorous and magnesium, the p-xylene selectivity is increased. However, the o-xylene shows no diffusion in this catalyst indicating that pore aperture and channels of the ZSM-5 are blocked partially.

(H) Surface Acidity

The ZSM-5 zeolite is a potential catalyst for the conversion of petroleum feedstocks and some oxygenated species like methanol[52], because of its shape selective

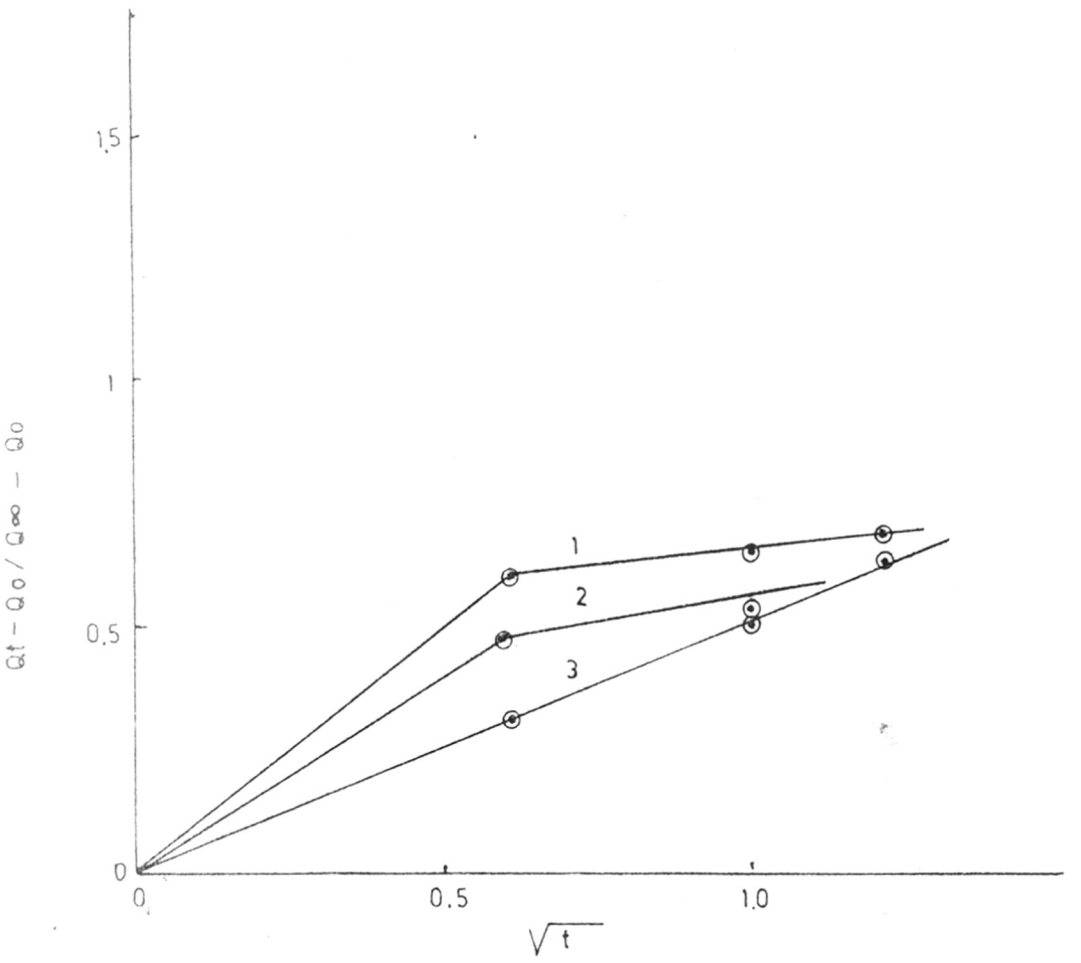

FIG. 2.15. DIFFUSION RATES OF TOLUENE, P-XYLENE AND O-XYLENE (CURVES 1-3 RESPECTIVELY) THROUGH HZSM-5, SiO_2/Al_2O_3 = 36.

TABLE - 2.7

Diffusivity of some sorbates in HZSM-5 at 298 K

Catalyst	SiO_2/Al_2O_3 molar ratio	Sorbate diffusivity D/a^2 cm^{-1}		
		P-Xylene	Toluene	O-xylene
HZSM-5	36	0.66	0.60	0.44
HZSM-5	86	0.69	0.65	0.36
HZSM-5	144	0.72	0.70	0.22
HZSM-5	165	0.70	0.73	0.16
HZSM-5	320	0.75	0.80	0.11
PMgHZSM-5 (2% P, 5% Mg)	36	0.33	-	-

behaviour and long lived activity. Such conversions have been understood to occur via carbonium ion type of intermediates[11,76b] and hence the Brönsted type of acid centres present on the surface of the zeolite are of particular interest. These centres are the results of the isomorphous substitution of trivalent aluminium (Al^{3+}) for tetravalent silicon (Si^{4+}) in the zeolite lattice. A variation of the SiO_2/Al_2O_3 ratio would then affect both, the number and strength of acid sites. The alteration of the number and strength of Brönsted and Lewis acid sites occurs by incorporation of transition metals into the framework of zeolite by ion exchange[80].

Many techniques have been used for the characterization of the acid sites namely infrared spectroscopy[41,81], microcalorimetry[82], electron spin resonance[40,44,83,84] and temperature programmed desorption (TPD).

The type of active sites, their strength and number have been evaluated from a study of TPD of ammonia as a function of following parameters:

(i) Temperature of deammoniation of NH_4ZSM-5,

(ii) Calcination temperature,

(iii) SiO_2/Al_2O_3 ratio,

Procedure A

The TPD unit shown in Fig. 2.16 was used. In procedure (A), the sample NH_4ZSM-5 (200 mg. 10-30 mesh particles) was loaded in the stainless steel micro-reactor, connected on line to a gas chromatograph (AIMIL). The catalyst was then heated at a linear rate of 10 K min^{-1} using purified and dry nitrogen (100 ml/min) as carrier gas and amount of NH_3 in the gas stream was continuously monitored by thermal conductivity detector to yield the TPD spectrum. The concentration of NH_3 in the exit gas was estimated by titration against standard HCl (0.01 N) and the number of NH_3 molecules per unit cell (NH_3/UC) desorbed were calculated.

Procedure B

The deammoniated catalyst (obtained by following the procedure A) was further activated in vacuum at 673 K for 4 hrs and cooled to ambient temperature. The catalyst was saturated with a known volume of pure ammonia gas and the amount of NH_3 adsorbed was determined volumetrically. Then, physically absorbed NH_3 was removed by evacuating at ambient temperature and the sample was resaturated with NH_3 gas at same pressure as before. The quantity of NH_3 adsorbed in the second stage was determined. The difference in the NH_3 adsorbed on fresh catalyst and that on pre-chemisorbed catalyst was taken as chemisorbed ammonia.

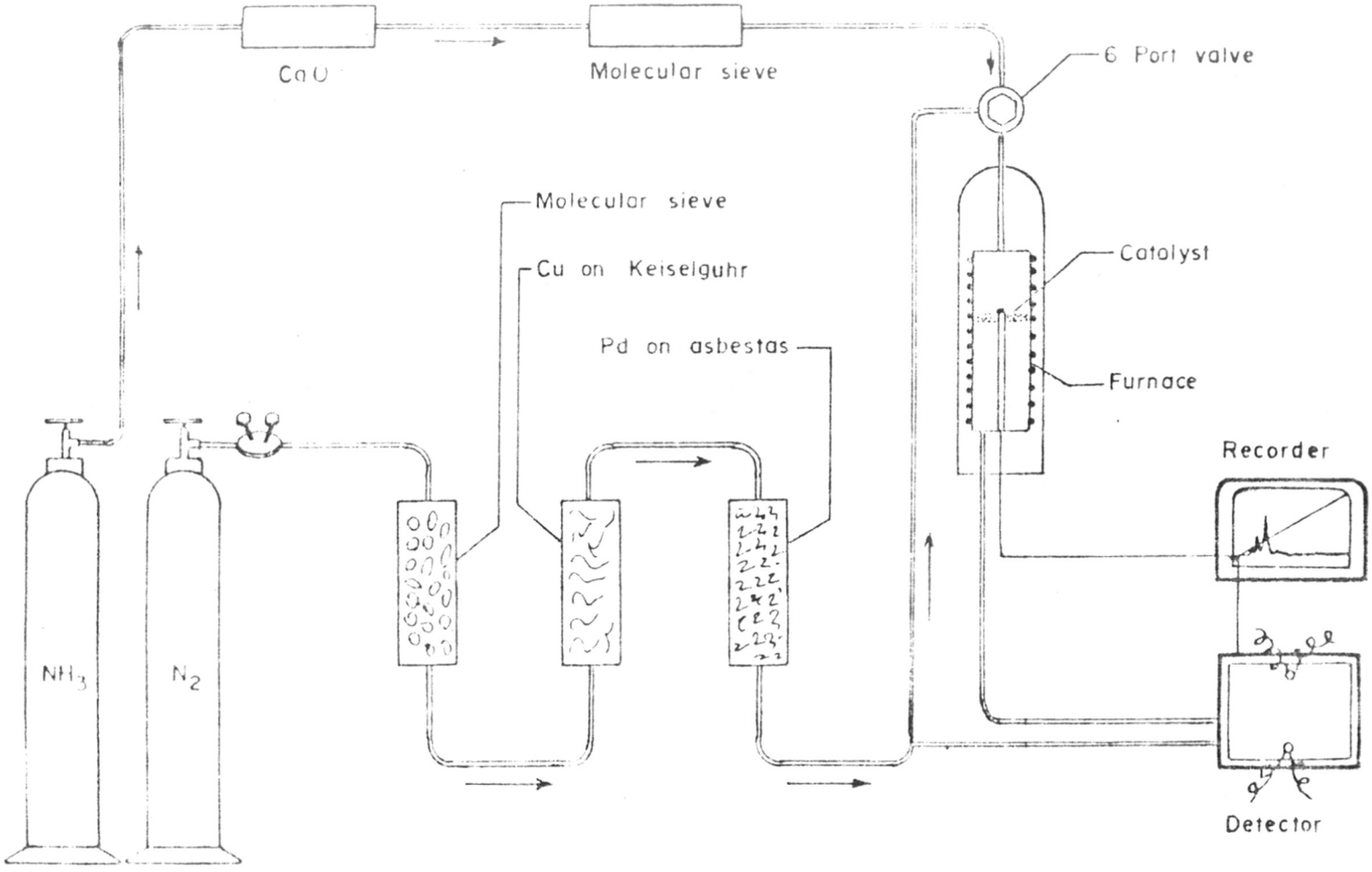

FIG. 2.16. SCHEMATIC DIAGRAM OF TPD UNIT

Then the catalyst sample was connected to the online gas chromatograph and heated at a linear rate of 10 K min^{-1}, as described in procedure A.

The desorption of chemisorbed NH_3 was continuously monitored by thermal conductivity detector to yield the TPD spectrum.

(i) Deammoniation of NH_4ZSM-5

The NH_4ZSM-5 zeolites of varying SiO_2/Al_2O_3 ratios (samples 1-5, Table 2.8) were obtained by ion exchange of NaZSM-5 with NH_4Cl solution (see Section 2.2). The TG was performed under similar conditions as described in the earlier section (2.3D) and the TPD was performed following procedure A.

Curve 1 in Fig. 2.17 shows weight loss obtained from thermogravimetry as a function of temperature. It can be seen that the TG thermogram exhibits three stages, 298-573 K, 573-823 K and above 873 K. The first two stages have been attributed to the loss of zeolitic water and to the simultaneous removal of residual water and NH_3 released during decomposition of NH_4ZSM-5 to form HZSM-5. The reversible deammoniation process can be represented as follows[85]:

TABLE - 2.8

The concentration of surface acid sites

Sample	SiO_2/Al_2O_3 molar ratio	Al/UC	Calcination temp. (K)	TM (K)	Acid sites/unit cell			
					Weak + medium	Strong	Total	Strong*
1. HZSM-5	36	5.02	823	680	8.81	3.34	12.15	3.02
2. HZSM-5	86	2.28	823	673	6.68	1.60	8.28	1.58
3. HZSM-5	144	1.31	823	665	5.72	0.92	6.44	1.01
4. HZSM-5	165	1.09	823	660.5	4.76	0.89	5.65	0.86
5. HZSM-5	320	0.64	823	635.5	1.84	0.45	2.29	0.48
6. HZSM-5	86	2.28	923	670.0	5.02	0.96	5.98	-
7. HZSM-5	86	2.28	973	670.0	4.28	0.81	5.09	-
8. HZSM-5	86	2.28	1273	-	0.60	-	-	-

TM = temperature for peak maximum for strong peak.

* Acid sites determined from the analysis of NH_3 gas evolved during temperature programmed decomposition of NH_4 form of the ZSM-5 samples.

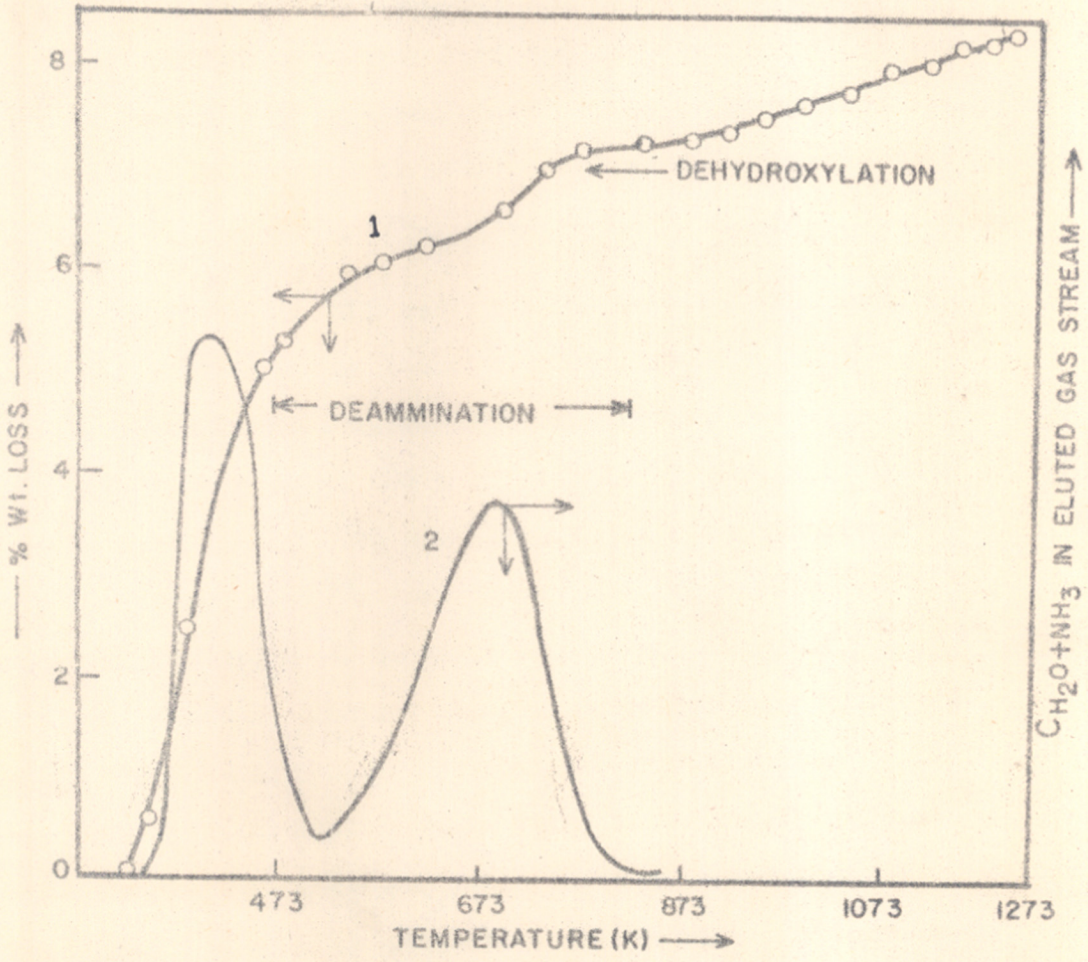

FIG.2.17. TG AND TPD CURVES OF NH_4ZSM-5 ZEOLITE (SiO_2/Al_2O_3=86), 1) TG AND 2) TPD

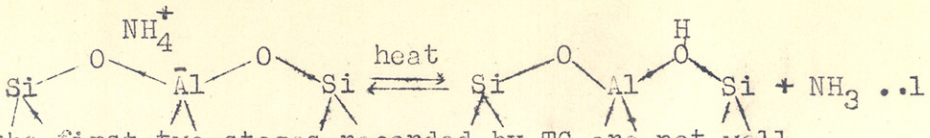

Although the first two stages recorded by TG are not well separated, these can be recognized in the two distinct TPD peaks (Curve 2, Fig. 2.7). The portion in the TG curve above 873 K shows continuous weight loss due to dehydroxylation which leads to conversion of Brönsted acid sites to Lewis acid sites as shown below by Hall et al[85] and Ward[86].

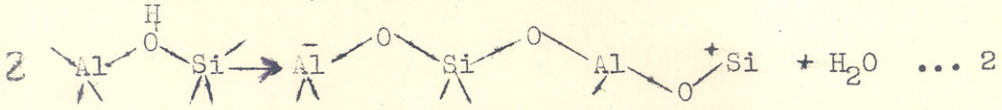

A part of the TPD curve in the temperature range 473-823 K for the samples 1-5 with different SiO_2/Al_2O_3 ratios is shown in Fig. 2.18. The temperature for peak maximum (TM) observed at 693 K for sample 1 (SiO_2/Al_2O_3 = 36, Table 2.8) agrees with that reported for an identical sample by Topsøe et al[44]. We observed a progressive decrease in the value of TM with increasing SiO_2/Al_2O_3 ratio from 36-320. Similar results have also been obtained when the TPD of chemisorbed ammonia desorbed from the corresponding protonated samples was carried out. Auroux et al[87] observed an increase in the heat of adsorption of ammonia as the aluminium content in the sample was increased from 1.5 to 4.8 (Al/UC). Further, the acid strength should increase with increase in the aluminium content in the zeolite samples, which would reflect in an increase

in the value of TM for the deammoniation of NH_4ZSM-5 measured by temperature programmed decomposition or TPD of NH_3 adsorbed on protonated samples.

The area under the peak (Fig. 2.18) increases linearly with increasing aluminium atoms in the zeolite framework. The number of ammonia molecules per unit cell (NH_3/UC) liberated for the various samples (samples 1-5, Table 2.8) has been plotted against the number of Al atoms per unit cell (Al/UC) in Fig. 2.19. Values obtained from the literature relevant to the present work are found to fit very well in the plot, further confirming that the number of acid sites increases linearly with increasing the number of aluminium atoms in the ZSM-5 framework. However, the ratio of the ammonia molecule to framework aluminium is 1:0.8 instead of the expected stoichiometric ratio 1:1. This lower ratio may be attributed to the fact that only part of the total aluminium atoms are present in the framework.

(ii) Influence of calcination temperature

Samples 6-8 (Table 2.8) were obtained from sample 2 by calcination at 923, 973 and 1273 K respectively, in static air for 8 hours. After thermal treatment the samples were cooled to room temperature and kept ovdr saturated NH_4Cl solution for about 24 hours for hydration.

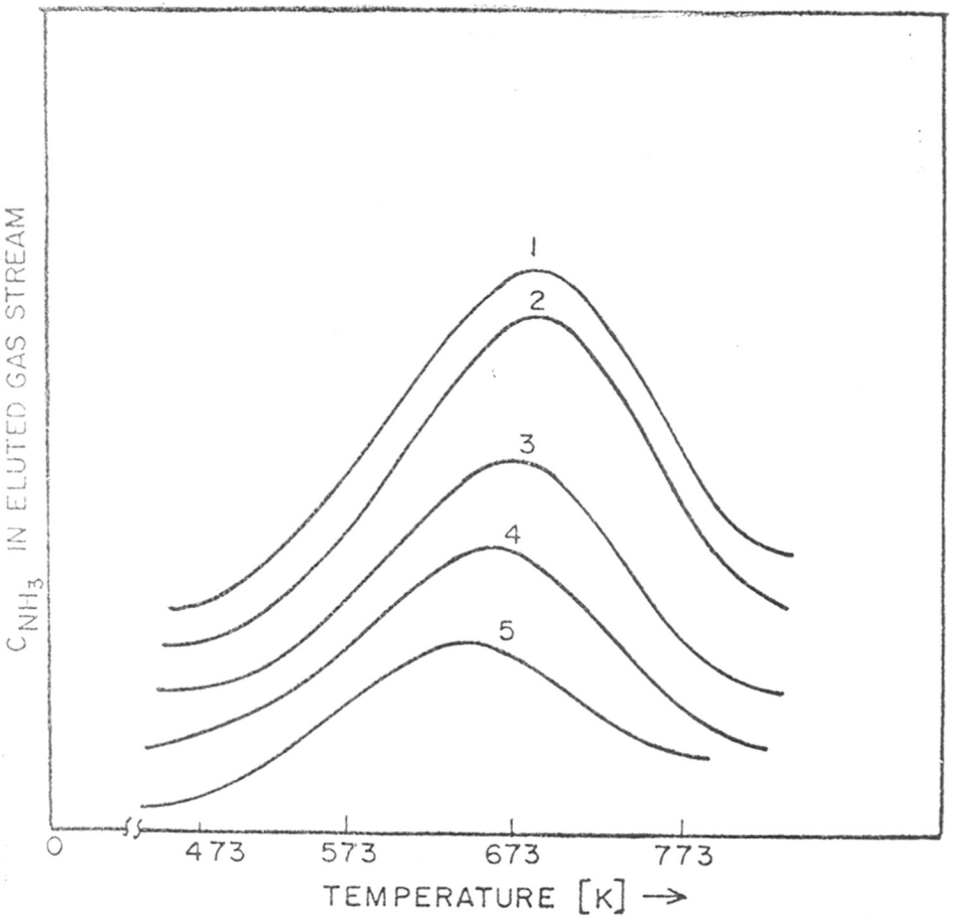

FIG.2.18. TPD CHROMATOGRAMS OF NH_4ZSM-5 ZEOLITES. NOS 1-5 REFER TO SiO_2/Al_2O_3 RATIOS, 36, 86, 144, 165 AND 320 RESPECTIVELY.

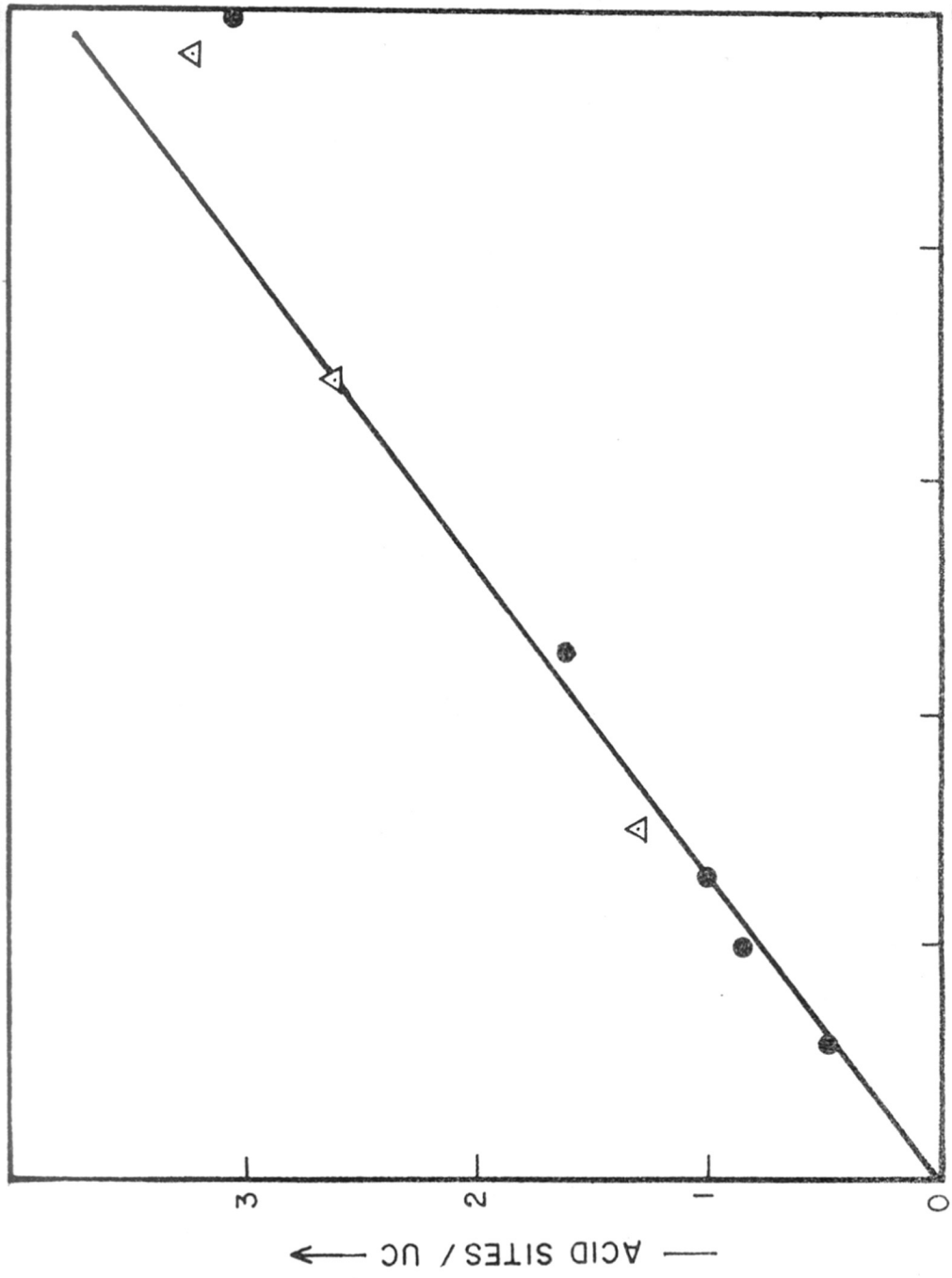

FIG.2.19. VARIATION OF ACID SITES WITH ALUMINIUM CONCENTRATION IN ZSM-5 ZEOLITES.
(● THIS STUDY, △ REF.88)

The TPD curves for these samples are shown in Fig. 2.20 (Curves 6-8). The three peaks show TM at 373-390, 420-470 and 620-677 K corresponding to weak, medium and strong acid sites respectively. The absolute concentration of these acid sites were calculated as follows: The total amount of chemisorbed ammonia was determined by volumetric adsorption method. Knowing the detector response factor (for NH_3) and area under the individual peak, the number of ammonia molecules corresponding to each TPD peak was evaluated. The concentration of these sites are summarized in Table 2.8 (Samples 6-8). The results show that the concentration of acid sites depends upon the calcination temperature. Upon increasing calcination temperature from 823 to 1273 K, there is a marked decrease in the peak intensity and total number of these sites. In the case of sample calcined at 1273 K, the adsorption peaks turned vestigial, showing a considerable reduction of its weak and medium acid sites and absence of strong acid sites. This observation is consistent with gradual decrease in the number of strong Brönsted acid sites with increasing calcination temperature from 2.6 (823 K) to 1.8 (1075 K) per unit cell[88].

The x-ray diffraction pattern showed 80% crystallinity (Fig. 2.21) after heating the sample at 1273 K. Moreover, HZSM-5 calcined at 1273 K did not exhibit any

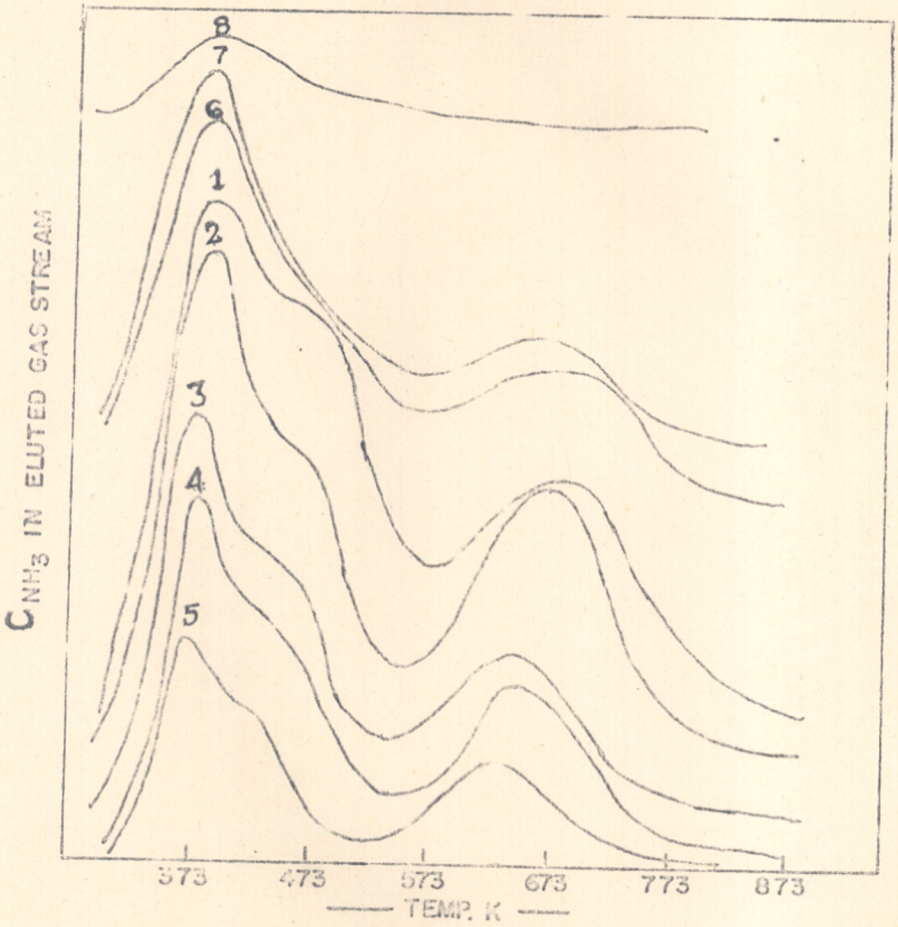

FIG.2.20. THE TEMPERATURE PROGRAMMED DESORPTION OF NH_3 FROM HZSM-5 ZEOLITES. CURVES NOS 1-5 REFER TO THE SiO_2/Al_2O_3 RATIOS 36,86,144,165,320 AND CURVES 6-8 REFER TO THE SAMPLE 2 CALCINED AT 923,983 AND 1273 K RESPECTIVELY.

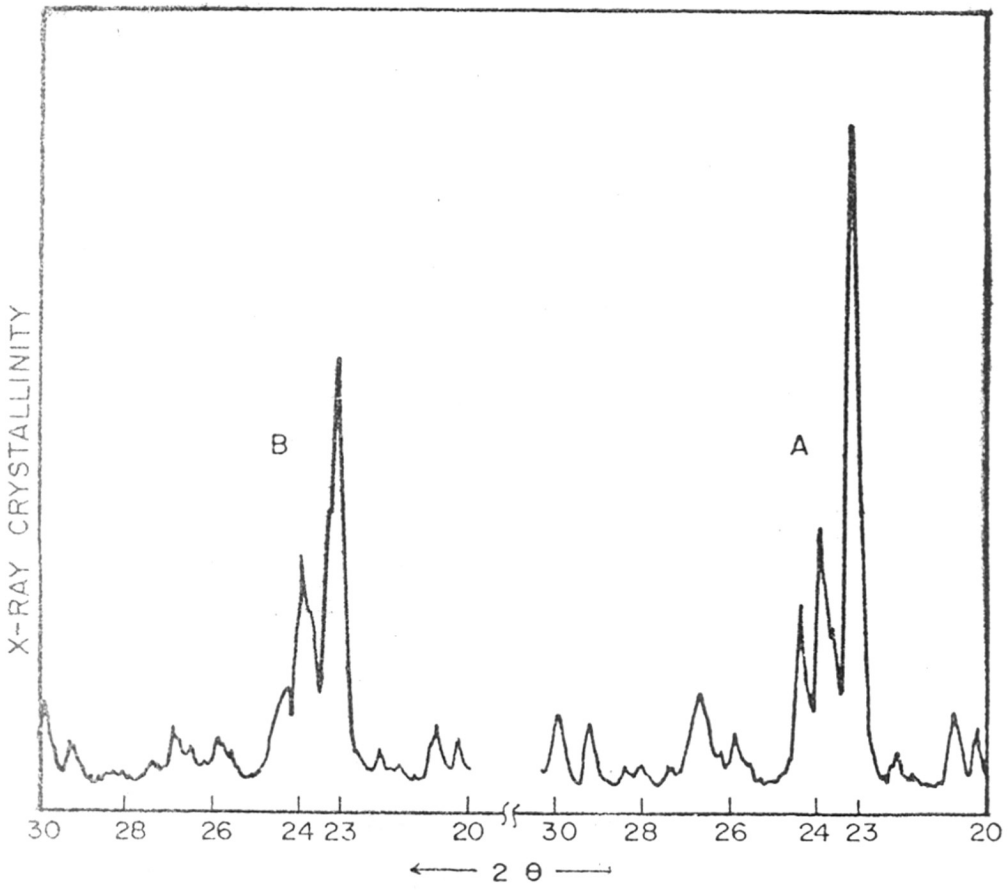

FIG.2.21. X-RAY DIFFRACTOGRAMS OF HZSM-5 ZEOLITE SiO_2/Al_2O_3 =86: CALCINED AT A)823K AND B) 1273K.

dealumination. Therefore, the loss of acid sites in these samples may be attributed to the conversion of Brönsted acid sites to Lewis acid sites due to dehydroxylation as described by Hall et al[85].

Benesi[11] reported that the hydrogen free form (Lewis acid) of mordenite and Y-faujasite regained their original activity by addition of water and suggested that acid sites in these zeolites are interconvertible. The present results show that the rehydration of the ZSM-5 samples calcined at 923-1273 did not regain the strong acid sites. Hence, we may infer that the strong Brönsted acid sites are converted to Lewis acid sites by an irreversible process.

(iii) Effect of SiO_2/Al_2O_3 ratio

The TPD of the HZSM-5 samples (Samples 1-5, Table 2.8) was performed following the procedure B, as described earlier. The TPD profiles are shown in Fig. 2.20 (Curves 1-5). It can be seen that the intensity of the three adsorption peaks and strength of binding are strongly dependent on the SiO_2/Al_2O_3 ratio. There is a progressive decrease in the intensity of the peaks as the SiO_2/Al_2O_3 ratio increases from 36-320 (Curves 1-5). There is also a shift in TM towards lower temperature, due to increase in the SiO_2/Al_2O_3 ratio as observed earlier in deammoniation of NH_4ZSM-5.

Jacobs et al[81] reported that a pure HZSM-5 zeolite contains only one type of hydroxyl group characterized by a band at 3600 cm^{-1}. Other workers[44,82] have shown three hydroxyl bands at 3600, 3650 and 3720 cm^{-1}. The band at 3720 cm^{-1} has been assigned to extra framework aluminium occluded in the pores[44,81]. The ir spectra of our samples shown in Fig. 2.22 exhibit two major absorbance bands at 3600 cm^{-1} and 3720 cm^{-1} followed by a small band at 3660 cm^{-1}. The latter two are OH bands arising from aluminium atoms outside the framework and terminal silicons.

The TPD results obtained in the present study are consistent with those reported by Topsøe et al[44] for a similar material. The TPD peaks at 373 K and 430-470 K are attributed to adsorptionof NH_3 on the loosely bonded hydroxyl groups attached to terminal silicon atoms and some occluded aluminium in the amorphous material. The peak at 677 K (strong) is assigned to the hydroxyl group attached to the framework aluminium atom which corresponds to ir band at 3600 cm^{-1}. These sites (weak, medium and strong) are designated as α, β and γ sites by Topsøe et al[44].

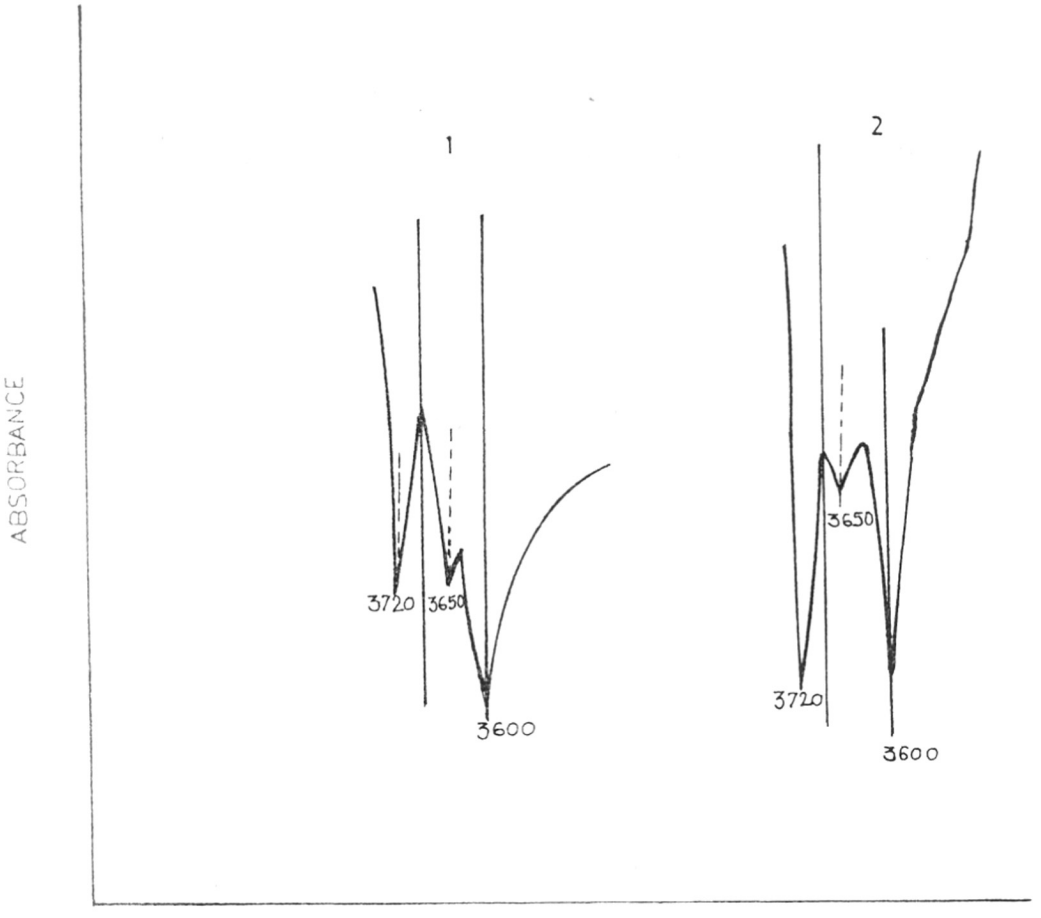

FIG. 2.22. INFRARED SPECTRA OF HZSM-5. NUMBERS 1 AND 2 FOR SAMPLES OF SiO_2 / Al_2O_3 RATIO 36 AND 86 RESPECTIVELY.

(iv) Effect of impregnation with P, B, Mg, etc.

Fig. 2.23 (Curves 1-5) represent the TPD profiles of HZSM-5 and modified NiHZSM-5 (1% wt.), BHZSM-5 (3% B) and PMgHZSM-5 and PHZSM-5 (8% P) respectively. The number of acid sites (Table 2.9) and corresponding values of TM show a decrease upon incorporation of these additives indicating interaction with the proton sites associated with framework aluminium atoms. However, the relative decrease in the total number of acid sites in case of magnesium phosphorous and boron impregnated samples is larger than that in the nickel impregnated sample. It is suggested by Kaeding and Butter[77] that elemental phosphorous binds to the zeolite framework through oxygen as indicated

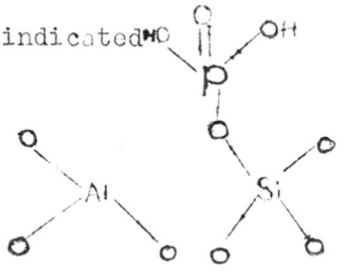

They have also reported the presence of phosphorous in the ZSM-5 channel which neutralises the strong acid sites and increases the acid sites which are weaker in strength compared to those in unmodified zeolites. However, all the acid sites determined from the TPD (Table 2.8) decrease progressively with increasing phosphorous concentration, in agreement with the findings of Vedrine et al.[89]

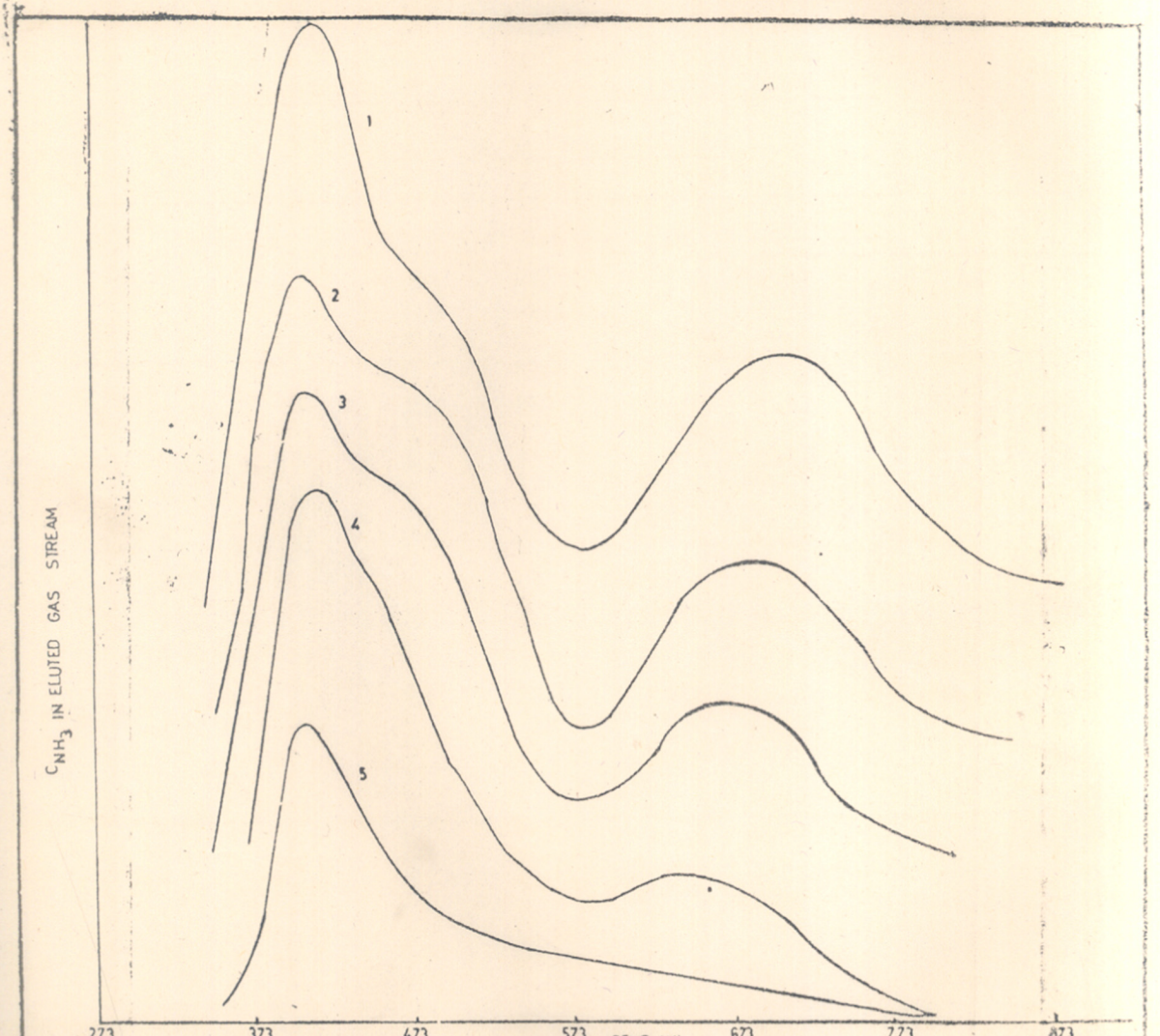

FIG. 2-23- TPD CHROMATOGRAMS OF HZSM-5 AND MODIFIED HZSM-5 ZEOLITES: 1) HZSM-5 2) NiHZSM-5 3) PMg HZSM-5 4) BHZSM-5 5) PHZSM-5

TABLE - 2.9

The concentration of surface acid sites in modified HZSM-5 zeolites

S. No.	Sample	SiO_2/Al_2O_3 molar ratio	Calcination temp. (K)	TM (K)	Acid sites/unit cell		
					Weak + medium	Strong	Total
1.	HZSM-5	36	823	680	8.81	3.34	12.15
2.	NiHZSM-5 (1.1% Ni)	36	823	673	9.15	2.71	11.85
3.	P-MgHZSM-5 (2% P, 5% Mg)	36	823	670	6.42	1.14	7.56
4.	BHZSM-5 (3% B)	36	823	650	4.12	1.50	5.62
5.	PHZSM-5 (8% P)	36	823	600	3.12	0.64	3.76

In NiHZSM-5 (1% Ni) zeolite, the area under the strong and medium peak increased relative to that in the parent HZSM-5 zeolite (Fig. 2.22, Curves 1-2). The value TM also shifted to lower side indicating redistribution of acid sites in agreement with that reported[90-92] for Fe and Co impregnated HZSM-5 zeolites. During reduction of the impregnated transition metal ions, the metal ions migrate in the channel and interact with strong protonic sites as described below.

In the NiHZSM-5, even after reduction at 873 K in presence of hydrogen, XPS shows only Ni^{2+} which indicates the absence of metal crystallite Ni^{o} (please see under XPS of NiZSM). Hence, the reduction of the number and strength of the strong acid sites is attributed to the interaction of the Ni^{2+} species with strong protonic sites.

(I) XPS of NiHZSM-5

Nickel, palladium and platinum supported catalysts are widely used for the hydrogenation reactions[93]. Moreover, a small amount of metal is usually incorporated in commercial zeolite catalysts for maintaining stable activity and for keeping the surface clean during the reaction. Minachev et al[94] had

found that by treating a zeolite containing nickel ion with hydrogen at elevated temperature, metallic nickel was formed as shown below

$$2(AlO_4)^- + Ni^{2+} + H_2 \longrightarrow 2Ni^{o} + 2(AlO_4)^- + 2H^+$$

However, Badrinarayan et al[95] reported that nickel (Ni^{o}) species were not formed over HZSM-5 after long reduction with hydrogen.

In present study, attempt has been made to examine the nickel species formed after reduction of NiHZSM-5 with hydrogen at different temperatures from 723 to 823 K by using highly surface sensitive XPS technique.

The samples designated a, b, c and d contain 2.22% wt. nickel (Section 2.2). About 1-2 grams of a sample (10-20 mesh particles) was loaded in silica reactor and dehydrated at 823 K in nitrogen (sample 'a') and then reduced in purified and dry hydrogen at 723, (Sample b), 823 (sample c) and 873 K (sample d) respectively. The samples were cooled to room temperature in flowing hydrogdn. The XPS measurements were performed with a commercial XPS spectrometer (Vacuum Generator ESCA 3MK II). MgK_{α} x-ray source ($h\nu$ = 1253 ev) was used. The slit width was 4 mm and analyzer energy 50 ev.

The XPS parameters of the samples a, b, c and d are summarized in the Table 2.10. A binding energy of 103.3 ev for the Si_{2p} level was used as internal standard for all the samples. The binding energy (BE) and FWHM (full width at half maximum) values of O_{1s}, Ni_{2p} and Si_{2p} determined from the spectra are given in Table 2.10. The surface Si/Ni atom ratios were calculated by the use of Wagner's[96] sensitivity factors,

$$\frac{Si}{Ni} = \frac{I_{Si}}{I_{Ni}} \times \frac{\sigma N_i}{\sigma Si} \times \frac{(E_{kSi})^{1/2}}{(E_{kNi})^{1/2}}$$

where I_{Si} and I_{Ni} are the heights of Si_{2p} and Ni_{2p} peaks respectively. The σ and E_k values refer to the sensitivity of detection[96] and the kinetic energy of photoelectron respectively.

Both , BE and FWHM for the Ni_{2p} in the four samples are constant (855.9 and 5.6 ev) within experimental error, which implies that the same species of the nickel must be present in all the samples. Moreover, the presence of Ni^{o} in the reduced NiZSM-5 samples can be ruled out since the BE and FWHV values for Ni^{o} are 852.6 and 2.0 ev respectively, which are different from those for samples a, b and c (Table 2.10). In other words, the nickel ions that were present in the fresh, calcined catalyst sample 'a' had not undergone any major chemical modification (like

TABLE - 2.10

XPS parameters of NiHZSM-5 zeolite

Sample	Reduction temp.(K)	Si_{2p} B.E.	Si_{2p} FWHM	O_{1s} B.E.	O_{1s} FWHM	Ni_{2p} B.E.	Ni_{2p} FWHM	Si/Ni	Ref.
a	Fresh	103.3	4.8	531.2	3.4	856.2	5.8	0.33	This study.
b	723	103.3	4.8	531.1	3.1	856.3	5.6	0.27	This study.
c	823	103.3	4.8	531.3	3.0	856.1	5.6	0.22	This study.
d	873	103.3	4.8	531.2	3.2	856.1	5.6	0.19	This study.
NiHZSM-5	773	103.2	2.4	532.5	2.4	856.5	4.3	-	95
Ni^{o}						852.6	2.0		98
NiO						854.6	4.2	-	98
Ni_2O_3						855.8		-	97
$Ni(OH)_2$						855.6		-	97
NiNaY						856.9	4.0		99
$Ni-Al_2O_3$ (7% Ni)						856.2	3.6	-	100

reduction to Ni^{o}) during reduction at higher temperature. The Ni_{2p} spectra for the four samples are similar. The possibility of NiO being present in the samples may also be ruled out since the BE and FWHM for NiO are 854.6 and 2 ev respectively. The binding energy of the present samples matches with that of $Ni(OH)_2$. Kim et al[97] reported that even under argon bombardment, $Ni(OH)_2$ is not reduced. Therefore, the Ni^{2+} species coordinated with OH groups may be present in the samples. The peak intensities for Ni_{2p} increases with increasing reduction temperature (Fig. 2.24) This may be due to some nickel species sticking out from the channels at high temperature.

C O N C L U S I O N S

(1) The variation in the SiO_2/Al_2O_3 ratios does not influence the XRD and IR patterns of the ZSM-5 zeolites significantly except the intensities of the XRD peaks.

(2) The DTA/TG analyses can be used to estimate the thermal stability as well as the number of acid sites and their distribution in the catalyst samples.

(3) The sorption of water and hydrocarbons showed that with increase in the SiO_2/Al_2O_3 ratios, the zeolites tend to become more hydrophobic. The uptake of benzene, para-xylene and toluene did not significantly vary with the SiO_2/Al_2O_3 ratio, whereas the sorption of cyclohexane,

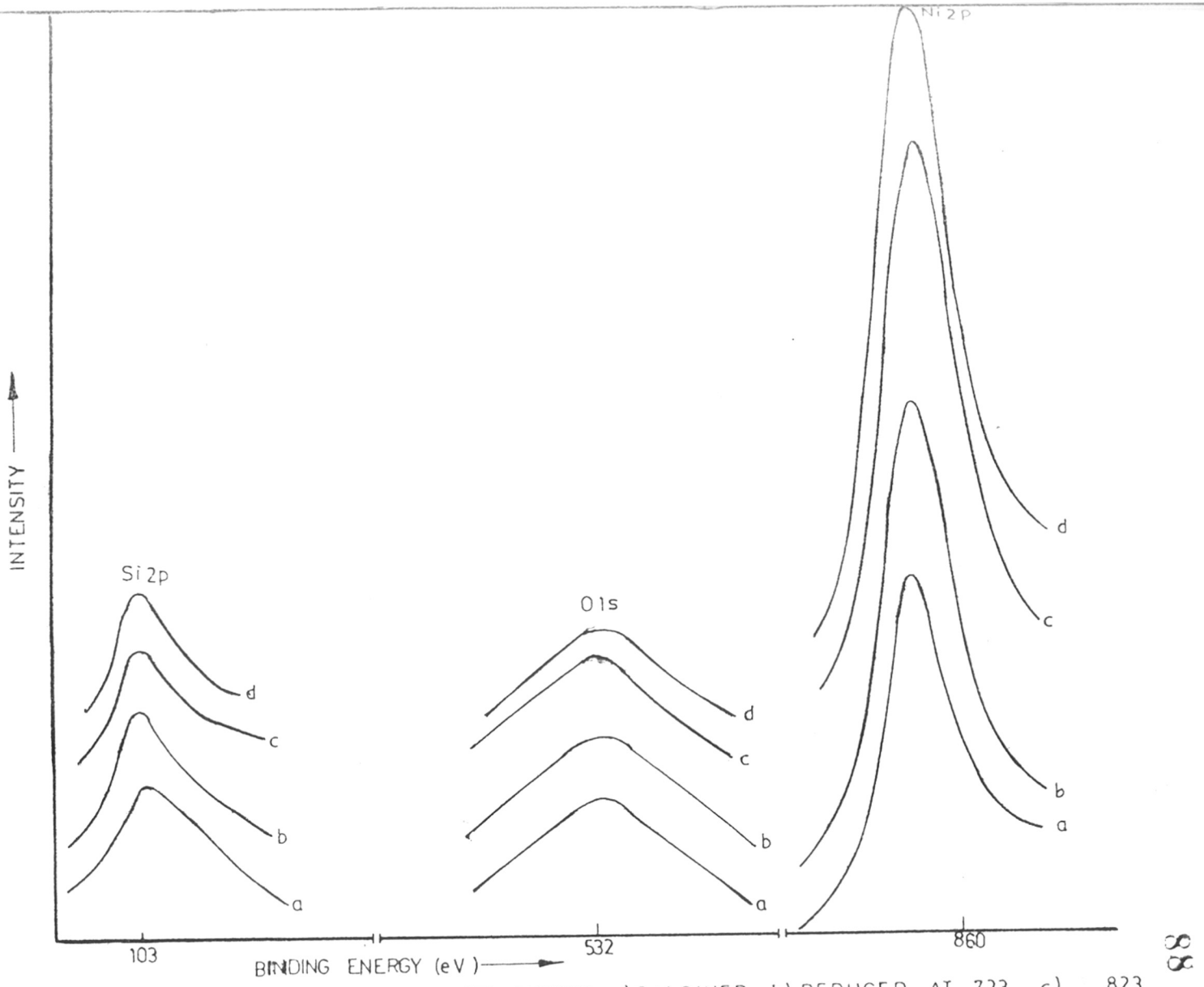

FIG. 2·24 XPS SPECTRA OF NiHZSM-5 ZEOLITE CURVES a) CALCINED, b) REDUCED AT 723, c) 823, d) 873 K RESPECTIVELY

orthoxylene and 1,2,4 trimethylbenzene was considerably reduced.

(4) The incorporation of modifiers like B, P, Mg, reduced the diffusivity and sorption capacity of the HZSM-5 catalysts.

(5) The TPD of NH_3 leads to the estimation of the number and strength of acid site distribution in the catalyst sample and shows a good correlation with the activity of the catalyst samples.

(6) It may be concluded from the above results that highest number of strong acid sites (Y sites) are formed when the NH_4ZSM-5 or HZSM-5 is calcined at 823 to 873 K.

(7) The decomposition of NH_4ZSM-5 monitored by TPD can be used to determine the number of strong acid sites and the ion exchange capacity of the ZSM-5 zeolite.

(8) The incorporation of nickel in the HZSM-5 zeolite may be creating the sites of lower acid strength.

CHAPTER III
TOLUENE DISPROPORTIONATION

3.1. INTRODUCTION

Toluene disproportionation to benzene and xylenes was first observed by Anschutz[103] (1884) by refluxing toluene at atmospheric pressure with aluminium chloride as a catalyst. Toluene disproportionation is important in the petrochemical industry since it provides an alternative route for para-xylene production which is used for the fibre production. Extensive research on the development of an active catalyst and process has been carried out[104-106]. The catalysts used for the toluene disproportionation can be divided into three categories, namely (1) Friedel-Crafts[107-110], (2) amorphous silica-alumina[111,112], and (3) synthetic zeolites[113].

In contrast to the first two catalysts, synthetic zeolites are known to be superior in the toluene disproportionation reaction. Mordenite[16] and zeolite HY[114] possess high initial activity for the disproportionation of toluene. However, due to predominance of toluene dealkylation and cracking reaction these catalysts show poor selectivity. Apart from the low selectivity, the activity of these catalysts falls within a few hours due to the formation of carbonaceous deposit.

Recent introduction of ZSM-5 zeolite has provided a novel route for the selective disproportionation of toluene[115,116a]. The architecture and the size of the channel system which matches with the size of benzene, toluene and para xylene molecules is one of the factors for the high selectivity in this reaction. Kaeding et al[28] have reported selective disproportionation of toluene into one mole of benzene and one mole of para xylene with ZSM-5 based catalysts modified with boron, magnesium and phosphorous.

3.2. EXPERIMENTAL

The toluene disproportionation reactions were carried out at atmospheric pressure using a fixed bed, down flow integral reactor (Fig. 3.1). The zeolite, HZSM-5 (1-2 grams, 10-20 mesh particles) was loaded in silica glass reactor, and was first activated in a dry air at 823-873 K for 5 hours and then cooled to reaction temperature in the flow of dry nitrogen. Toluene (99.5% BDH) and H_2 (IOL, Bombay), were mixed in a preheater. Toluene was fed by a metering pump (Model 352, Sage Instruments), vapourised in a preheater assembly and then passed through catalyst bed. The product was analysed by gas chromatography (HP Model 5840A) using 5% diisodecyl phthalate and 5%

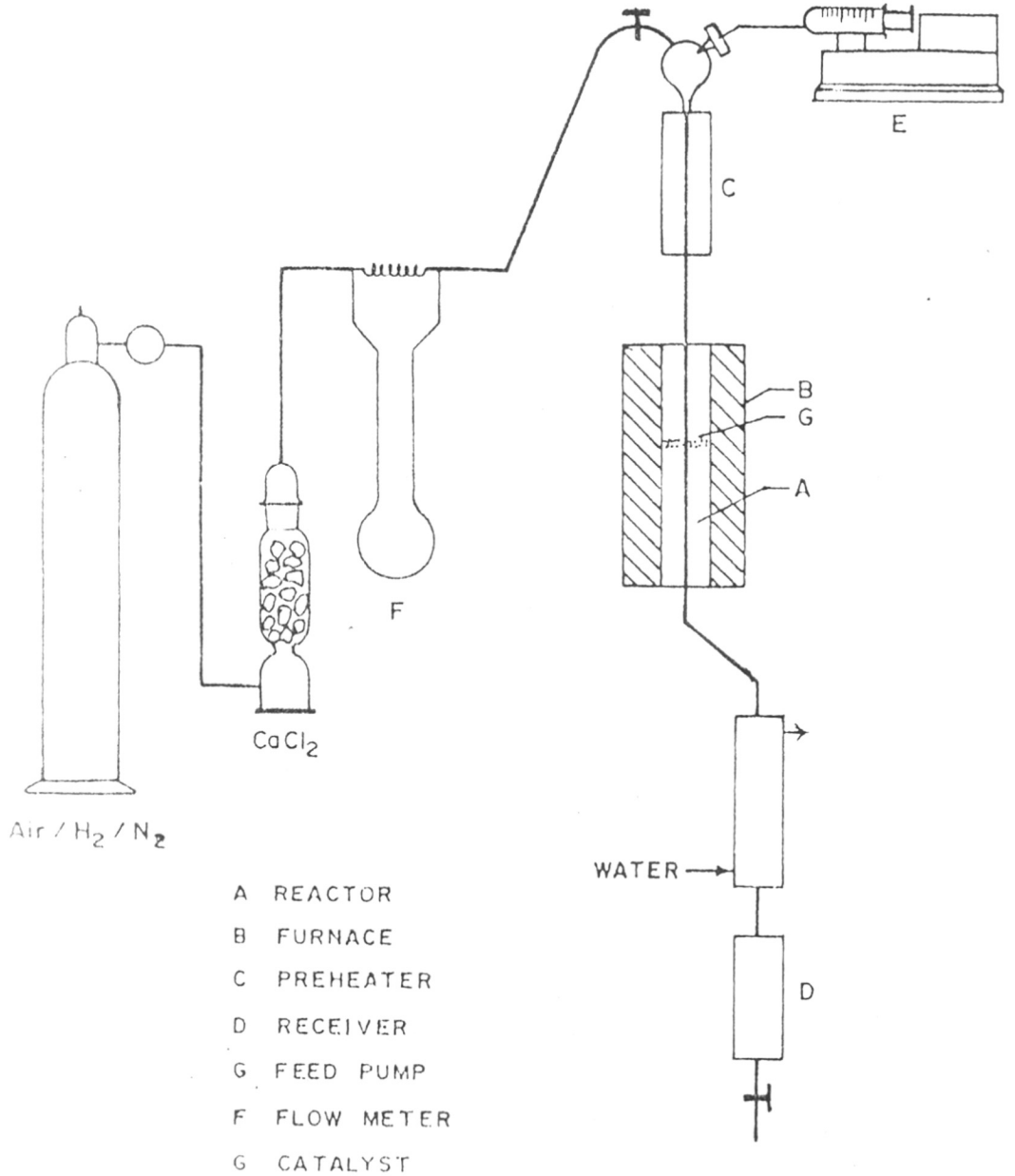

FIG. 3.1. SILICA REACTOR USED FOR CATALYTIC REACTIONS AT ATMOSPHERIC PRESSURE.

Bentone-34 on chromosorb W column (2 meters). A typical chromatogram is shown in Fig. 3.2. The reproducibility of the data was about ± 0.3%.

High pressure reactions were carried out in a "Catatest" unit (Geomechanique Model B, France), shown in Fig. 3.3. The stainless steel reactor was used both as a preheater and a reactor. The reactor had an internal diameter (i.d.) of 1.8 cms, with centered thermowell of 0.6 cm. diameter. The reactor was provided with four thermocouples for measuring temperatures at four different points in the reactor. The catalyst in the form of extrudates (ZSM-5 + binder) was loaded in the middle of the reactor and top as well as bottom portions were filled with inert alumina balls of 2-3 mm diameter. The catalyst was activated following the procedure described above for the atmospheric/pressure reactions. The toluene was fed by a metering pump into the vapouriser and passed through the catalyst bed. The reaction products from the reactor were cooled in chilled water condenser and collected in a high pressure separator where hydrogen and liquid products were separated. The products were collected periodically and analysed by gas chromatography as described above.

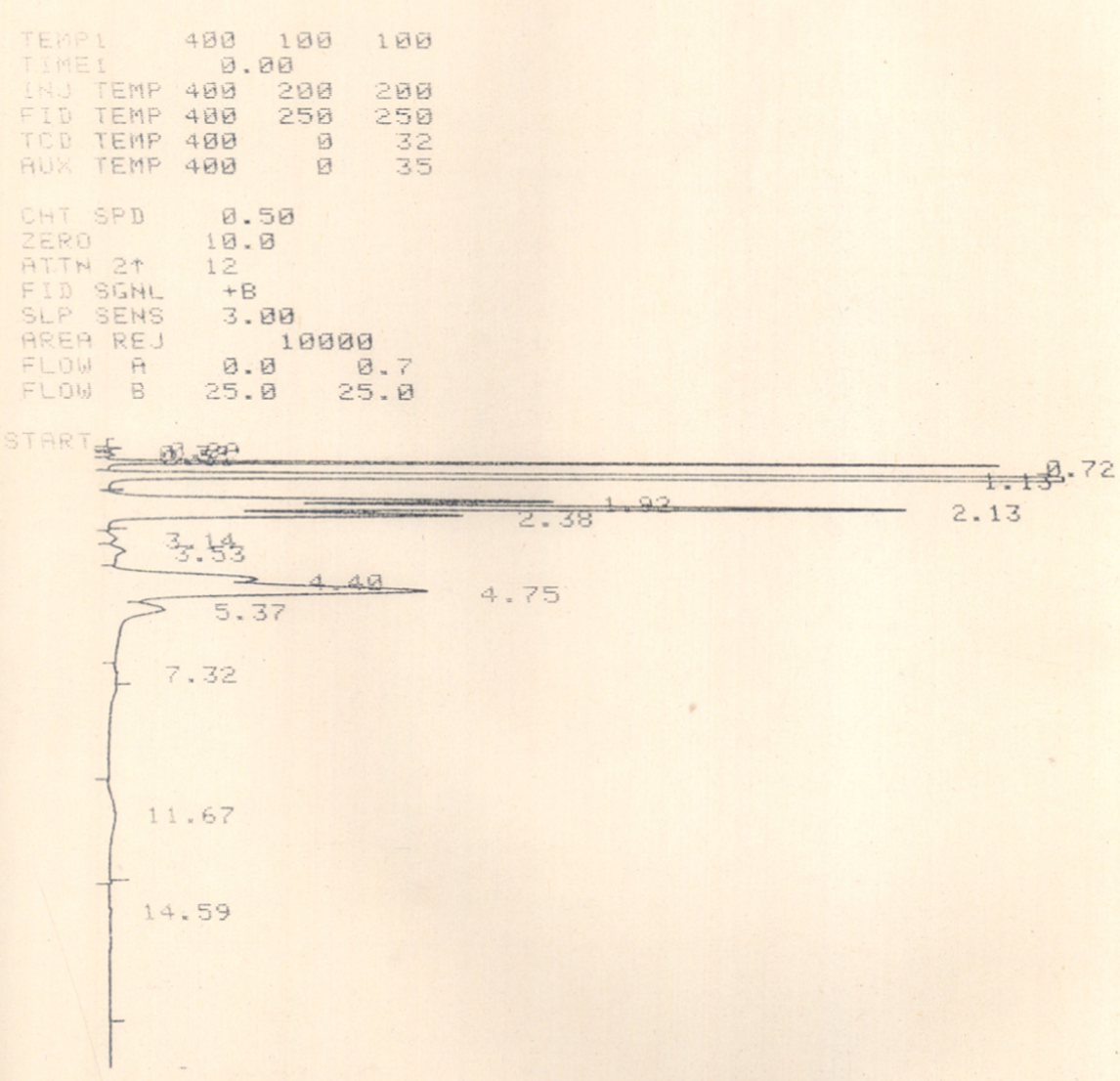

FIG.3.2. A TYPICAL CHROMATOGRAM OBTAINED BY ANALYSIS OF THE REACTION PRODUCTS IN THE DISPROPORTIONATION/TRANSALKYLATION REACTION OF TOLUENE. THE MAIN PRODUCTS ARE BENZENE(RETENTION TIME, t_r=0.72),TOLUENE(t_r=1.13)XYLENE(t_r=1.92-2.38),ETHYL TOLUENES (t_r=3.12-3.53)AND TRIMETHYLBENZENE(t_r=4.40-5.37).

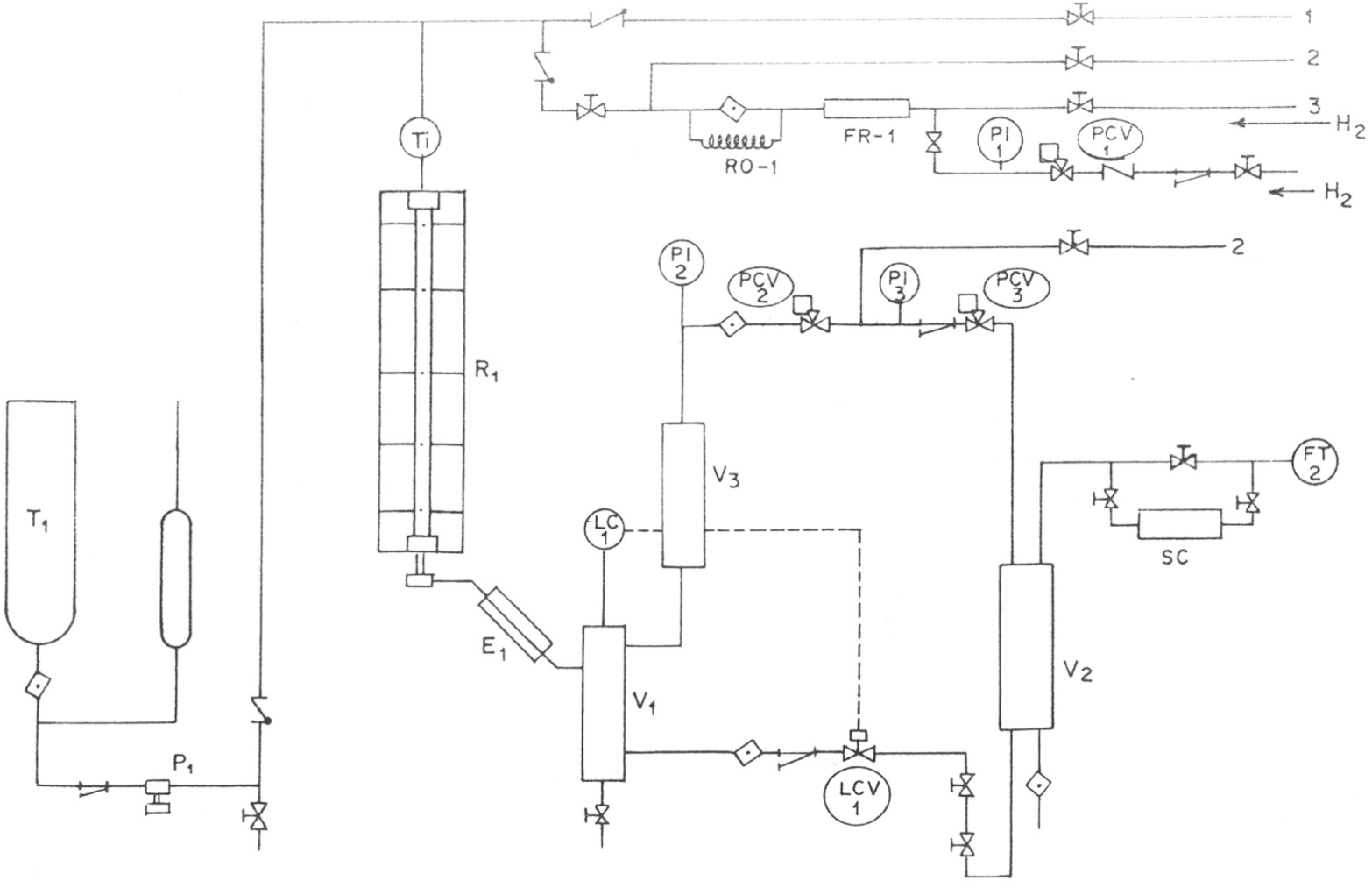

FIG. 3.3. CATATEST UNIT USED FOR HIGH PRESSURE REACTIONS.

DESCRIPTION OF THE PARTS OF CATATEST UNIT

T_1	-	Feed Reservoir.
P_1	-	Feed pump.
R_1	-	Reactor.
E_1	-	Condenser.
V_1	-	High Pressure Separator.
V_2	-	Product Separator.
V_3	-	Uncondensed Gas.
LC	-	Level Controller.
LCV	-	Level Controlling Valve.
TC	-	Thermocouple.
PCV	-	Pressure Control Valve.
PI	-	Pressure Indicator.
SC	-	Gas Sampling Column.
FT	-	Wet Flow Meter.
RO	-	Capillary.
RI	-	Gas Flow Meter.
	-	One-way Valve.
TI	-	Temperature Indicator.
RC	-	Recycle.

3.3. RESULTSAND DISCUSSION

(A) Reaction of toluene on the catalyst surface

The reactions which can occur along with toluene disproportionation are illustrated in Fig. 3.4. Toluene disproportionation (which yields benzene and xylenes) and toluene dealkylation (benzene and methane) are prominent reactions observed over HZSM-5 zeolites. However, the disproportionation of xylenes to toluene and trimethylbenzenes occurs to a smaller extent because of the restrictions on the formation of transition state in the ZSM-5 cavities as illustrated by Derouane[26].

(B) Effect of calcination temperature

The zeolite HZSM-5 which is active for toluene disproportionation reaction is prepared by the thermal decomposition of NH_4ZSM-5. It has been noted previously that the temperature at which NH_4ZSM-5 catalyst is calcined has a significant influence on the toluene disproportionation activity. In fact, it is a key step in converting NH_4ZSM-5 to catalytically active HZSM-5. The conversions obtained at each calcination temperature and the product distribution are summarized in the Table 3.1. Among the NH_4ZSM-5 samples activated between 723 to 1273 K, the zeolite activated at 823 to 873 had the highest toluene conversion activity.

TOLUENE DISPROPORTIONATION

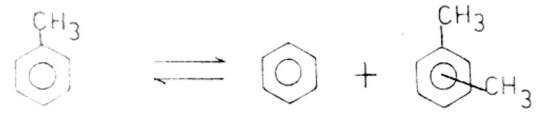

(1)

TOLUENE HYDRODEALKYLATION

(2)

XYLENE DISPROPORTIONATION

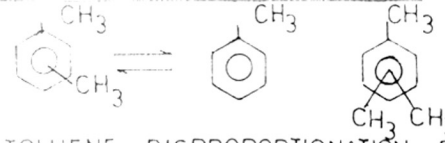

(3)

TOLUENE DISPROPORTIONATION REACTION MECHANISM

a) $HCl + AlCl_3 \rightleftharpoons H^{\oplus}AlCl_4^{\ominus}$ (4)

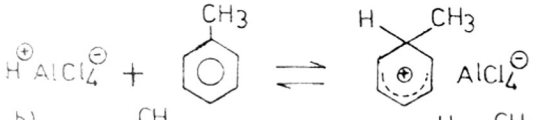

(5)

b)

(6)

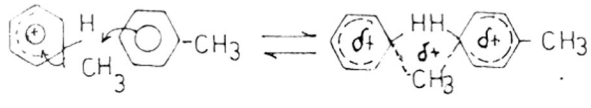

(7)

a)

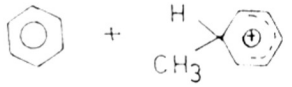

(8)

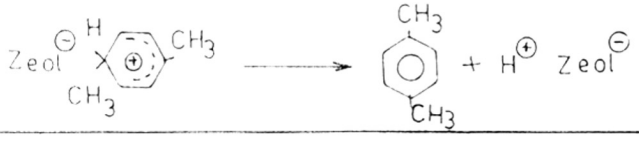

(9)

NET

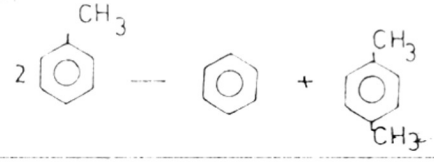

(10)

FIG. 3.4. POSSIBLE REACTIONS DURING TOLUENE DISPROPORTIONATION (1-3)
a) TOLUENE DISPROPORTIONATION MECHANISM ON FRIEDEL-CRAFTS CATALYST.
b) POSTULATED MECHANISM ON SHAPE SELECTIVE ZSM-5 CATALYST[28]

TABLE - 3.1

Influence of calcination temperature of NH_4-ZSM-5 zeolite on toluene disproportionation reaction

Reaction conditions:

Catalyst - NH_4ZSM-5(SiO_2/Al_2O_3 = 86)
Temp. (K) - 723
WHSV($hr.^{-1}$) - 2
H_2/Toluene(mol) - nil
Pressure (bar) - Atmospheric

Calcination Temp. (K)	723	773	823	873	973	1273
Product distribution - % mol.						
Aliphatics	0.29	0.19	0.53	0.92	0.82	0.1
Benzene	19.98	20.64	21.44	20.00	17.88	0.2
Toluene	67.30	63.43	49.64	50.05	57.02	98.72
p-Xylene	2.87	3.45	6.27	6.05	5.14	0.44
m-Xylene	6.53	7.5	11.11	10.94	9.68	0.38
o-Xylene	2.79	3.38	6.03	6.24	5.02	0.19
C_9^+ aromatics	1.40	1.9	4.00	4.20	3.38	-
B/X mol. ratio	1.63	1.44	1.25	1.17	1.29	1.17
% Mol. conversion of toluene	32.70	36.57	50.54	50.00	42.98	1.27

WHSV = Weight hourly space velocity = weight of feed per unit weight of catalyst per hour.
B/X = Benzene to xylene molar ratio.

These observations could be explained in terms of generation of Brönsted acid sites and dehydroxylation of Brönsted acid sites to Lewis sites at higher calcination temperature.

Benesi[11] examined the disproportionation of toluene on mordenite and faujasite based catalysts and found that the maximum activity had attained in both the cases when the zeolite was heated beyond the temperature at which ammonia was completely removed. These results strongly suggest that it is the hydrogen form of the zeolite which is catalytically active. The drop in conversion that occurs in case of each zeolite when hydrogen ions are removed as water shows that hydrogen free form is inactive. He, therefore, concluded that Brönsted rather than Lewis acid sites are seats of activity for toluene disproportionation in the above two zeolites.

The present results with the NH_4ZSM-5 are consistent with the above findings. From the temperature programmed decomposition of NH_4ZSM-5, it was noticed that the evolution of ammonia stops at 823-873 K indicating that NH_4ZSM-5 was converted fully into the hydrogen form. Moreover, the temperature programmed desorption of ammonia (TPD) of the samples activated between 823 to 1273 K and

thermogravimetric studies of NH_4ZSM-5 had shown that the catalyst activated at 823 to 873 K has highest number of Brönsted acid sites. Therefore, the dedrease in the conversion in case of samples activated at 723 and 773 K is attributed to the incomplete release of Brönsted acid sites and maximum conversion at 823 to 873 to complete release of Brönsted acid sites and fall in conversion at 973 to 1273 to the reduction in the number of Brönsted acid sites due to dehydroxylation.

The x-ray diffraction of the samples activated at 923 and 1273 K showed that 80 to 90% crystallinity was retained which indicates that the high temperature treatments did not alter the crystal structure. Hence, the drop in conversion in sample activated at 923 and 1273 K may be due to dehydroxylation and not due to any structural breakdown.

(C) Effect of reaction temperature and contact time

Table 3.2 gives the theoretical equilibrium concentration of methylbenzenes at different temperatures[127]. The results of toluene disproportionation obtained in the temperature range 673 to 873 K on HZSM-5 catalyst (SiO_2/Al_2O_3 = 86) is illustrated in the Table 3.3 and plotted as function of temperature in Fig. 3.5B. A near

TABLE - 3,2

Theoretical equilibrium concentrations of methylbenzenes (mol.%)

Temp. (K)	Benzene	Toluene	Xylenes	Trimethyl benzenes	Tetra methyl benzenes
300	30.0	44.0	22.2	3.6	0.2
400	30.2	43.1	22.7	3.8	0.2
500	31.2	42.2	22.6	3.7	0.3
600	31.5	41.7	22.7	3.8	0.3
700	31.9	41.1	22.7	3.9	0.4
800	32.0	40.6	23.1	3.9	0.4
900	32.3	40.6	22.7	3.9	0.5
1000	32.4	40.3	22.8	4.0	0.5

See Ref. 127.

TABLE - 3.3

Influence of temperature on toluene disproportionation reaction

Reaction conditions:

Catalyst - HZSM-5 (SiO_2/Al_2O_3 = 86)
WHSV (hr^{-1}) - 2
H_2/Toluene (mol) - 2
Pressure (bar) - Atmospheric

Temp. (K)	673	723	773	798	823	848	873
Product distribution(% mol)							
Aliphatics	0.79	0.80	1.02	1.0o	1.10	1.20	1.80
Benzene	8.02	11.51	19.78	23.35	26.67	29.52	33.53
Toluene	84.56	77.30	62.58	58.67	53.69	51.81	48.73
P-Xylene	1.40	2.31	3.86	4.06	4.43	4.29	4.12
M-Xylene	2.95	4.77	8.11	8.50	9.37	9.09	8.68
O-Xylene	1.02	2.16	3.80	4.30	4.30	4.50	4.30
C_9^+ aromatics	1.95	1.44	1.31	1.23	1.26	1.21	1.10
B/X mole ratio	1.50	1.25	1.25	1.38	1.47	1.65	1.96
% Mol toluene conversion	15.44	22.70	37.42	40.33	46.31	48.19	51.27

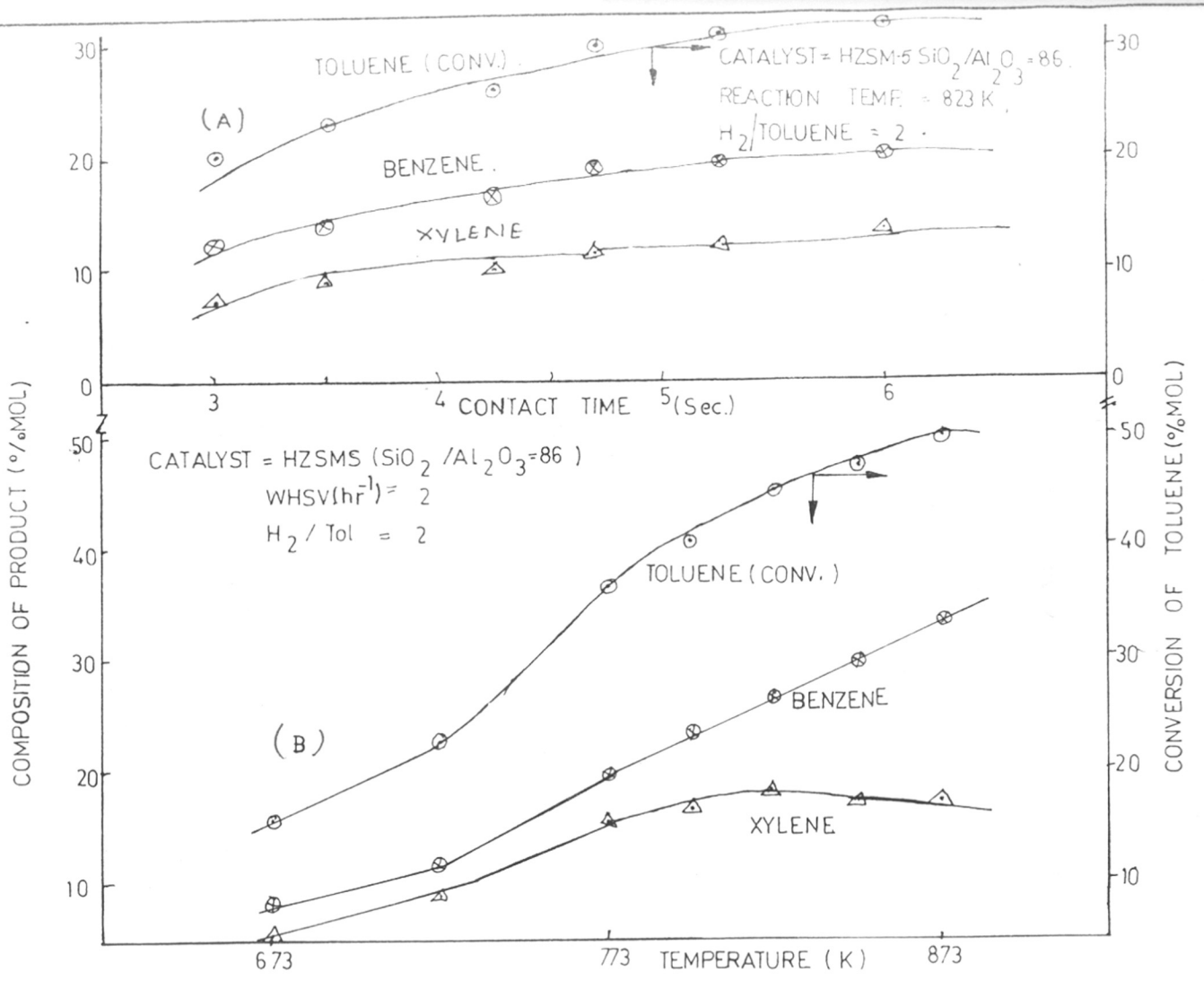

FIG. 3.5. A AND B SHOW THE INFLUENCE OF CONTACT TIME (W/F) AND TEMPERATURE ON PRODUCT DISTRIBUTION RESPECTIVELY.

equilibrium mixture of three xylenes is obtained at all temperatures. A small amount of trimethyl benzene isomers predominantly , 1.2.4 trimethylbenzene is obtained, indicating the poor performance of ZSM-5 zeolite for transalkylation reaction. Toluene conversion increases in direct proportion to temperature from 15 to 49.5% mol. showing toluene disproportionation to be a temperature dependent reaction. However, the selectivity (defined as the benzene to xylenes molar ratio in the product which should be equal to unity for maximum selectivity) decreases with increase in the reaction temperature i.e. the B/X molar ratio increases from 1.25 to 1.96. Beyond 823 K, the concentration of benzene (Fig. 3.5B) increases monotonically without changing the xylenes concentration due to dealkylation and cracking of toluene. These results indicate that the dealkylation reaction requires a higher activation energy than toluene disproportionation and/or the stronger acid sites, (generated at higher temperatures) are the active centres for the dealkylation and cracking reaction of toluene. It may be noted here that thermodynamically the dealkylation reaction is more favoured than the disproportionation reaction (ΔF_{298} =-10.7 vs + 1.4 Kcal mol^{-1}).[116b]

In order to choose appropriate reaction conditions, the effect of contact time was studied using HZSM-5 zeolite (SiO_2/Al_2O_3 = 86). Fig. 3.5A illustrates the effect of contact time (W/F) on toluene disproportionation. Toluene conversion increased with increasing contact time and attained equilibrium. However, the selectivity is found to be independent of the contact time.

(D) Effect of SiO_2/Al_2O_3 mol. ratios

The catalytic activity of the samples 1-5 (Table 3.4) having different SiO_2/Al_2O_3 ratios, for disproportionation of toluene at various temperatures is shown in the Fig. 3.6. The toluene conversion decreases at each temperature for the HZSM-5 sample with higher SiO_2/Al_2O_3 ratio indicating that the surface acid sites are active centres for toluene disproportionation since the concentration of the acid sites also decreases with increasing SiO_2/Al_2O_3 ratio (Table 3.4). For the sample 1 (SiO_2/Al_2O_3 = 36) an equilibrium conversion is attained above 800 K. Fig. 3.7 illustrates the influence of SiO_2/Al_2O_3 ratio on product selectivity. The B/X molar ratio for the samples 3-5 with higher SiO_2/Al_2O_3 ratios, is close to unity whereas the B/X molar ratio in case of samples 1 and 2 with lower SiO_2/Al_2O_3 is greater than unity and indicates a predominance of toluene dealkylation and cracking reactions. This can be explained

TABLE - 3.4

Influence of SiO_2/Al_2O_3 molar ratio on toluene disproportionation reaction

Reaction conditions

Temp. (K) - 673
WHSV(hr^{-1}) - 2
H_2/Toluene (mol) - 2
Pressure (bar) - Atmospheric

Sample	1	2	3	4	5
SiO_2/Al_2O_3 molar ratio	36	86	144	165	320
Al/Unit Cell	5.02	2.28	1.31	1.09	0.59
Strong acid sites/ Unit cell	3.02	1.59	1.01	0.86	0.48
Product distribution (% mol)					
Aliphatics	0.27	0.79	0.62	1.18	0.37
Benzene	15.51	8.02	4.65	3.9	1.92
Toluene	69.69	84.56	87.33	88.37	95.86
Para-Xylene	3.08	1.40	1.20	1.02	0.60
Meta-Xylene	6.45	2.95	2.39	1.95	0.86
Ortho-Xylene	2.84	1.02	1.0	0.84	0.34
C_9^+ aromatics	2.4	1.95	1.53	1.50	0.05
B/X molar ratio	1.25	1.5	1.01	1.02	1.06
% Mol conversion	30.31	15.44	12.67	11.63	4.14
*Specific activity (N) x 10^3	10.13	5.72	3.80	3.45	0.90

Specific activity (N), defined as number of molecules of toluene that undergo conversion per second per unit cell of zeolite.

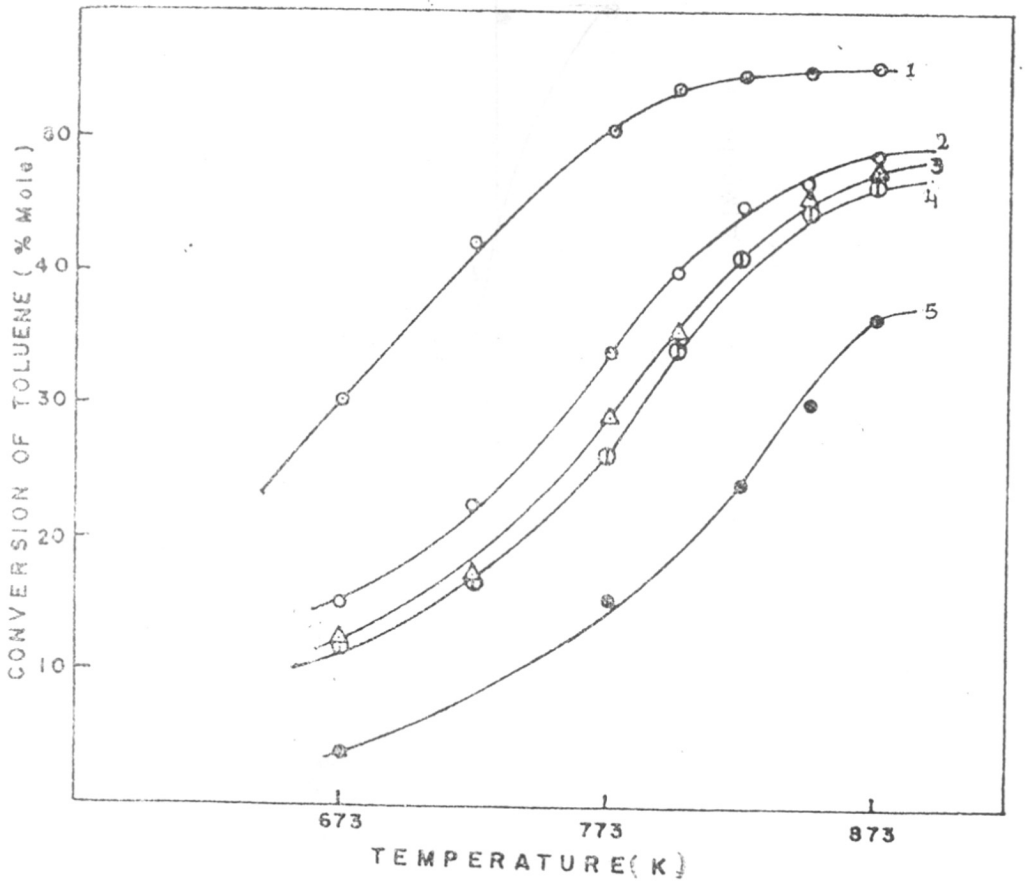

FIG.3.6. THE CATALYTIC ACTIVITY OF HZSM-5 ZEOLITES IN TOLUENE DISPROPORTIONATION . THE NOS. 1-5 REFER TO THE SiO_2/Al_2O_3 RATIOS 36,86,144,165 AND 320 respectively. [REACTION CONDITIONS: WHSV=2, H_2/TOLUENE (mole)=2, PRESSURE= ATMOSPHERIC]

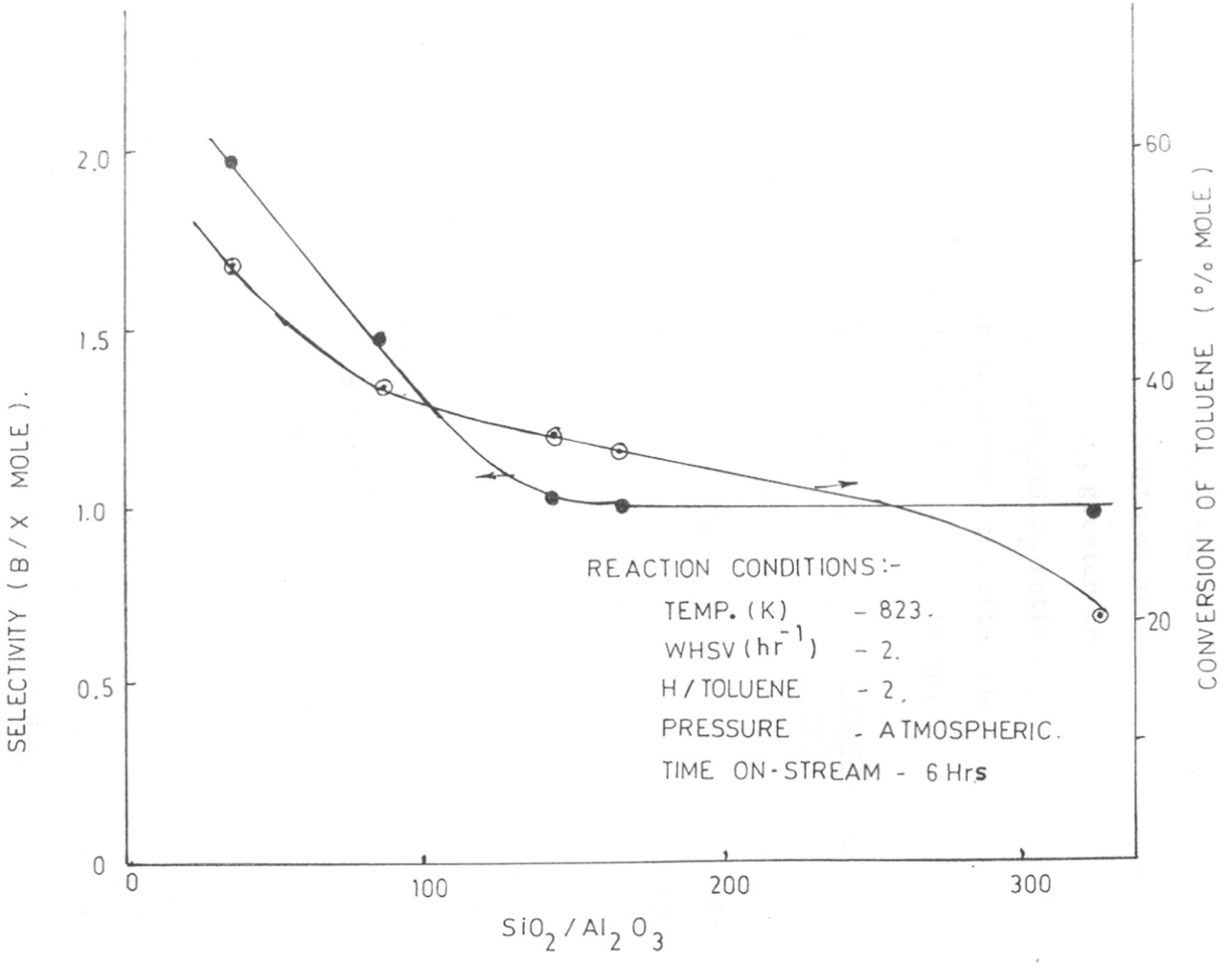

FIG. 3.7. THE INFLUENE OF SiO_2 / Al_2O_3 (MOLE) RATIO OF THE HZSM-5 ZEOLITES ON CATALYTIC ACTIVITY AND SELECTIVITY.

in terms of the strength of acid sites. In the TPD spectra it was noticed that the increase in SiO_2/Al_2O_3 ratio decreases the strength of acid sites. The observed B/X molar ratio, greater than unityin the case of samples with low SiO_2/Al_2O_3 ratio may be due to the highest strength of strong acid sites which are active in cracking and dealkylation of toluene.

(E) Relationship between surface acidity, framework aluminium atoms and catalytic activity

It is well known that hydrogen form of zeolites promotes acid-catalysed reactions and that the activity generally originates with the protons associated with the negatively charged aluminium (framework) tetrahedra. Olson et al[55] reported the cracking of n-hexane over a series of HZSM-5 zeolites. They showed that the catalytic activity is a linear function of alumina content, i.e. the activity per aluminium atom is constant, even over a 400 fold change in aluminium content. They also reported that the non-framework aluminium is catalytically inactive.

Having characterized both, the surface acidity and catalytic features of the samples with different aluminium content in semiquantitative detail, an attempt

was next made to delineate the relationship, if any, between them. The specific activity (N), defined as the number of molecules of toluene that undergo disproportionation per second per unit cell, was taken as the index of catalytic activity. Data collected at lower conversion levels (at low temperature) were used for this purpose. A relationship was sought between N and concentration of aluminium or the acid sites. The acid sites determined from the TPD peak maxima at 650-673 K were used. Figs. 3.8A and 3.8B show a linear relationship between N and acid sites and framework aluminium atoms respectively.

In case of o-xylene isomerization over HZSM-5 zeolites, Babu et al[83] had shown a linear relationship between the turnover number (TON), defined as the number of molecules of ortho-xylene that undergo isomerization per second per unit cell) and strong acid sites, suggested that the same strong acid sites responsible for 650-673 K peak maximum in TPD are the main loci of catalytic activity which are located at channel intersections. The straight line obtained in the Fig. 3.8 shows that the same strong acid sites are the active centres for toluene disproportionation. The activity values per acid site and per aluminium atom/sec. which are estimated from the slopes (Fig. 3.8A and 3.8B) are

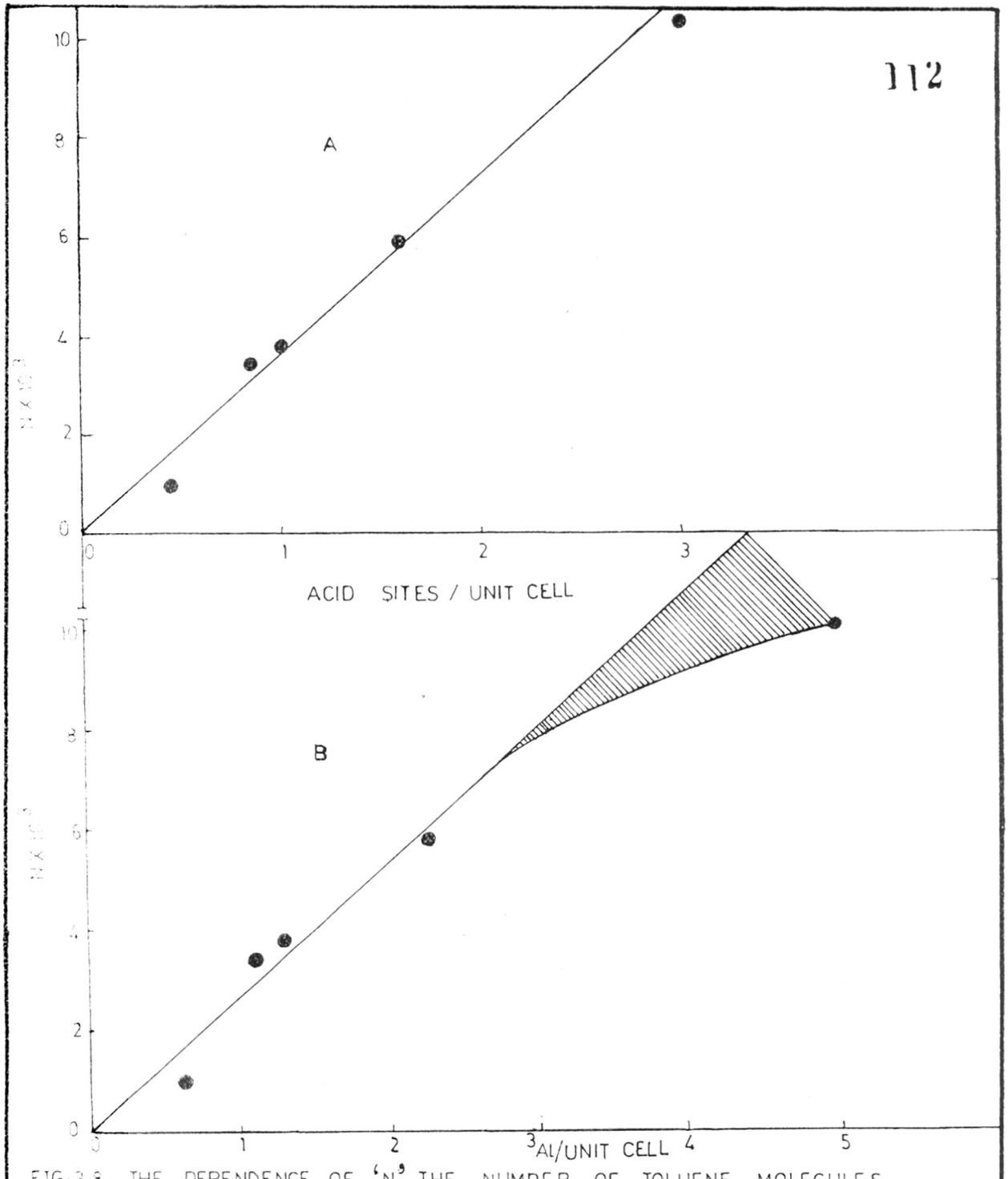

FIG. 3.8. THE DEPENDENCE OF 'N', THE NUMBER OF TOLUENE MOLECULES CONVERTED/UNIT CELL/SECOND ON CONCENTRATION OF STRONG ACID SITES (A) AND Al / UNIT CELL (B.)

3.6×10^{-3} and 2.6×10^{-3} respectively. The activity per Al atom is lower than that per acid site.

It is well known that the Brönsted acid site in zeolites is a result of nett unit negative charge created by trivalent aluminium atom which is forced to assume a tetravalent coordination in zeolites. In case of HZSM-5 zeolite, it has been shown by the temperature programmed desorption of ammonia that the acid sites with peak maximum at 650-673 K in the TPD spectrum result from the framework aluminium atoms[44]. One would therefore expect the same activity per aluminium atom and/or per acid site. However, the present results show the activity for the toluene disproportionation obtained per aluminium atom is lower than that obtained per acid site. This indicates that all the aluminium atoms in the HZSM-5 samples are not totally in the framework position which is in good agreement with the data from the NH_3/Al ratio (lower than unity)obtained in the temperature programmed decomposition of NH_4ZSM-5 zeolites. Apart from these, the activity per aluminium atom is not constant (Fig. 3.8B). The activity per aluminium atom decreases further when the aluminium content per unit cell increases from 3 to 5 (see Fig. 3.8B), indicating that the aluminium content outside the framework increases with decreasing SiO_2/Al_2O_3 ratio in the ZSM-5 zeolite.

Similar result has been reported by Romannikov et al[128]. Thus, the lower rate of specific activity (N) per aluminium atom than per acid site indicates that the extra framework aluminium atoms are inactive for toluene disproportionation. This was also proved to be inactive in n-hexane cracking by Olson et al[55]. These results further support our conclusion that the acid sites responsible for the TPD peak maximum at 650-673 K are active in toluene disproportionation whereas the acid sites which are associated with the extra framework aluminium are inactive.

(F) Influence of SiO_2/Al_2O_3 ratio on para-xylene selectivity

The xylene isomer composition obtained in toluene disproportionation reaction (for the samples 1-5 of different SiO_2/Al_2O_3 ratios) at 773 K is given in Table 3.5. It is seen that the para-xylene content among the xylenes increases from 24.48 to 28.78% mole (against 22.8% equilibrium) at the expense of ortho-xylene with increasing SiO_2/Al_2O_3 ratio from 36 to 320. The formation of trimethylbenzene also decreases from 2.13 to 0.14% with increasing SiO_2/Al_2O_3 ratio. This increase in selectivity for para-xylene could be explained on the basis of their relative diffusivity in the ZSM-5 channel. The size of the intersecting channels of ZSM-5 matches closely with the size of para-xylene molecule which, in turn, greatly favours the diffusion and the formation

TABLE - 3.5

Influence of SiO_2/Al_2O_3 molar ratio on para-xylene selectivity

Reaction conditions

Temp. (K) = 773
WHSV(hr^{-1}) = 2
H_2/toluene (mol) = 2
Pressure(bar) = Atmospheric

Sample	1	2	3	4	5	*Equilibrium at 800 K
SiO_2/Al_2O_3 (mol ratio)	36	86	144	165	320	
Toluene conversion % mole	50.90	36.66	29.74	26.50	7.28	
Xylene composition % mole						
Para-Xylene	24.57	24.48	25.00	25.74	29.78	23.10
Meta-Xylene	50.81	51.43	50.92	50.74	49.18	51.35
Ortho-Xylene	24.62	24.11	24.08	23.52	21.03	25.60
C_9^+ aromatics	2.13	13.5	1.30	1.30	0.18	-

* Ref. 139.

of para-xylene. On the other hand, the diffusion restrictions are strongly imposed on o- and m-xylene molecules because their sizes are greater than the channel dimensions. At higher SiO_2/Al_2O_3 ratio there may be partial shrinking of the unit cell which is enough to reduce the conversion of xylene to trimethylbenzene. Apart from the partial shrinking, the crystallite size in the present sample was found to increase with increasing SiO_2/Al_2O_3 ratio. These factors may be responsible for further reduction in the diffusivity of o- and m-xylene as compared to that of para-xylene which influences the selectivity factor.

(G) Influence of incorporation of Ni^{2+}, P^{5+} Mg^{2+} and B^{3+} in HZSM-5

HZSM-5 zeolites are very active for toluene disproportionation. However, due to predominance of dealkylation and cracking reactions, the selectivity to xylenes decreases leading to higher B/X molar ratios and results in deactivation of the catalyst due to the formation of carbonaceous deposits. This type of catalyst deactivation can be reduced or even eliminated either by modifying the strength of active sites which are responsible for the dealkylation or cracking reactions of toluene or by incorporating metals which are active in hydrogenation reactions.

Table 3.6 shows the influence of the incorporation of metal ions (Ni^{2+}, P^{5+}, Mg^{2+}) in the HZSM-5 on the product distribution and selectivity to xylenes (B/X mole ratio). Fig. 3.9 shows that the toluene conversion is dependent on reaction temperature and steadily increases upto 855 K and then attains a constant value. The order of activity in the present samples is as follows : HZSM-5 > NiHZSM-5 > PMgHZSM-5 > BHZSM-5. This order is consistent with the number of acid sites calculated from the TPD spectra. The B/X molar ratio in case of HZSM-5 and PMgHZSM-5 is greater than unity indicating appreciable dealkylation and cracking of toluene. However, B/X molar ratio in case of NiHZSM-5 is near to unity. Thus, the sites present over NiHZSM-5 may be selective for the disproportionation of two moles of toluene to one mole of benzene and one mole of xylene. In the TPD profile, it was noticed that on incorporation of nickel in HZSM-5, there is a shift in T_M (temperature for peak maxima) to the lower side as compared to HZSM-5 indicating a decrease in the strength of acid sites. Therefore, we propose that the presence of nickel on HZSM-5 may create new sites (Brönsted acid type) which are lower in strength but are active in toluene disproportionation with increased selectivity to xylene.

TABLE - 3.6

Catalytic activity of modified HZSM-5 in toluene disproportionation

Reaction conditions

Temp. (K) - 673
WHSV(hr^{-1}) - 2
H_2/toluene (mole) - 2
Pressure(bar) - Atmospheric

Catalyst	HZSM-5	NiHZSM-5	PMgHZSM-5
Product distribution(% mole)			
Aliphatics	0.50	0.43	0.50
Benzene	15.51	7.9	3.30
Toluene	69.31	81.45	93.18
P-Xylene	3.08	2.19	1.75
M-Xylene	6.45	3.82	0.85
O-Xylene	2.84	1.63	0.39
C_9^+ aromatics	2.4	1.63	0.04
B/X mole	1.25	1.03	1.10
Toluene conversion (% mole)	30.69	18.55	6.80

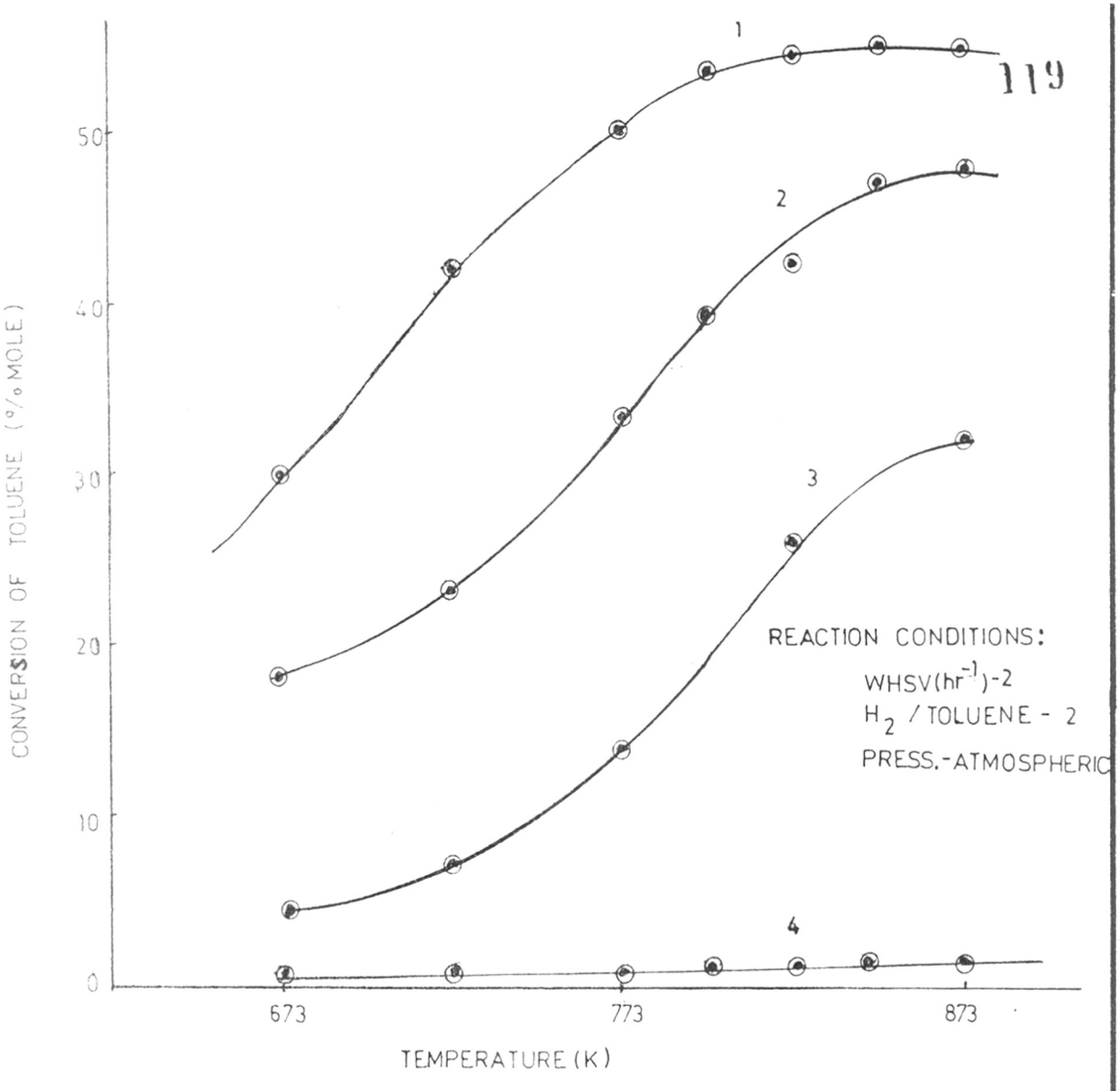

FIG 3.9. THE CATALYTIC ACTIVITY OF MODIFIED HZSM-5 ZEOLITES IN TOLUENE DISPROPORTIONATION: 1) HZSM-5 2) NiHZSM-5 3) PMg HZSM-5 4) BHZSM-5

(H) Shape selective properties of modified HZSM-5 zeolites

Molecular shape selective catalysis was first reported by Weisz and Frilette[117] in 1960 with zeolite 5A which has a pore opening of 5Å in diameter. Straight chain molecules such as normal paraffins, normal olefins, straight chain primary alcohols, etc. were selectively converted in presence of their branch isomers. The latter, because their molecular diamensions exceeded those of the catalyst pore opening, could not enter in zeolite cavities and react. Similarly, only straight chain molecules small enough to diffuse out of zeolite pores appeared in the product.

The interconnected channels formed by ten membered rings of oxygen, such as in ZSM-5 zeolite are especially interesting because certain benzene derivatives which fit closely are able to diffuse into pores, reach catalytic sites, and undergo reactions and products may diffuse out. Other isomer may be too large to be formed easily or may diffuse out at greatly reduced rate.

Chen et al[33] and Kaeding et al[28] further modified the diffusional characteristicsof ZSM-5 significantly by incorporating a variety of chemical reagents such as the compounds of boron, magnesium and phosphorous and reported

70-80% para selectivity in the toluene disproportionation and 90-97% para xylene in the alkylation of toluene with methanol.

Toluene disproportionation results obtained with modified HZSM-5 using compounds of boron, magnesium and phosphorous are summarized in Table 3.7. About 70-80% para-xylene selectivity in xylenes has been achieved with catalyst modified with magnesium and phosphorous. The toluene conversion at each temperature was varied by changing the space velocity. The amount of para-xylene among the xylenes over these catalysts is found to increase with increasing the space velocity. This may be due to the reduction of residence time for isomerization in the catalyst bed.

Adsorption studies carried out with argon and different hydrocarbons (Table 2.5 and 2.6 respectively) for these catalysts indicate that there is a reduction in the pore volume on incorporation of phosphorous, magnesium and boron in the HZSM-5. The diffusion study showed that the diffusivity of ortho-xylene decreased drastically as compared to the diffusivity of para-xylene on incorporation of these modifiers (Table 2.7). Therefore, the high para-xylene selectivity in case of modified catalysts with boron, magnesium and phosphorous may be attributed to partial reduction of pore openings and channel dimensions of ZSM-5 crystals

TABLE - 3.7

Toluene disproportionation with modified ZSM-5 zeolites

Catalyst	Temp. K	WHSV (hr^{-1})	H_2/ toluene (mol)	Toluene conversion (% mole)	Xylene isomer composition %		
					Para	Meta	Ortho
1. HZSM-5	823	2	2	54.83	24.58	50.52	24.90
2. BHZSM-5 (3% B)	823	2	2	0.63	49.0	39.25	11.75
3. PMgHZSM-5 (2% P, 5% Mg)	723	2	2	8.22	60.98	28.92	10.11
	823	2	2	26.86	52.32	35.47	12.25
	823	4	2	18.44	57.27	31.57	11.16
	873	4	2	26.63	50.36	34.38	15.25
4. PMgHZSM-5 (4% P, 3% Mg)	673	4	2	3.76	78.31	15.93	5.76
	723	2	2	5.36	62.89	27.83	9.28
	723	4	2	3.87	77.08	17.39	5.53
	773	2	2	7.66	66.29	25.57	8.15
	773	4	2	6.19	75.00	19.05	5.95
	823	4	2	9.57	62.96	28.11	8.93
5. PHZSM-5 (8% P)	873	4	2	0.38	53.76	37.10	9.14
*Equilibrium	700				23.50	52.10	24.40
	800				23.10	51.35	25.60
	900				22.8	50.6	20.6

* Ref. 139.

which restrict the diffusion of orthoxylene and meta-xylene. These selective catalysts, with channels reduced in size, may favour transfer of methyl group to the least hindered position of toluene and the resultant para-xylene formed diffuse out of the pores at a relatively fast rate. The ortho- and meta-isomer formed, due to their low diffusivity, may spend enough time in the channels, encounter with adjacent active site and rearrange to para-isomer.

It is seen that the toluene conversion decreases drastically on incorporation of phosphorous in the HZSM-5 zeolite. For example, the toluene conversion is 55% mol for HZSM-5 zeolite whereas 27% mol for PMgHZSM-5 under identical conditions (samples 1 and 3, Table 3.7) The conversion further decreases with increasing the content of phosphorous in the HZSM-5 zeolite (Samples 2 to 5, Table 3.7). However, the selectivity to para-xylene increases with increasing phosphorous content. This indicates that the phosphorous in the channels of the ZSM-5 neutralizes the strong acid sites which are responsible for the toluene conversion in addition to partial channel blockage. The results show good agreement with acid sites determined by TPD of these samples

(Table 2.9). However, catalysts, BHZSM-5 (3% boron, Fig. 3.9) and PHZSM-5 (8% phosphorous, Table 3.7) are inactive in the toluene disproportionation although these catalysts had shown considerable strong acid sites. This may be attributed to the higher concentration of the boron and phosphorous in the ZSM-5 channels which may not sterically inhibit the chemisorption and diffusion of small ammonia molecule, but may inhibit the adsorption and diffusion of larger toluene molecules to the active sites in the channels. This observation is confirmed from adsorption data given in Table 2.6. These catalysts do not adsorb toluene molecules significantly.

The p-xylene selectivity of the modified sample (samples 3 and 4) is compared at different toluene conversion levels in Table 3.7. The conversion of toluene increased by raising reaction temperature. It can be seen that the p-xylene selectivity (among the xylenes) decreases significantly with increasing reaction temperature indicating that the p-xylene selectivity is affected by the diffusivity of o- and m-xylene. The critical dimensions of o- and m-xylene are larger than that of p-xylene, hence their diffusivity is lower due to steric hindrance. However, at higher temperature their diffusivity increases with increasing temperature which, in turn, decreases the conversion of o- and m-xylene to p-xylene by isomerization. A similar

effect was reported by Chen and Garwood[27]. They have shown that at 648 K, n-hexane was converted 8.8 times faster than 3-methylpentane which is a larger molecule than n-hexane; raising temperature to 783 K both molecules were converted at the same rate. This result confirms the fact that diffusivity of o- and m-xylene has significant effect on para-xylene selectivity.

(I) Effect of reduction temperature on the activity of NiHZSM-5 catalyst

The NiHZSM-5 catalyst (2.22% Ni) was dehydrated at 823 K in presence of air and subsequently reduced at 723, 823 and 873 K in presence of pure and dry nitrogen for about 8 hours. The resulting catalyst was then tested for toluene disproportionation at 723 K. The toluene conversion was found to increase with increasing the reduction temperature of the NiHZSM-5 catalyst. The catalyst reduced at 873 K had highest activity (Table 3.8).

The XPS results for the reduced samples show that the Si/Ni ratio decreases on increasing reduction temperature. The nickel in the form of NiO may agglomerate on the ZSM-5 surface at the higher temperature of reduction unlike that on hydrogen mordenite[118A]. The high toluene conversion in case of the sample reduced at 873 K may be due to NiO species in addition to nickel ion in the

TABLE - 3.8

Influence of reduction temperature on the activity of NiHZSM-5 catalyst

Reaction conditions

Reaction Temp.(K) - 723
WHSV (hr^{-1}) - 3
H_2/Toluene (mole) - 2
Pressure (bar) - Atmospheric

Reduction Temp. (K)	723	823	873
Product distribution % mol.			
Aliphatics	0.40	0.38	0.50
Benzene	4.89	5.91	7.82
Toluene	89.44	88.07	83.63
Para-Xylene	1.39	1.55	2.15
Meta-Xylene	2.83	3.02	4.30
Ortho-Xylene	1.28	1.38	1.97
C_9^+ aromatics	0.05	0.06	0.04
B/X molar ratio	0.90	0.99	0.93
% Mole conversion	10.56	11.93	16.37

channels. Shopov et al[20] have reported that the nickel ion in the zeolite crystal lattice or nickel oxide on the surface are only active species of nickel in toluene disproportionation. Moreover, Davidova et al[118B] reported that when Ni(II) is reduced to metallic state, only dealkylation of toluene takes place. In the present results, the B/X molar ratio in case of three samples is around unity. Therefore, the increase in the activity at higher reduction temperature may not be due to the formation of metallic nickel.

(J) Effect of nickel concentration

To establish the content of nickel on HZSM-5 which is favourable for toluene disproportionation, the nickel concentration was varied from 0.55 to 5.5 % wt. Fig. 3.10 represents the effect of nickel loading on toluene conversion. The toluene conversion increases with increasing nickel concentration from 0.55 to 2.22 % wt. but falls sharply with further increase in the nickel content to 5.5% wt. This may be due to either blocking of active sites at high nickel concentration (5.5 % wt.) or reduction in the active sites for toluene disproportionation.

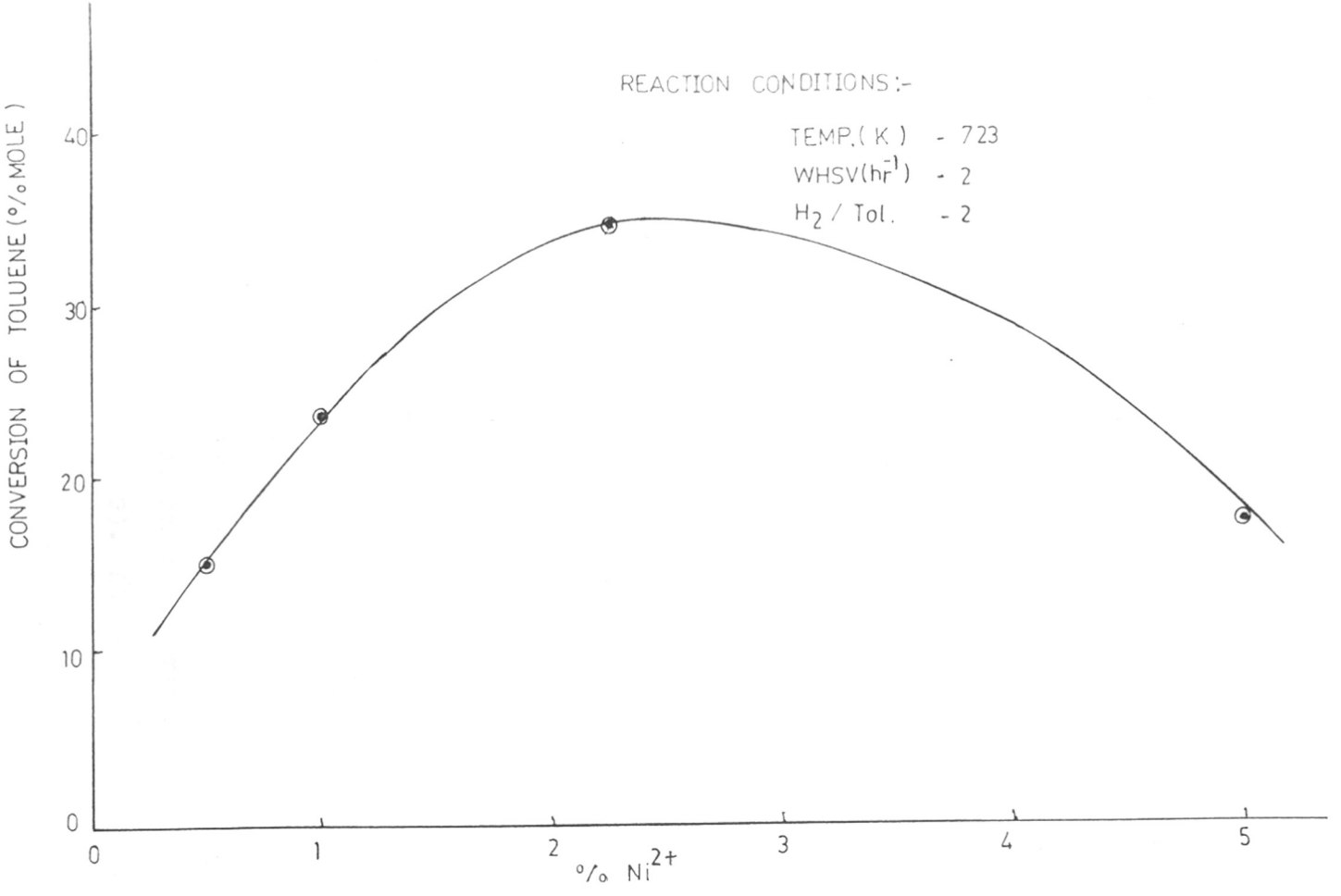

FIG 3.10 INFLUENCE OF INCORPORATED NICKEL CONTENT IN HZSM-5 ON TOLUENE DISPROPORTIONATION REACTION.

(K) High pressure toluene disproportionation reaction

(i) Pressure Effect

The influence of pressure on the activity and selectivity in toluene disproportionation reaction has been studied using 'Catatest' Unit described in the experimental section (3.2). Fig. 3.11 represents the effect of pressure (catalyst Ni, PtHZSM-5, SiO_2/Al_2O_3 = 36). The selectivity, B/X molar ratio, is unity and it is independent of pressure while the toluene conversion increases with increasing pressure and levels off above 20 kg/cm^2. However, the formation of trimethylbenzene increases at higher pressure as compared to the atmospheric pressure. The increase in the conversion of toluene and the formation of trimethyl benzene may be attributed to the enhanced adsorption and retention of reactants and products on the surface under these conditions.

(ii) Temperature Effect

It has been noticed that the toluene disproportionation reaction is highly temperature sensitive. To establish the ideal temperature for the disproportionation of toluene at higher pressure, the reaction was carried at 553-768 K. The near equilibrium conversion of toluene is achieved at 768 K (Table 3.9). At lower temperatures

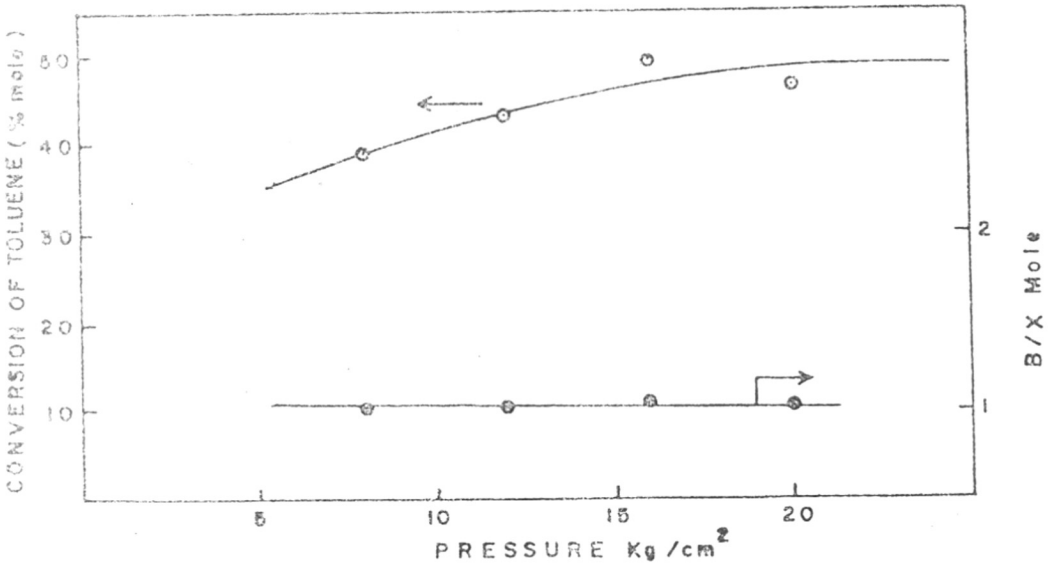

FIG.3.11. THE INFLUENCE OF PRESSURE ON ACTIVITY AND SELECTIVITY IN THE TOLUENE DISPROPORTIONATION. REACTION CONDITION: TEMP.=763K, WHSV=2, H_2/TOLUENE(mole)=5, TIME ON STREAM= 6 HOURS.

TABLE - 3.9

Effect of temperature on toluene disproportionation

Reaction conditions

Catalyst - NiHZSM-5 (SiO_2/Al_2O_3 = 36 with 0.5% Ni)

Pressure (bar) - 40

H_2/toluene (mol) - 0.50

WHSV (hr^{-1}) - 1.0

Reaction Temp. K	553	673	723	768
Product (mole %)				
Aliphatics	1.90	1.20	0.62	0.71
Benzene	1.04	12.66	21.03	30.82
Toluene	95.21	70.61	57.22	45.57
Total xylenes	1.02	13.21	19.86	21.67
C_9^+ aromatics	0.71	2.01	1.4	2.6
B/X molar ratio	1.00	0.96	1.05	1.42
% Mol. conversion.	4.79	29.39	42.78	54.43

(553-723 K), the toluene cleanly disproportionates into one mole of benzene and xylenes. However, at higher temperatures (768 K), the conversion of toluene increases and benzene and gaseous products are formed due to dealkylation and cracking of toluene rather than disproportionation.

(iii) Effect of Space Velocity (F/W)

The results obtained with NiHZSM-5 catalyst at different space velocities are shown in Table 3.10. At 768 K, H_2/toluene, 0.5, and 40 bar pressure, the toluene conversion is not affected by the variation in the space velocity. However, the selectivity i.e. B/X molar ratio is very much influenced. The selectivity is found to increase with increasing space velocity.

(iv) Activity of metal loaded ZSM-5 zeolites

In Table 3.11, the catalytic activity of the HZSM-5, NiHZSM-5 and Ni/Pt HZSM-5 catalyst for toluene disproportionation have been compared. The toluene disproportionation activity decreases in the order, HZSM-5 > NiHZSM-5 > Ni/PtHZSN-5. The lower activity of the nickel and nickel-platinum ZSM-5 zeolite as compared to HZSM-5 zeolite is due to a decrease in the number of acid sites by the incorporation of metal in the zeolite. However, the selectivity is improved on incorporation of nickel and phosphorous. A change in the strength of the acid sites could possibly account for an improved selectivity.

TABLE - 3.10

Effect of space velocity (WHSV)

on toluene disproportionation

Catalyst - NiHZSM-5 (SiO_2/Al_2O_3 = 36 with 0.5% Ni)
Temp. K - 768
H_2/toluene (mole) - 0.50
Pressure (bar) - 40

WHSV (hr^{-1})	0.50	1	1.38	1.73	2.02
Product (% mol.)					
Aliphatics	0.37	0.71	0.79	0.63	0.62
Benzene	32.73	30.82	29.04	26.79	25.38
Toluene	42.71	44.57	46.71	47.53	27.97
Total e xylenes	22.89	21.67	22.26	23.79	24.43
C_9 aromatics	1.49	2.6	2.8	1.7	1.73
B/X mole ratio	1.43	1.42	1.30	1.12	1.04
% Mole conversion	56.29	54.43	53.3	52.47	52.03

Note : WHSV= Weight of feed per unit weight of catalyst per hour.

TABLE - 3.11

Toluene disproportionation with modified HZSM-5 zeolites

Temperature (K) - 773

Pressure (bar) - 20

WHSV (hr^{-1}) - 2

H_2/toluene (mol) - 2

Product (% mole)	HZSM-5	NiHZSM-5	NiPtHZSM-5
Aliphatics	0.46	0.36	0.25
Benzene	32.89	23.12	14.25
Toluene	48.71	53.50	69.91
P-Xylene	4.54	5.64	3.74
M-Xylene	9.19	10.59	7.53
O-Xylene	4.04	5.29	3.65
C_9^+ aromatics	2.48	1.07	0.96
B/X molar ratio	1.85	1.07	0.96
% Mole conversion	51.29	46.50	30.09

(L) Catalyst Deactivation

The zeolites show unusual behaviour for their shape selective properties. Their intracrystalline built active sites are accessible only to those molecules whose size and shape permits the sorption through the entry pores. The deactivation is known to be associated with the synthesis and occlusion of large molecules within the catalyst pores which prevents the access of reactants to the active sites[119]. Rollmann and Walsh had demonstrated[120,121,53] that the intracrystalline coking of zeolites is a shape selective process which largely depends on the size and architecture of their channels. They have explained the mechanism of coke formation on zeolites, especially on ZSM-5 zeolite and proposed that an increase in the acid site density leads directly to an increase in the paraffin cracking into fragments within the pore system and thus to greater paraffin participation in coke formation.

(i) Effect of SiO_2/Al_2O_3 ratio

The influence of SiO_2/Al_2O_3 ratio on catalyst stability during toluene disproportionation reaction is shown in Fig. 3.12. There is a significant aging in the sample with low SiO_2/Al_2O_3 ratio. This aging is due to the deposition of carbonaceous matter on the catalyst

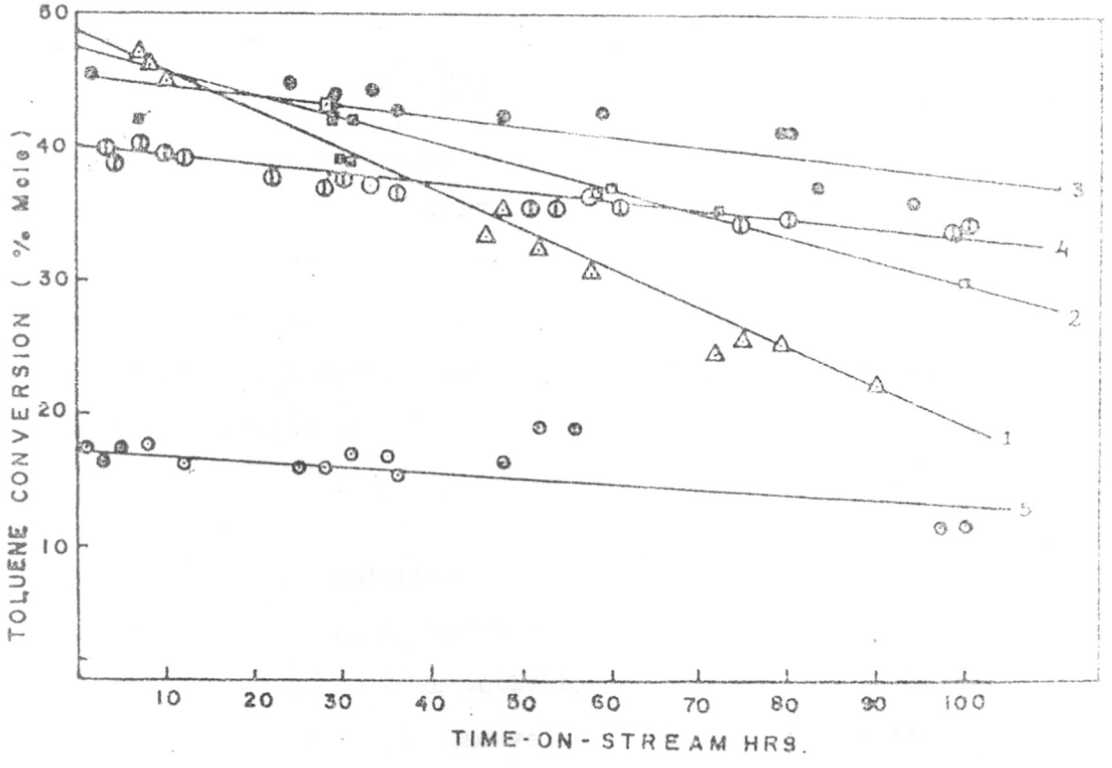

FIG.3.12. THE DEACTIVATION OF HZSM-5 ZEOLITES IN THE DISPROPORTIONATIO OF TOLUENE. THE NOS. 1-5 REFER TO THE SiO_2/Al_2O_3 RATIOS 36, 86,144,165 AND 320 RESPECTIVELY. [REACTION CONDITIONS: TEMP.=823, WHSV=2, H_2/TOLUENE(mole)=2, PRESSURE=ATMOSPHERIC]

surface and not due to the structural changes in the catalysts. The x-ray diffraction patterns of the coked and fresh samples were almost identical. An attempt has been made to describe the rate of deactivation of the zeolite samples of different SiO_2/Al_2O_3 ratios in the toluene disproportionation reaction in a semiquantitative detail. For this purpose, the activity of the catalyst was characterized by an apparent first order rate constant K, where

$$K = 1/W \ln 1/1-X \quad \ldots (1)$$

It may be noted that Gnep and Guisnet[122] had earlier reported that toluene disproportionation follows a first order reaction rate. In the above equation, W = the weight of catalyst in grams and X = fractional conversion. The values of K derived from equation (1) above were fitted to the following equation,

$$K = K_o \, e^{-\alpha Y} \quad \ldots (2)$$

where Y is the cumulative amount of toluene that had been converted to products and K_o and α are the constants which characterize the initial activity and aging rate of the catalyst respectively. The values of K_o and α for the samples 1-5 calculated from Fig. 3.13A are given in Table 3.12. The values α and K_o increase with decreasing SiO_2/Al_2O_3 ratio in the ZSM-5 zeolite. Fig. 3.13B shows

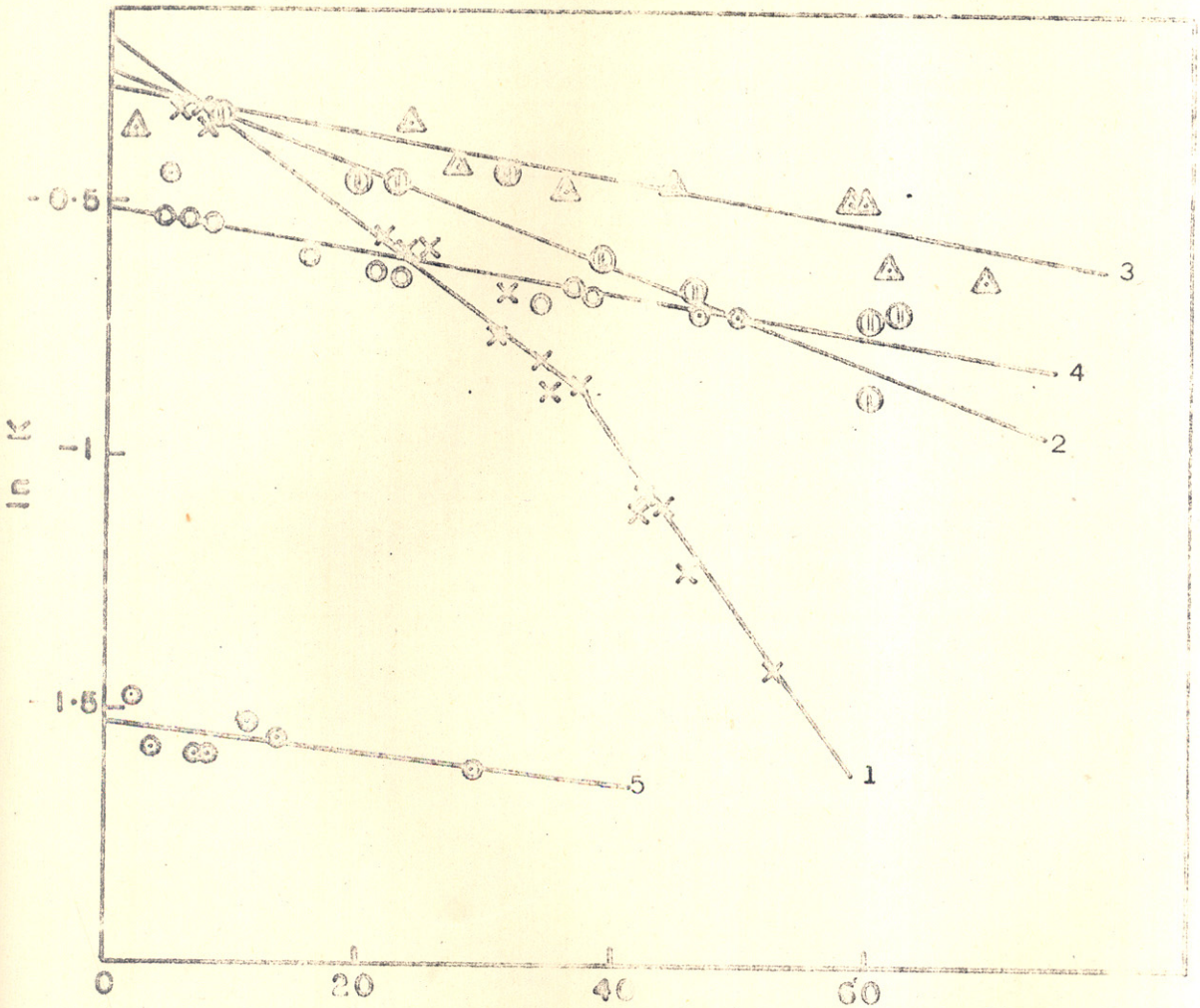

FIG.3.13A. INFLUENCE OF SiO_2/Al_2O_3 RATIO ON THE AGING OF THE HZSM-5 ZEOLITES. NOS. 1-5 REFER TO SiO_2/Al_2O_3 RATIOS 36,86,144,165 AND 320 RESPECTIVELY. (REACTION CONDITIONS ARE THE SAME AS THOSE MENTIONED IN FIG.3.12)

TABLE - 3.12

Catalytic deactivation (α) and initial activity (K_o) parameters

Sr.No.	Sample	$\alpha(10^2)(g^{-1}sec^{-1})$	$K_o(sec^{-1})$
1.	HZSM-5(36)	1.53	0.84
2.	HZSM-5(86)	0.96	0.79
3.	HZSM-5(144)	0.43	0.62
4.	HZSM-5(165)	0.41	0.60
5.	HZSM-5(320)	0.30	0.22

The number in bracket refers to SiO_2/Al_2O_3 ratio.

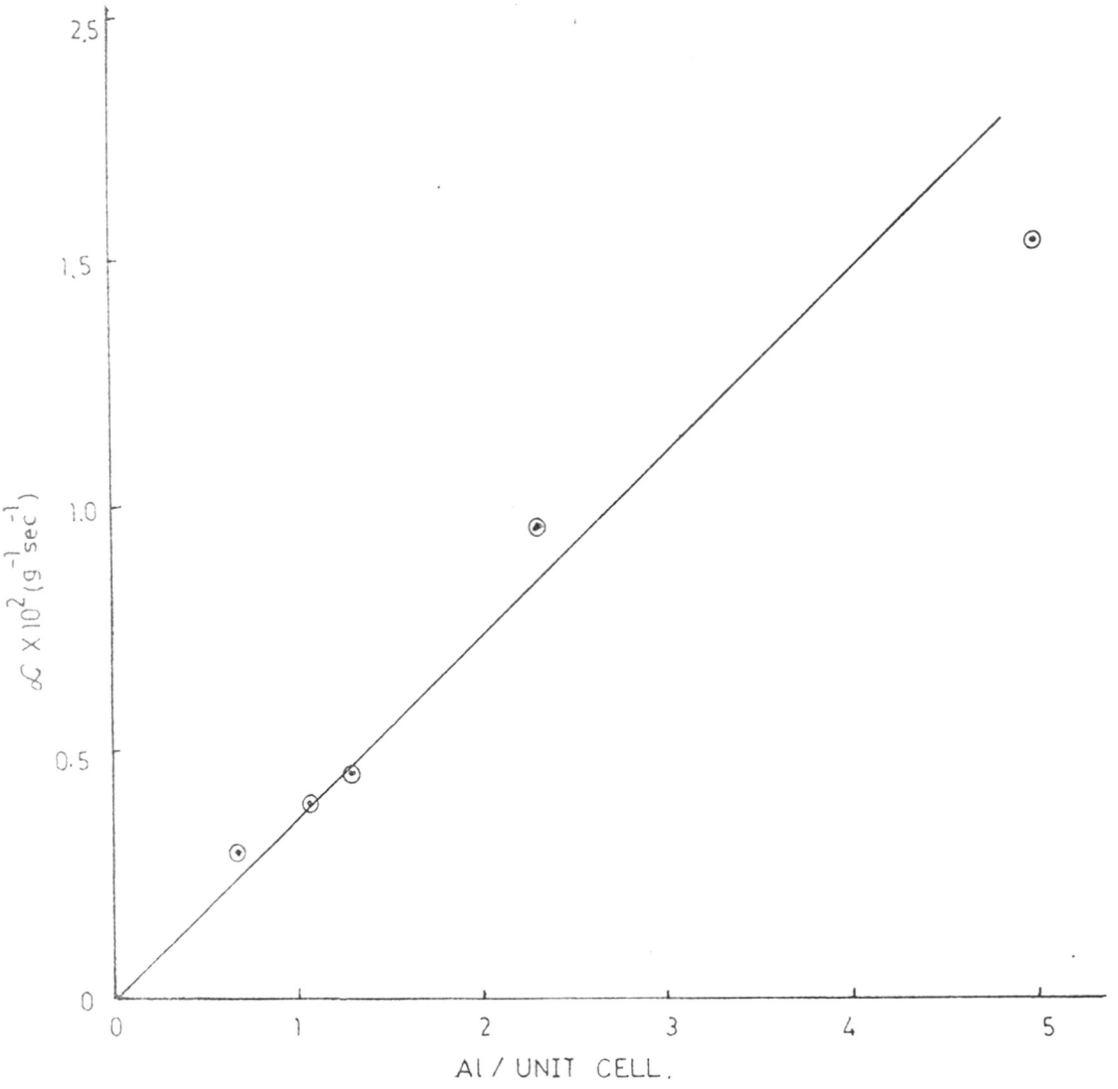

FIG.3·13B. DEPENDENCE OF α (DEACTIVATION PARAMETER) ON FRAMEWORK ALUMINIUM ATOMS OF THE HZSM-5 ZEOLITES.

the dependence of α (deactivation constant) on aluminium content in the ZSM-5 zeolites. Our results show good agreement with the results reported by Ione et al[123]. They have reported that the stable activity of ZSM-5 zeolite catalysts decreases with increase in aluminium content in the ZSM-5 zeolite.

The coke formation on the acid catalysts occurs by reaction and conversion of alkylaromatics (by cyclisation, dehydrogenation, further alkylation ...) to polyalkyl-aromatics and polyaromatics, the coke precursor causes more or less rapid deactivation. Coke deposits lower the catalyst activity by site coverage (poisoning),and/or by pore blocking which prevents the access of the reactants to the active sites. Aging of an acid catalyst can, therefore, be tested by comparing the acidity of both fresh and aged samples[54].

To describe the acid sites poisoned during toluene disproportionation, the coked catalyst (sample 2, SiO_2/Al_2O_3 ratio = 86, Table 3.12) was subjected to acidity measurement by temperature programmed desorption (TPD) as described below:

The toluene disproportionation reaction was carried out for about 24 hours in the first series and 100 hrs in the second series and the catalysts were unloaded from the catalytic reactor and loaded in the TPD reactor.

The coked catalyst was flushed with dry and purified nitrogen at 823 K for about 4 hours. The TPD run was then carried out as described in the earlier section. The TPD profiles of the fresh and coked samples after 24 and 100 hours reaction are shown in Fig. 3.14,(curves A,B,C, respectively). The peak maxima at 373, 420-470 and 650-673 K in the TPD have been assigned to the weak, medium and strong Brönsted acid sites respectively.The active sites poisoned in the coked catalyst do not impose restriction to the access of ammonia to the weak, medium and strong acid sites as evidenced by TPD spectrum. The intensity of the first two peaks (sample B) namely weak and medium is reduced strongly as compared to the third (strong) peak indicating that the acid sites of weak and medium strength are poisoned rapidly during toluene disproportionation unlike in the methanol conversion reaction[54]. However, the strong acid sites in sample C (after 100 hr reaction) are reduced drastically. This result is consistent with that reported by Topsøe et al[44] for methanol conversion reaction, indicating that the strong acid sites are poisoned either by site coverage or by pore blocking which may have prevented the access of the ammonia molecules to the active sites.

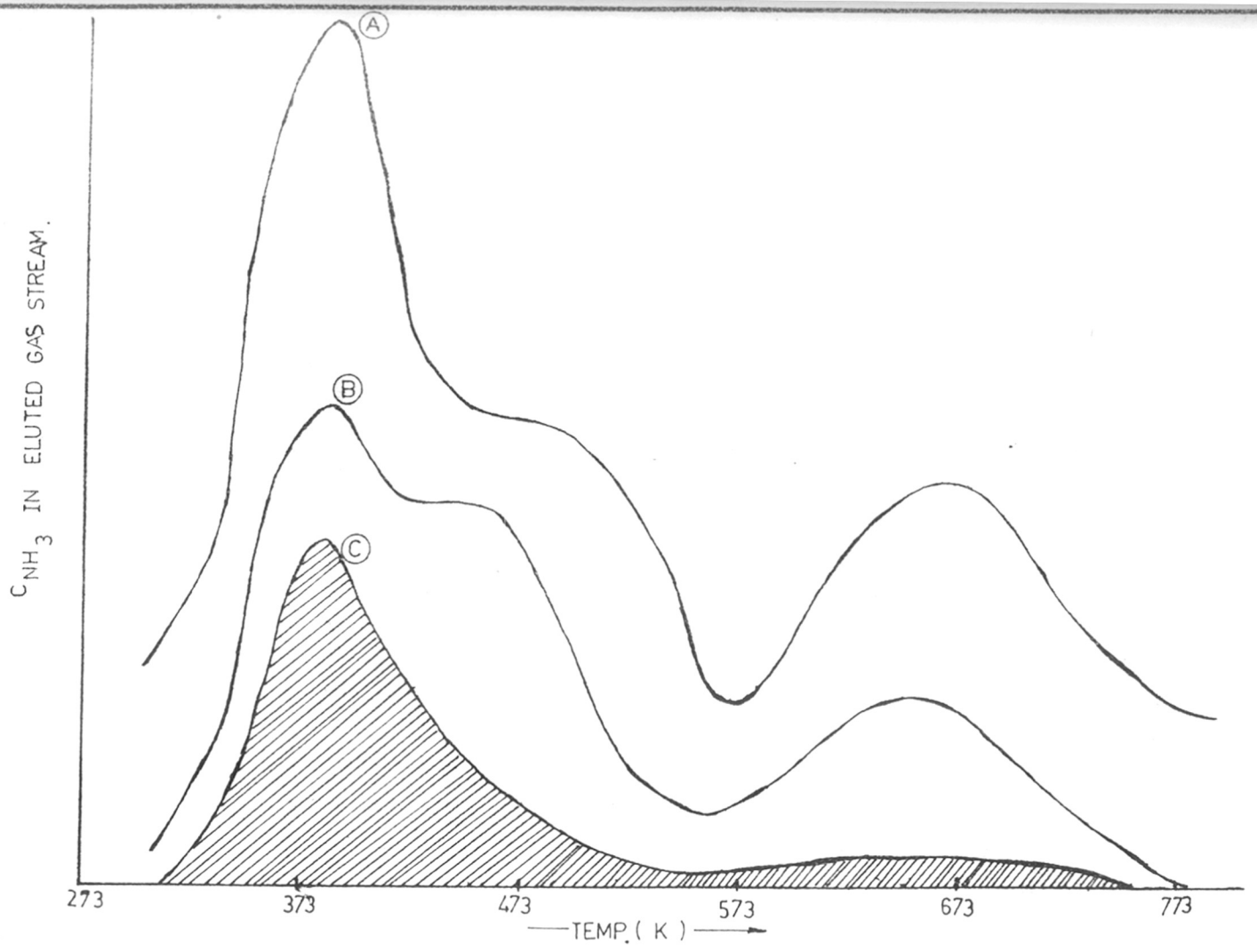

FIG. 3.14. THE TPD CHROMATOGRAMS OF CHEMISORBED AMMONIA : A) FRESH CATALYST(HZSM-5 SiO_2/Al_2O_3 86) B) AFTER 24 HOURS' C) AFTER 100 HOURS' REACTION.

The amount of deposited coke residue on the catalyst surface was determined by using thermogravimetric technique. The decoking was performed in the presence of dry air. The decoking was complete between 723 to 950 K as shown in the DTA profile in Fig. 3.15. The amount of coke estimated from the DTA/TG analysis is directly proportional to the number of strong acid sites determined from the TPD spectra (Fig. 3.16) indicating that mainly the strong acid sites take part in the reactions. It may be noted that Eisenbach and Gallei[124] who examined the influence of OH groups (ir bands at 3640 and 3740 cm^{-1}) had shown that the influence of external OH groups (3740c cm^{-1}) on coke formation was low below 773 K while the highest activity for coking was shown by the OH groups in the supercages in the catalysts CaY and PtCaY during n-hexane reaction.

It was observed that the partially deactivated surface of ZSM-5 showed reduction in the pore apertures and channel dimensions which favours the para-xylene formation[125]. The results given in the Table 3.13 show that the para-xylene selectivity increases with increasing time on stream. This indicates that partial blocking of pore aperture and channel, which occurs due to the deposition of coke during reaction, favours para-xylene formation. It may be seen from the data in Table 3.13 that para-xylene selectivity of HZSM-5 catalyst (SiO_2/Al_2O_3 = 36) increases from nearly 23% to 28% in 100 hrs

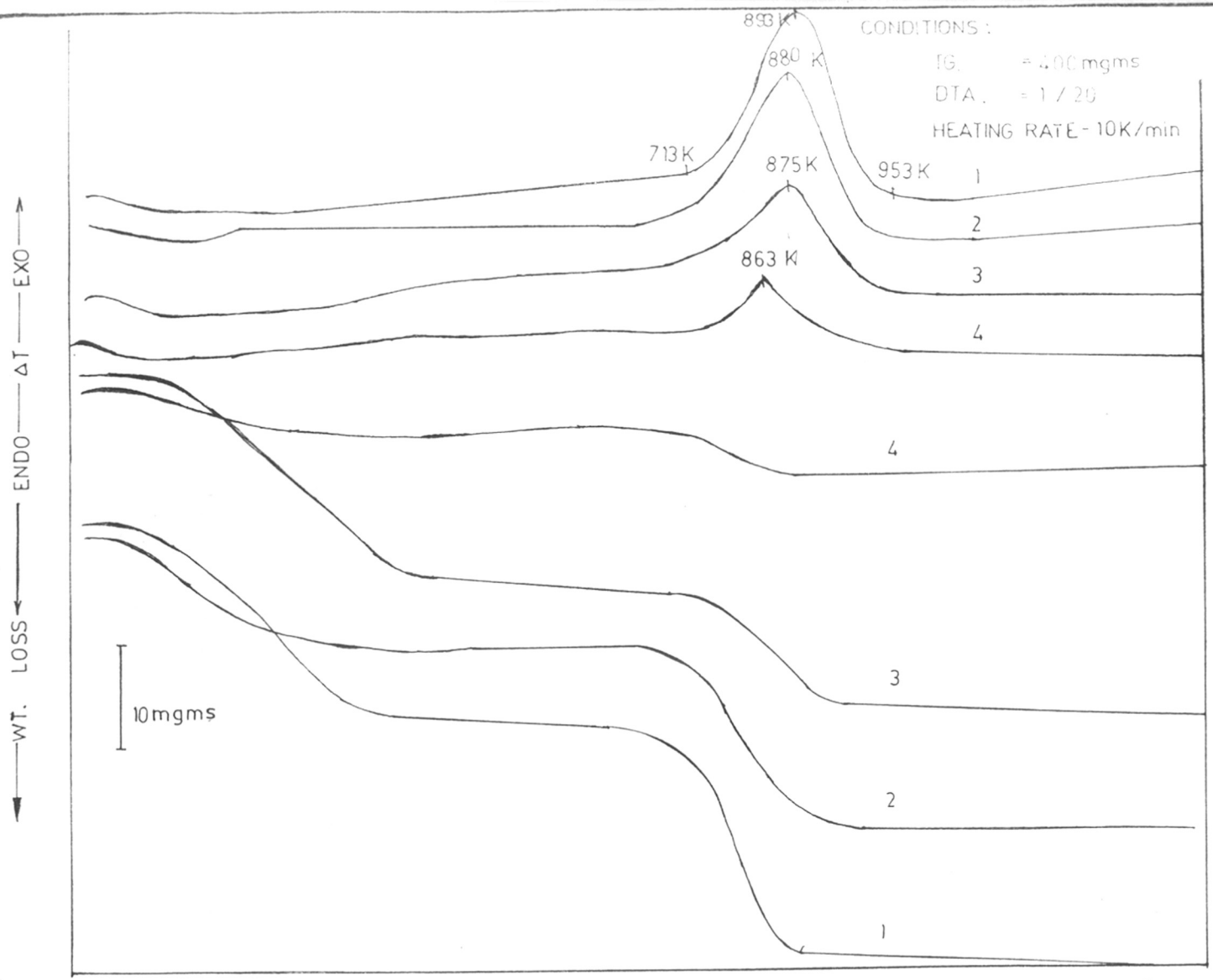

FIG.3-15. DTA AND TG THERMOGRAMS OF COKED HZSM-5 ZEOLITES. NUMBERS 1-4 REFER TO SiO_2/Al_2O_3 RATIO 86, 144, 165 AND 320 RESPECTIVELY.

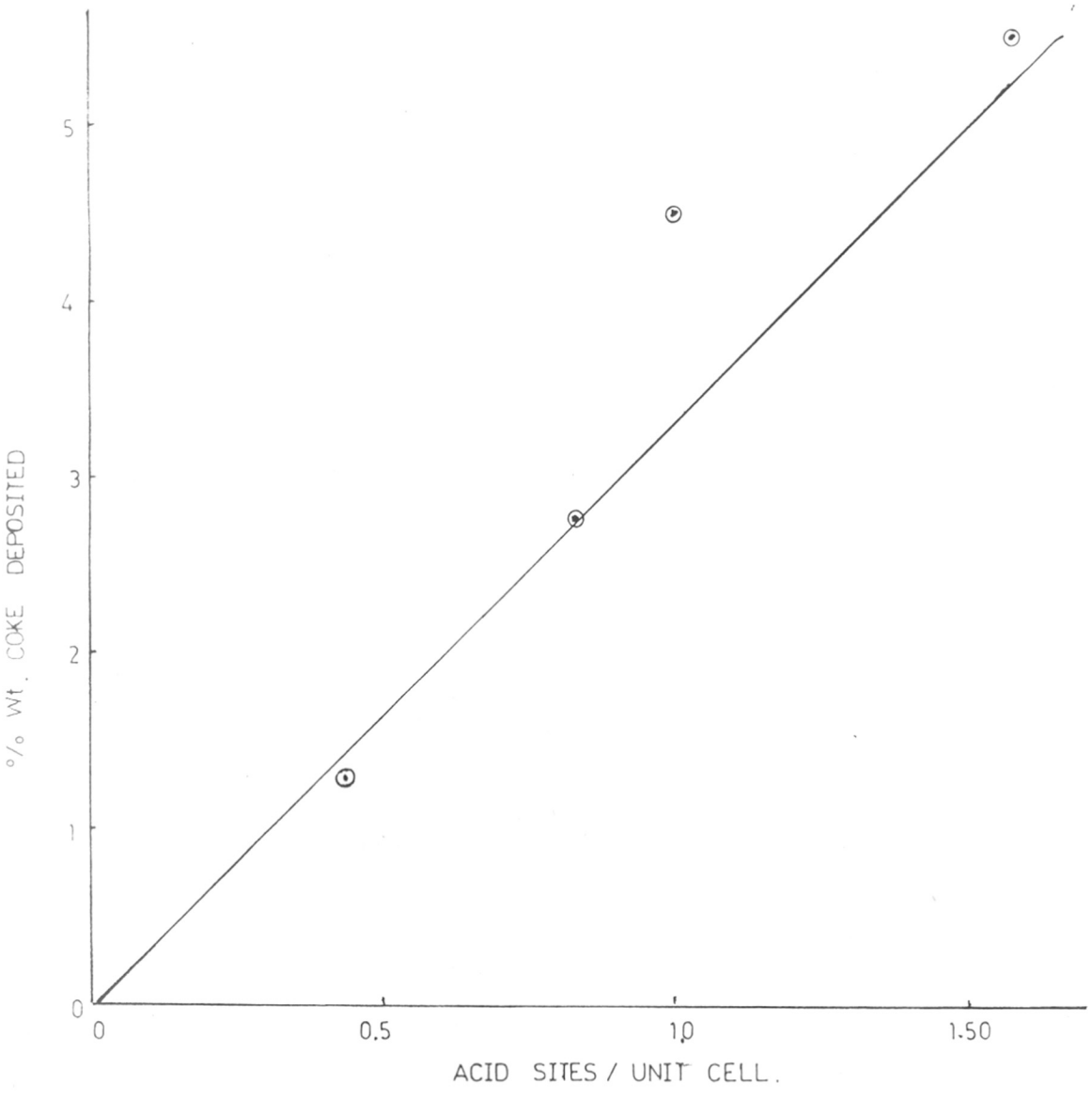

FIG.3.16. DEPENDENCE OF COKE FORMATION ON ACIDTY OF HZSM-5 ZEOLITES.

TABLE - 3.13

Effect of coke deposition on selectivity of para-xylene in xylenes

Reaction condition

Temp. (K)	-	823
Pressure (bar)	-	Atmospheric
WHSV (hr^{-1})	-	2
H_2/toluene (mol)	-	2

Time on stream(hrs.)		1	12	30	48	100
Sample						
HZSM-5(36)	a :	22.98	24.46	25.58	25.97	27.81
	b :	50.23	48.13	48.38	48.78	49.34
	c :	26.79	27.41	26.04	25.25	22.95
HZSM-5(86)	a :	26.53	25.05	29.21	26.53	27.01
	b :	47.92	49.68	47.24	49.56	49.45
	c :	25.55	25.27	23.25	23.90	23.54
HZSM-5(144)	a :	25.40	25.34	26.92	26.25	26.96
	b :	49.44	49.00	48.69	49.60	50.09
	c :	25.16	25.66	24.39	24.15	22.94
HZSM-5(165)	a :	25.68	26.01	26.63	26.75	27.48
	b :	47.72	47.56	47.18	47.25	47.12
	c :	26.60	26.43	26.19	26.00	25.40
HZSM-5(320)	a :	28.56	28.83	29.10	29.39	29.35
	b :	49.50	49.63	49.36	49.02	49.12
	c :	21.94	21.53	21.53	21.58	21.53

Note : a % mole para-xylene
b % mole meta-xylene
c % mole ortho-xylene

The figure in bracket refers to SiO_2/Al_2O_3 ratio.

while that for SiO_2/Al_2O_3 = 320 shows an increase from 29% to 30%. The results can also be explained on the basis of extensive coking of the former catalyst.

What is the location of carbonaceous matter? Whether it is on the external crystal surface or inside the channel of ZSM-5 zeolite? Rollmann and Walsh[53] and Djaifve et al[54] by taking variety of zeolites have shown that the coking of the zeolite is a shape selective reaction intimately controlled by its pore size and geometry. Especially, in the case of ZSM-5 they have proposed that coking takes place on the external surface of the ZSM-5 crystals because the smaller channels of the ZSM-5 which are free from cages do not allow the synthesis of bulky polyaromatics which are the coke precursors. If we assume that the coke deposition takes place only on the external crystal surface, then the toluene conversion should not decrease till its access to the active sites is prevented by blocking the pore aperature. However, the present results show that the toluene conversion is decreased from 48% to 30% at the end of 100 hrs although there are no diffusional restrictions imposed on the access of toluene molecules in the channels. This is evidenced by adsorption of benzene on fresh and coked catalyst after 100 hrs reaction. The size of the benzene molecules is equal to size of toluene

molecule but larger than ammonia molecule[26]. The uptake vs time curve for benzene on fresh and coked catalyst is shown in Fig. 3.17. The sorption was performed at 298 K. The equilibrium is attained after a lapse of 10 to 15 minutes on coked catalyst as well as on the fresh catalyst indicating that the coking had not imposed any diffusional restrictions. However, the total uptake is decreased after coking which is attributed to reduction of the pore volume caused by the deposition of coke. Therefore, we would like to suggest that reduction in the number of strong acid sites is not due to the deposition of coke on the external surface of the ZSM-5 crystal. However, there is intracrystalline coking, although very slow, due to which the strong acid sites are reduced after about 100 hours of reaction.

Ione et al[126] reported the effect of aluminium content of ZSM-5 zeolite on catalyst stability in methanol reaction and explained the coke synthesising centres. They have suggested that the coke precursors and non-desorbed compounds are formed on these centres, $[(Si(OAl)_n]^{n-}Al^{3+}_{n/3}$, which show the properties of super acids. Probability of formation of such centres increases either by non-uniform distribution of aluminium or by increasing the aluminium content in ZSM-5 zeolite. This, in turn, leads to a decrease in the time of stable activity.

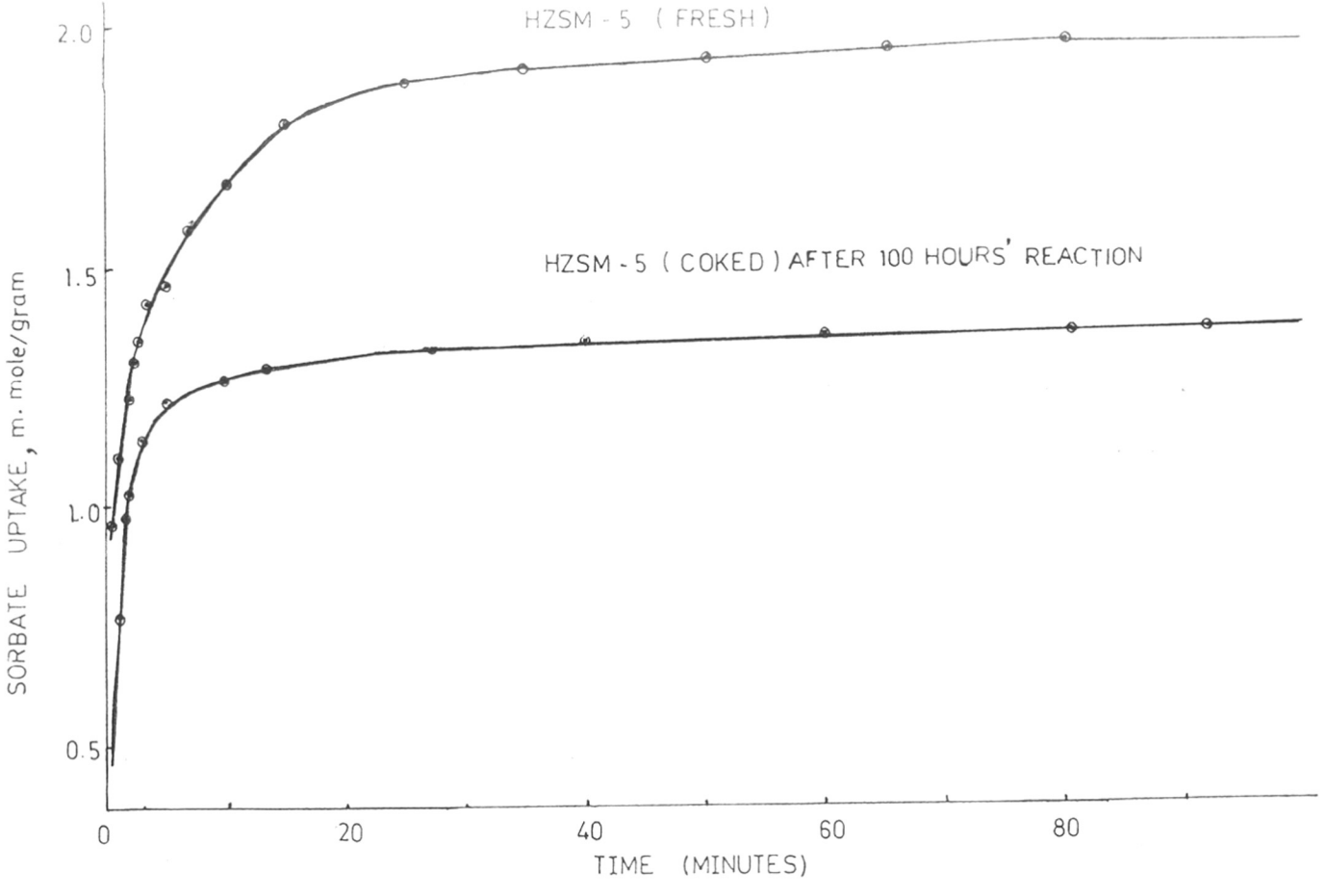

FIG.3.17. SORPTION OF BENZENE OVER FRESH AND COKED.

HZSM - 5 CATALYST SiO_2 / Al_2O_3 = 86.

During toluene conversion, the dealkylation and cracking of toluene which leads to conversion of toluene to benzene and gaseous products are the most prominent side reactions. In the present zeolite catalysts the dealkylation and cracking activity go on increasing with increase in aluminium content in the ZSM-5 zeolites (Fig. 3.7). This indicates that the strongest acid sites are the active sites for these side reactions since the strength of the active sites also increases with increasing aluminium content. This supports the idea that the formation of the super acid sites results from extra framework aluminium atom. Therefore, the extensive coking in case of sample (HZSM-5, SiO_2/Al_2O_3 = 36) is mainly due to the formation of such centres which facilitate the dealkylation and cracking of toluene that lead to the formation of coke precursors.

(ii) Effect of nickel

One of the drawbacks of the HZSM-5 zeolites investigated so far is their fast deactivation due to deposition of carbonaceous matter. The NiHZSM-5 zeolites prepared by impregnation method were tested for toluene disproportionation under conditions which had been employed for HZSM-5 zeolite. It can be seen from

Fig. 3.18, curves 1-3 that the presence of nickel in HZSM-5 helps to maintain a stable activity throughout the run. The improvement in the stability of the catalyst on nickel loading may be due to the bifunctional nature of nickel. In presence of hydrogen, nickel assists hydrogenation and thus eliminates some unsaturated hydro-carbons which otherwise would polymerise and block the active sites. To verify this argument, the catalytic activity of the catalyst was examined in presence of hydrogen, nitrogen and without carrier gas. Fig. 3.19, curves 1-3 show the catalytic activity in presence of hydrogen, nitrogen and without carrier gas respectively. The sharp fall in the toluene conversion observed in the presence of nitrogen as well as in the absence of the carrier gas is as expected. Thus, in presence of hydrogen only, nickel in zeolite prolongs the activity of the catalyst. The deactivation parameters for the above catalysts are given in Table 3.14

(M) Toluene disproportionation reaction mechanism

Toluene disproportionation and alkylation have been extensively studied using variety of alkylating agents and variety of Friedel-Crafts catalysts to elucidate the mechanism of catalytic alkylation reactions[5] (Fig 3.4) P.98. The combination of halogen acids and catalysts such as $AlCl_3$

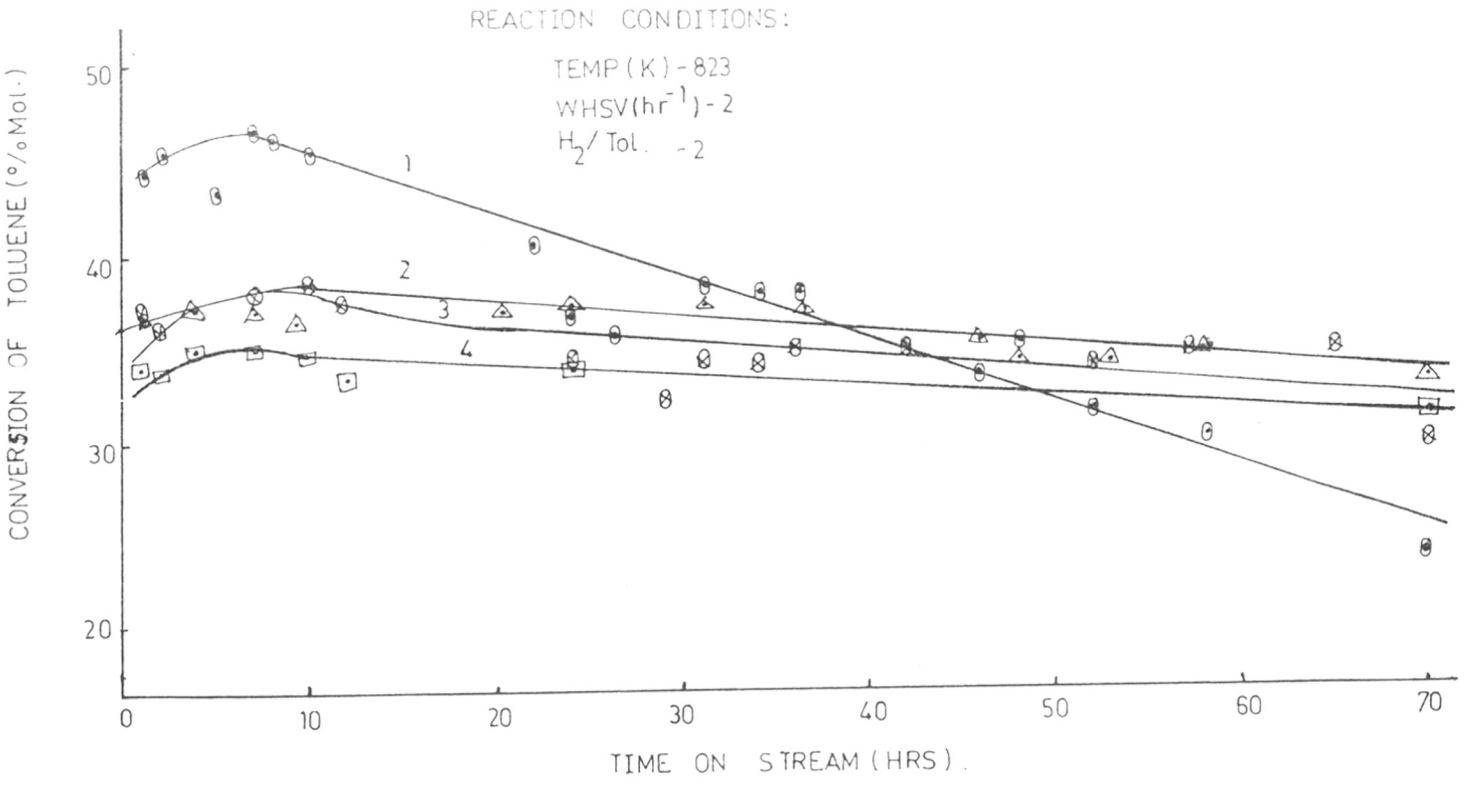

FIG. 3.18 CATALYTIC DEACTIVATION OF H ZSM-5 AND NiHZSM-5 . CURVES 1-4 ARE RESPECTIVELY FOR HZSM-5 NiHZSM-5 (2·20) NiHZSM-5 (1.1) AND NiHZSM-5 (0·55). THE FIGURES IN BRACKET REFER TO % Wt. OF NICKEL .

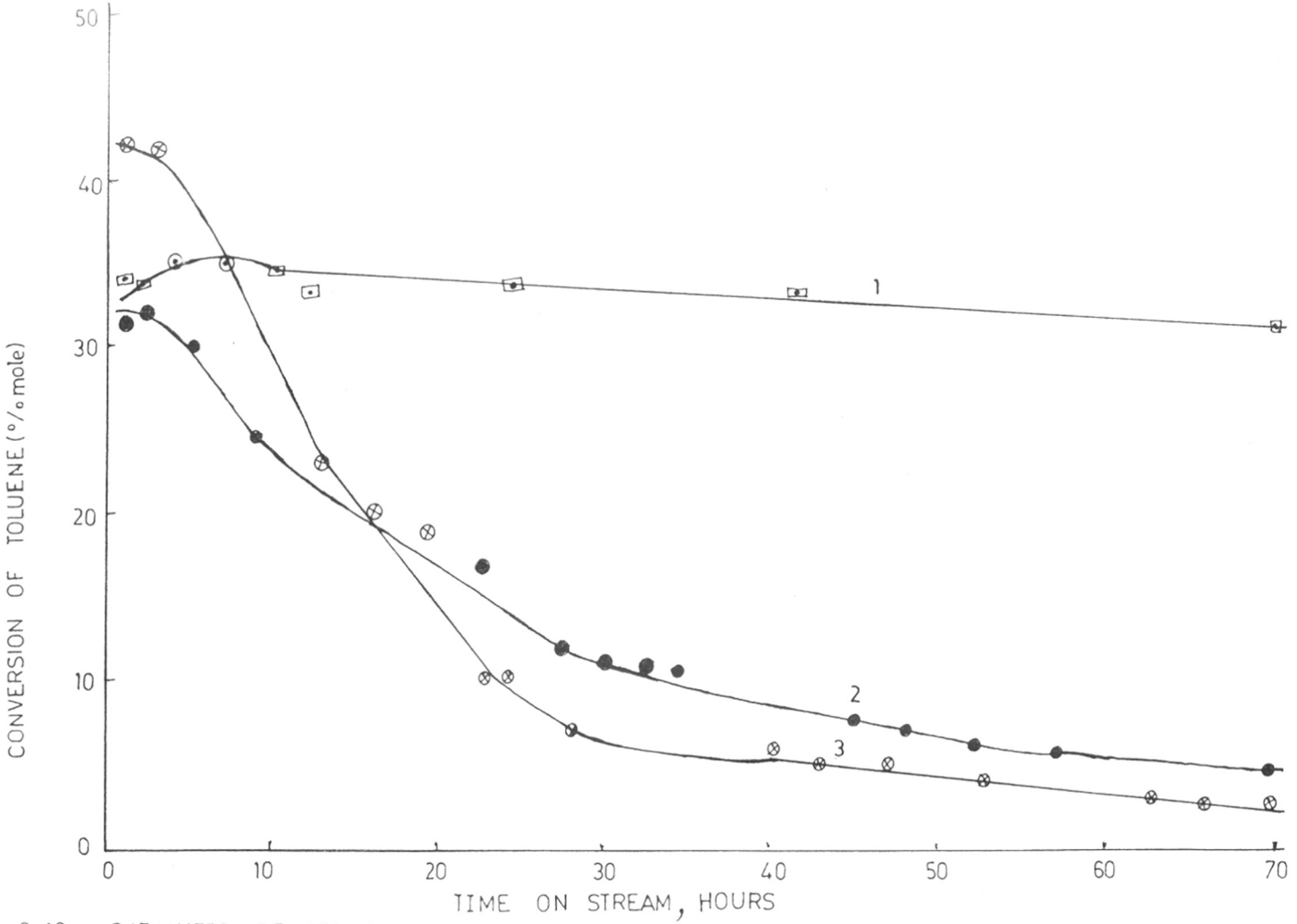

FIG. 3.19. CATALYTIC DEACTIVATION OF NiHZSM-5 ZEOLITE DURING THE DISPROPORTIONATION IN PRESENCE OF H_2,N_2 AND IN THE ABSENCE OF H_2 AND N_2 (CURVES 1-3 RESPECTIVELY).

TABLE - 3.14

Catalytic deactivation (α) and initial activity (K_o) parameters

Sr.No.	Sample	$\alpha(10^{-3})(g^{-1}sec^{-1})$	$K_o(sec^{-1})$
1.	HZSM-5	15.3	0.84
2.	NiHZSM-5 (0.55)	2.5	0.49
3.	NiHZSM-5 (1.11)	4.27	0.52
4.	NiHZSM-5 (2.22)	4.3	0.56
5.	NiHZSM-5 (2.22)	100	0.50
6.	NiHZSM-5 (2.22)	125	0.54

The figure in bracket represents the wt. % of Ni^{2+}.

Samples 1-4 represent reaction in presence of hydrogen and samples 5 and 6 represent reaction in presence of nitrogen and in absence of carrier respectively.

produce the hypothetical $HAlCl_4$ acids[3] (Eq.4). The proton from this acid attacks the ring carbon atom to form a carbonium ion salt (Eq.5). The alkyl group could then be transferred to a second aromatic ring in the transalkylation step. Zeolites are also known as strong proton donors having very strong protonic sites, hence an analogous mechanism to Friedel-Crafts reaction has been suggested[113,28]. The zeolites, such as X, Y and mordenite yield the equilibrium composition of o-, m- and p-xylene in the toluene disproportionation reaction. However, the ZSM-5 zeolite, a new shape selective catalyst, yields more p-xylene than its equilibrium composition among xylenes at the expense of o- and m-xylenes. The ZSM-5 zeolites modified with coke or/and easily accessible inorganic compounds yield near about 80-90% para-xylene. This selectivity of ZSM-5 for para-directed compound is well explained by Kaeding et al[28] who have suggested the mechanism for the formation of benzene and para-xylene. The proton from the acid form of the zeolite, H^+ zeolite $^-$ attacks a toluene molecule at the ipso position [Eq. (6), Fig. 3.4]. This weakens the carbon-methyl bond [Eq.(7)] and initiates transfer to a second toluene molecule, Eq. (8). Since this reaction occurs within the zeolite pores, the para-position is least hindered by snug fitting of aromatic rings and consequently would be most available for

attack. Transfer of proton back to an anionic site in the catalyst from the protonated xylenes gives the xylene product and regenerates the acid site in the catalyst, Eq. (9)[p.98]. Ortho and meta-xylene also isomerize to para-isomer within the zeolite pores.

C O N C L U S I O N S

The conclusions drawn from the present results are:

(1) The temperature at which zeolite ZSM-5 is activated has significant effect on toluene disproportionation activity. The NH_4ZSM-5 zeolite activated at 823 to 873 K has the highest activity. This is consistent with the removal of the last ammonia molecule from NH_4ZSM-5 and generation of protons that form ultra-active Brönsted acid sites.

(2) The acid sites of highest strength are not suitable for toluene disproportionation reaction but lead to rapid coking of the surface of the zeolite. On the other hand, these promote the dealkylation and cracking of toluene to benzene and gaseous products like methane, ethane, etc.

(3) The HZSM-5 zeolite modified with nickel is capable of maintaining a high selectivity at high conversion and stable activity in the toluene disproportionation reaction.

(4) The HZSM-5 based catalysts modified with boron, magnesium and phosphorous provide a novel route for the synthesis of p-xylene via toluene disproportionation.

(5) The selectivity and deactivation due to coke formation in toluene disproportionation can be controlled either by controlling aluminium content in the ZSM-5 zeolite framework or by incorporating transition metals like nickel in the zeolite.

(6) The presence of nickel in the zeolite ZSM-5 catalyst does not confer on it any additional stability if there is no hydrogen in the reactant stream.

———— .... ————

CHAPTER IV

TOLUENE TRANSALKYLATION

4.1. INTRODUCTION

Aromatic hydrocarbons, especially benzene and xylenes, are major raw materials used in the manufacture of nylon, polystyrene, polyester fibres etc. These industrially important raw materials are obtained by the pyrolysis and catalytic reforming of naptha. In these processes, large amounts of less valuable toluene and C_9 hydrocarbons are formed and can be converted to benzene and xylenes by disproportionation and/or transalkylation reactions using suitable acidic catalysts, like Friedel-Crafts catalysts in the liquid phase and silica-alumina or synthetic zeolites in the vapour phase.

Different zeolites such as mordenite[11,19], faujasite[10] or ZSM-5 in the H form have been reported to be active catalysts for these reactions. Both mordenite and faujasite based catalysts are active for the transalkylation reaction, showing high initial activity. However, these catalysts deactivate fast due to the formation of carbonaceous deposits on the active sites within the pores of the catalysts. The catalyst deactivation can be diminished or even eliminated by modifying the acid strength distribution of the active sites or by incorporating metals which are active for hydrogenation of the coke precursor species in presence of hydrogen[19].

As discussed in Chapter I, mordenite is an active catalyst for disproportionation of toluene to benzene and xylene and has recently been examined for the transmethylation of toluene and pseudocumene as H and NiH mordenite[129]. In contrast to toluene disproportionation studies, the literature contains very few reports on the transalkylation of C_7 and C_9 aromatics to xylenes.

In view of the known superiority, especially catalyst stability over long period of time of the ZSM-5 zeolites over the earlier zeolites for the disproportionation of toluene, the transalkylation of C_7 and C_9 aromatic hydrocarbons over HZSM-5 zeolites, with different SiO_2/Al_2O_3 ratio was investigated. Likewise, a series of dealuminated mordenites and mordenite-HZSM-5 blends in varying proportions have been examined and their catalytic activity for transalkylation reported in the following.

4.2. EXPERIMENTAL

The synthesis and modification of the ZSM-5 zeolite have been described in the earlier Chapter. The hydrogen mordenite (Norton, $SiO_2/Al_2O_3 = 10$) was dealuminated according to a procedure described[130,131] elsewhere. The H mordenite (HM) was heated in presence of steam at 573 to 873 K, cooled and treated with 2 to 6N HCl to alter their

SiO_2/Al_2O_3 ratios. The samples thus treated were washed free of chloride ions, dried and water saturated over NH_4Cl solutions. The SiO_2/Al_2O_3 ratios were estimated by a wet chemical analysis and flame photometry. The unit cell compositions of the various dealuminated mordenites(DHM) are illustrated in Table 4.1. The XRD patterns (Fig.4.1) indicated that all the samples were at least 90% crystalline.

The adsorption of 1.3.5 and 1.2.4 - TMB isomers was measured at 298 K and P/P_o = 0.5 using the gravimetric McBain quartz balance following the activation procedure described earlier (Chapter 2). The procedure for performing the catalytic reactions, as described in Chapter 3, was followed.

4.3. RESULTS AND DISCUSSION

The SiO_2/Al_2O_3 mole ratio and adsorption of water, benzene, toluene, para-xylene, cyclohexane, ortho-xylene and 1,2,4-trimethylbenzene on HZSM-5 samples 1 to 5 have been summarized in Table 2.6 in Chapter 2. It was observed that the adsorption of benzene, toluene and para-xylene did not vary significantly in Samples 1 to 5, while the uptake of cyclohexane, o-xylene and 1,2,4-trimethylbenzene decreased in the samples with higher SiO_2/Al_2O_3 values. The restricted adsorption of the above molecules indicated a partial blocking of pore mouth in the sample with higher SiO_2/Al_2O_3 ratio.

TABLE - 4.1

Chemical composition of zeolite sample

Sr.No.	Sample	SiO_2/Al_2O_3	chemical formulae
1.	HZSM-5	36	$Na_{0.02}(SiO_2)_{90.98}(AlO_2)_{5.02}{}^{15}H_2O$
2.	HM	10.2	$Na_{0.1}(SiO_2)_{40.13}(AlO_2)_{7.87}{}^{25}H_2O$
3.	Dealuminated HM (DHM)	25.6	$Na_{0.08}(SiO_2)_{44.48}(AlO_2)_{3.52}{}^{20}H_2O$
4.	Dealuminated HM (DHM)	32.70	$Na_{0.06}(SiO_2)_{45.23}(AlO_2)_{2.77}{}^{12}H_2O$
5.	Dealuminated HM (DHM)	57.43	$Na_{0.05}(SiO_2)_{46.38}(AlO_2)_{16.2}{}^{9.5}H_2O$

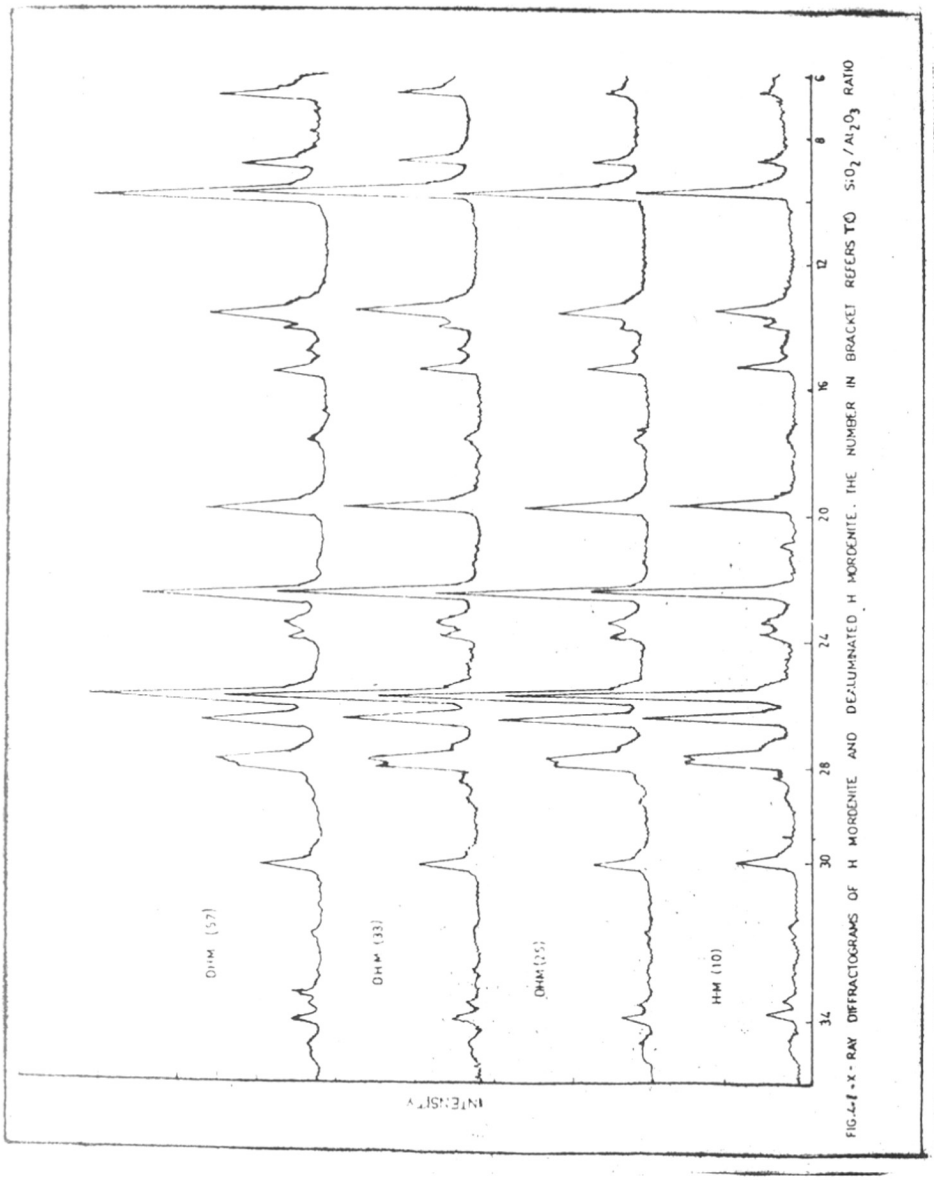

FIG. 4.1 X-RAY DIFFRACTOGRAMS OF H MORDENITE AND DEALUMINATED H MORDENITE. THE NUMBER IN BRACKET REFERS TO SiO_2/Al_2O_3 RATIO

(A): Influence of SiO_2/Al_2O_3 ratio on transalkylation reaction

The influence of SiO_2/Al_2O_3 ratio on the transalkylation reaction is shown in Table 4.2. The composition of the feed is given in Table 4.3. The xylenes in the product had an equilibrium composition. The aliphatic hydrocarbons comprised of methane and ethane. It may be noted that while xylene can be formed by the transalkylation of toluene and C_9 aromatics as well as by the dealkylation of trimethylbenzenes (TMB), benzene is formed mainly by the disproportionation of toluene. This is reflected in the lower benzene/xylene mole ratio in the product. While the conversion of toluene and C_9 aromatics decreasesat higher SiO_2/Al_2O_3 values, the selectivity (denoted by the B/X ratio) is almost independent of this parameter.

(B): Influence of temperature

The influence of temperature is shown in Table 4.3. The major reactions that occur during the transalkylation are summarized in Fig. 4.2. As reaction temperature is increased, the following features are observed:

(i) The conversion of both toluene and C_9 aromatics to products increases. Among the C_9 aromatics, the ethyltoluenes (mostly the para-isomer) are easily dealkylated to toluene while the 1.3.5 TMB isomer does not undergo any

TABLE - 4.2

Influence of SiO_2/Al_2O_3 ratio in HZSM-5 zeolites on transalkylation of toluene with C_9 aaromatics

Reaction conditions

Temperature (K)	-	723
Pressure (bar)	-	Atmospheric
H_2/HC(mol)	-	2
WHSV (hr^{-1})	-	2

Product(% mole)	Feed	Sample (SiO_2/Al_2O_3 ratio)				
		36	86	144	165	320
Aliphatics	-	0.50	0.40	0.10	0.10	0.30
Benzene	-	6.60	7.90	3.60	3.80	1.70
Toluene	77.5	68.20	68.10	73.8	74.5	76.5
Ethylbenzene	0.22	0.62	0.71	0.52	0.48	0.38
Xylenes	-	9.4	10.20	5.30	5.40	3.30
C_9 aromatics	21.4	15.3	13.40	17.20	16.30	18.20
Benzene/xylenes mole ratio	-	0.70	0.77	0.68	0.70	0.52
% Toluene Conversion		12	12.1	4.77	3.87	1.29

TABLE - 4.3

Influence of temperature on the transalkylation reaction

Reaction conditions

Sample -- HZSM-5 (SiO_2/Al_2O_3 = 36 with 15 % binder).

Pressure (bar) - 20

WHSV (hr^{-1}) - 0.70

H_2/HC (mol) - 2

Product (% wt.)	Feed	Temperature (K)			
		633	673	723	773
Aliphatics	-	0.4	0.6	0.7	0.8
Benzene	-	6.7	11.1	19.2	26.4
Toluene	77.2	64.6	58.7	47.9	45.9
Ethylbenzene	0.22	0.62	0.57	0.68	0.84
P-Xylene	-	2.5	3.8	5.4	4.0
M-Xylene	-	5.4	8.3	10.7	8.80
O-Xylene	1.24	2.9	3.9	4.5	4.8
Ethyl toluenes	7.0	4.3	2.5	1.4	1.2
1,3,5 TMB	2.4	2.6	2.5	2.2	1.7
1,2,4 TMBB	9.4	8.4	7.4	6.4	4.9
1,2,3 TMB	1.9	1.5	1.3	1.2	1.0
C_{10} aromatics	0.9	0.7	0.6	0.5	0.5
B/X mole ratio	-	0.84	0.94	1.27	2.0
% Tol. Conversion	-	16.65	24.26	38.19	40.77

Note - TMB = trimethylbenzene

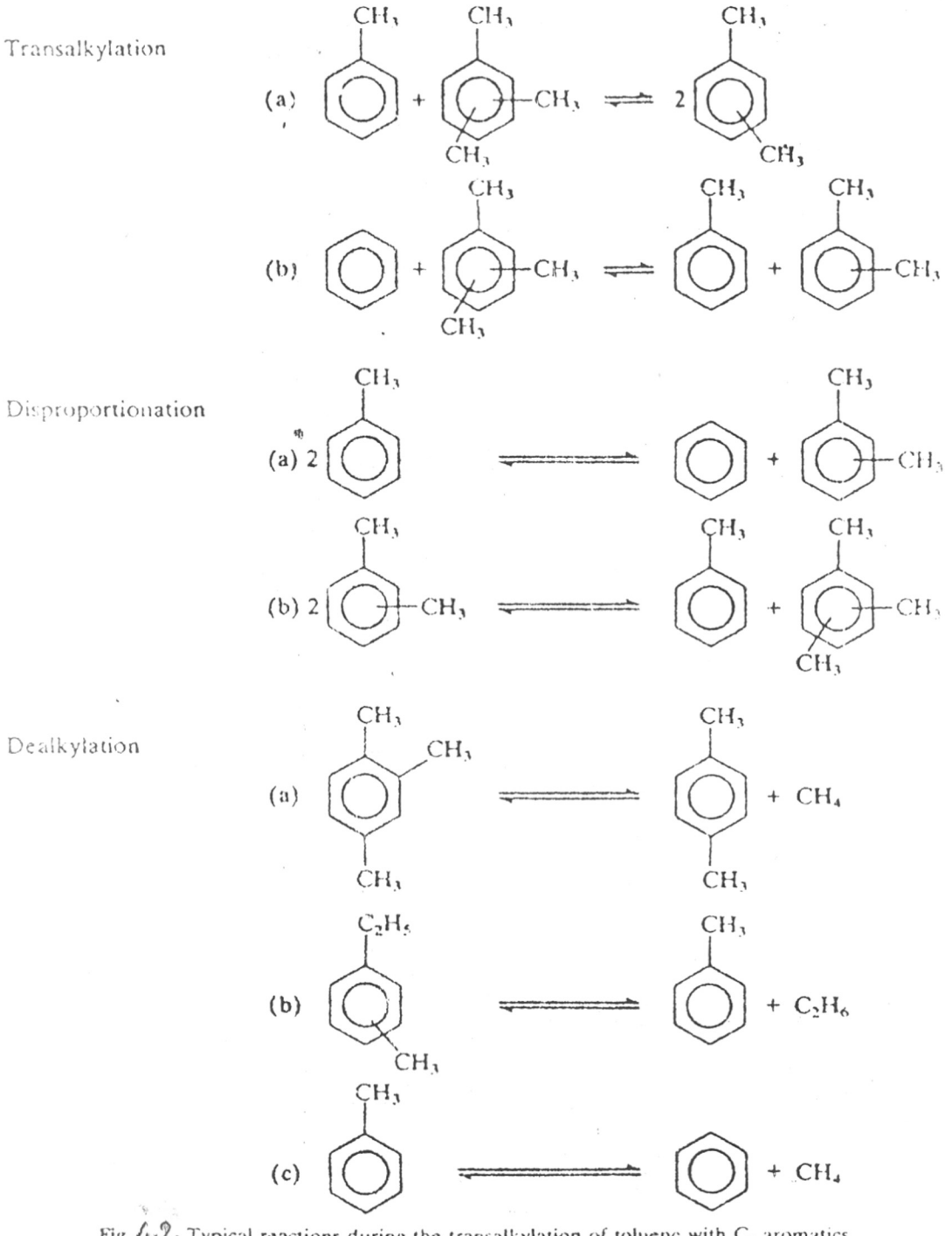

Fig. 4.2. Typical reactions during the transalkylation of toluene with C_9 aromatics.

significant conversion except at 773 K. The lower reactivity of the 1.3.5 TMB isomer is due to its restricted access into the pores of ZSM-5 zeolites. It may be noted that while the kinetic diameter of 1.3.5 TMB is 0.86 nm, the diameters of pores in ZSM-5 zeolite channel is only 0.56 nm.

(ii) The molar ratio of benzene to xylenes in the product increases from 0.84 to 2.0 in the temperature range 633 to 773 K and benzene is formed mainly by the disproportionation/dealkylation of toluene. At higher temperatures the toluene conversion increases due to predominance of the dealkylation reaction. Our results indicate that the dealkylation reactions require a higher activation energy than toluene disproportionation and that the stronger acid sites generated at higher temperatures are the active centres for the dealkylation of toluene. It may be remembered that thermodynamically dealkylation reaction is more favoured than disproportionation reaction (Δ F 298 = - 10.7 vs + 1.4 K Cal mol^{-1})[116b].

(C) Influence of H_2/hydrocarbon ratio

The influence of H_2/hydrocarbon ratio on the transalkylation reaction is shown in Table 4.4. A decrease in the hydrocarbon partial pressure (i.e. by increasing the H_2/hydrocarbon ratio) leads to the

TABLE - 4.4

Influence of hydrogen/hydrocarbon ratio

Sample - HZSM-5, SiO_2/Al_2O_3 = 36 with 15% binder

Reaction conditions

Temp. (K) - 773

WHSV (hr^{-1}) - 1.2

Pressure(bar) - 20

Product (% wt.)	Feed	Hydrogen/hydrocarbon(mol)		
		2	5	10
Aliphatics	-	0.8	0.5	0.3
Benzene	-	24.4	21.0	16.9
Toluene	77.5	44.5	46.8	49.6
Ethylbenzene	0.22	0.74	0.64	0.5
P-Xylene	-	4.4	4.6	5.1
M-Xylene	-	10.0	9.8	9.9
O-Xylene	1.20	5.2	5.1	4.6
Ethyl toluenes	7.0	1.1	1.2	1.1
1,3,5 TMB	2.4	1.9	2.4	2.6
1,2,4 TMB	9.4	5.3	7.0	7.9
1,2,3 TMB	1.9	1.0	1.3	1.4
C_{10} aromatics	0.9	0.8	0.5	0.5
B/X mole ratio		1.67	1.46	1.17
% Tol. Conversion		42.5	39.61	36.00

TMB = Trimethyl benzene

following changes in the product distribution:

(i) A decrease in the production of benzene without significant change in the xylene concentration;as a consequence, B/X ratio decreases.

(ii) A decrease in the conversion of trimethylbenzene and toluene, due to the decrease in the contact time. It is significant to note that the production of para-xylene is increased among the xylenes. This may be due to the reduction of residence time in the catalyst bed for isomerization.

(iii) The hydrocracking of ethyl toluenes to toluene and ethane is insensitive to the H_2/hydrocarbon ratio under these conditions.

(D): Influence of pressure

The influence of pressure on transalkylation reaction is illustrated in Table 4.5. The toluene conversion increases with increasing pressure. However, it is surprising to note that the conversion of trimethylbenzenes (TMB) is not affected by increasing the pressure. This is probably due to fact that since the kinetic diameter of the TMBs are larger than those of the pores in the ZSM-5 zeolites, they are not able to enter the pores and undergo transalkylation. The transalkylation reactions (especially

TABLE - 4.5

Influence of pressure on the transalkylation reaction

Sample - HZSM-5, SiO_2/Al_2O_3 = 36 with 15% binder

Reaction conditions

Temperature (K)	673
WHSV (hr^{-1})	0.70
H_2/hydrocarbon (mol)	2

Product (% wt)	Feed	Pressure (bar)			
		15	20	24	30
Aliphatics	-	0.5	0.6	0.50	0.6
Benzene	-	9.3	11.1	11.6	11.8
Toluene	77.5	60.5	58.7	58.3	56.6
Ethylbenzene	0.22	0.73	0.57	0.54	0.72
P-Xylene	-	4.3	3.8	3.8	4.0
M-Xylene	-	6.7	8.3	8.3	8.40
O-Xylene	1.2	2.9	3.9	4.0	3.9
Ethyl toluenes	7.0	3.5	2.5	2.3	2.1
1,3,5 TMB	2.4	2.5	2.5	2.5	2.5
1,2,4 TMB	9.4	7.9	7.4	7.4	7.5
1,2,3 TMB	1.9	1.5	1.3	1.3	1.3
C_{10} aromatics	0.9	0.40	0.6	0.5	0.6
B/X mole ratio		0.91	0.94	0.98	0.98
% Tol. conversion		21.94	24.26	24.77	26.97

of the bulky 1.3.5 TMB) occurs essentially on the external surface, while the disproportionation of toluene takes place within the pore system. This is confirmed by the fact that when the transalkylation reaction was carried out over a prolonged period of time, the deactivation of the transalkylation reaction (to yield xylenes) was faster than the toluene disproportionation (to yield benzene and xylenes). If it is assumed that 'coking' occurs initially on the external surface of ZSM-5 crystals, wherein trimethylbenzene molecules are adsorbed and undergo transalkylation, the deactivation of such sites would suppress mainly the transalkylation reaction. Toluene disproportionation, on the other hand, occurs mainly within the zeolite pore system due to much smaller kinetic diameter of the toluene molecule and hence would not be affected to the same extent.

(E): NiHZSM-5 Catalyst

One drawback of the HZSM-5 zeolites investigated so far, is their relatively fast deactivation during toluene disproportionation/transalkylation as shown in Fig. 4.3, curve 1. Incorporation of nickel was found to suppress catalyst aging as shown in Fig. 4.2, curve 2. The product distribution at two different reaction conditions over NiHZSM-5 zeolite is illustrated in Table 4.6. At 773 K, 20 bar pressure and WHSV = 2, the disproportionation/trans-

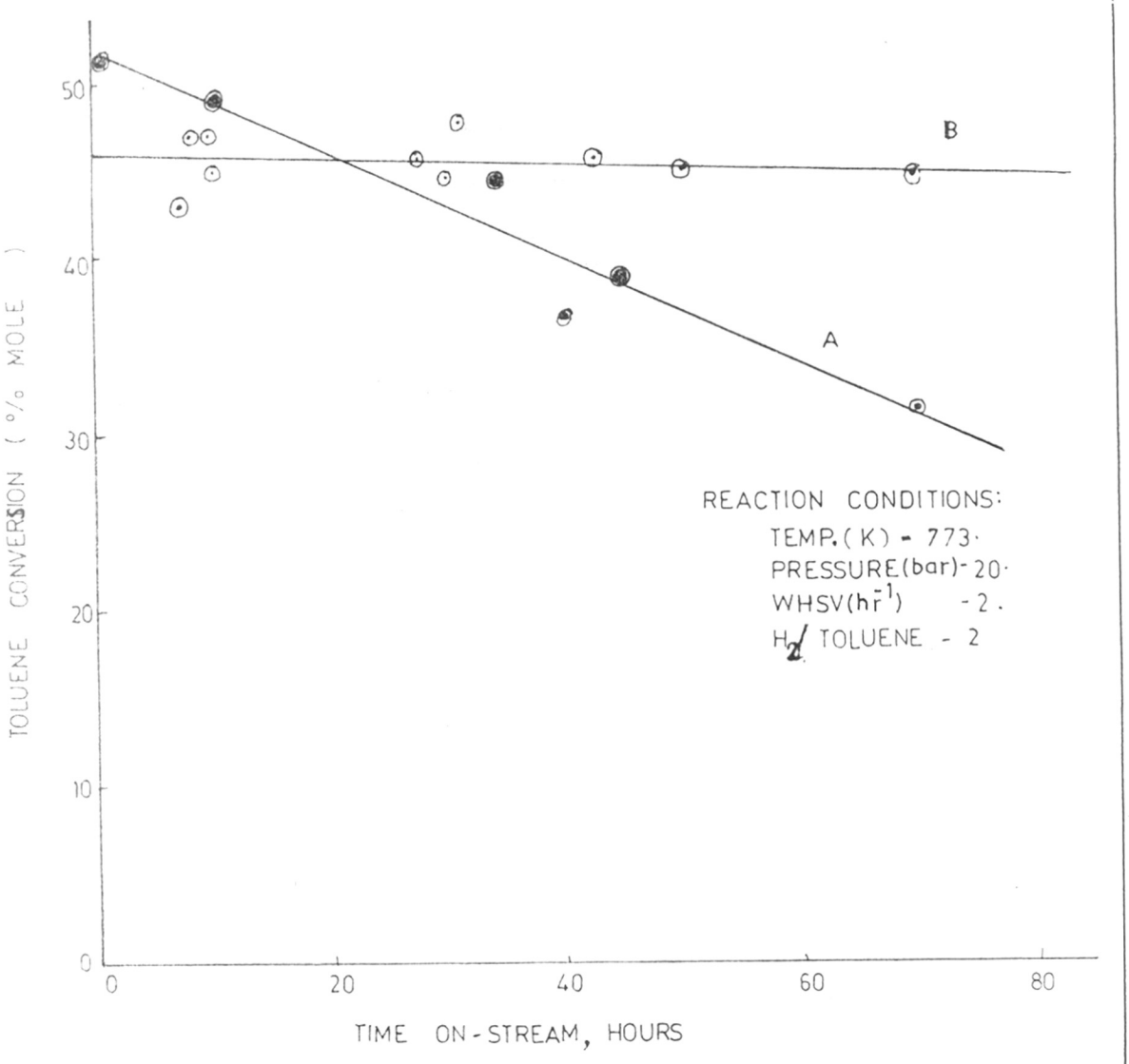

FIG. 4.3. CATALYTIC DEACTIVATION OF HZSM-5 (A) & NiHZSM-5(B) DURING TOLUENE TRANSALKYLATION.

TABLE - 4.6

Transalkylation reaction over NiHZSM-5

Sample - NiHZSM-5, (SiO_2/Al_2O_3 = 36 with 15% binder)

H_2/hydrocarbon (mol) - 2

Pressure (bar)	-	20	30
WHSV (hr^{-1})	-	2	4
Temperature (K)	-	773	743

Product (% wt.)	Feed		
Aliphatics	0.9	0.8	0.8
Benzene	0.2	17.6	15.4
Toluene	71.2	40.0	42.4
Ethylbenzene	-	1.0	0.6
P-Xylene	-	5.5	6.4
M-Xylene	-	11.6	11.6
O-Xylene	1.3	5.4	5.0
1,4 Ethyltoluene	2.7	0.4	0.9
1,3 Ethyltoluene	4.6	1.0	2.2
1,2 Ethyltoluene	1.4	0.7	0.9
1,3,5 TMB	3.1	3.4	2.4
1,2,4 TMB	10.8	9.6	8.4
1,2,3 TMB	2.2	1.8	1.7
C_{10} aromatics	0.9	1.2	1.4
B/X mole ratio		1.06	1.0
% Tol. conversion		43.82	40.31

alkylation of toluene was maintained above 44% (wt.) for a period of more than 70 hours without any deactivation. Unlike NiH mordenites the NiHZSM-5 zeolites suppressthe coke formation. The main role of nickel is in keeping the surface clean by hydrogenating the coke precursors that are formed during the transalkylation process.

4.4. Catalytic activity of dealuminated mordenites in C_7 and C_9 transalkylation reaction

The dealumination of zeolites has been widely employed in catalyst preparation to enhance their activity, thermal and hydrothermal stability and prolong the active life. It has been found that controlled dealumination of zeolites, X, Y and mordenite, can be achieved without altering their crystal structure while simultaneously improving their sorption characteristics and surface acidity.

(A): Adsorption of TMB isomers

It was observed earlier[132] that 1.2.4 TMB was predominantly formed during the shape selective disproportionation of xylene on CuH mordenite, the fraction of 1.2.4 isomer in the TMB formed being 78% at 20% total yield. This was attributed to smaller (0.76 nm) molecular dimension of 1.2.4 TMB as compared to 1.3.5 isomer (0.86 nm). The sorption curves of 1,2,4 and 1.3.5 TMB isomers in mordenites

at 298 K are illustrated in Figs. 4.4 and 4.5 respectively. The uptake of 1.3.5 TMB in HM-10 (H mordenite SiO_2/Al_2O_3 = 10) and DHM-25 (dealuminated mordenite) is slow and equilibrium is not reached even after exposing the sample to the 1,3,5-trimethylbenzene vapour for 120 minutes, probably due to diffusional restrictions, imposed on the bulky 1,3,5-trimethylbenzene molecules in the H mordenite pores. On the other hand, the uptake is fast and equilibrium adsorption is reached within 20 minutes exposure in HM-33 and DHM-57. Furthermore, the sorption capacity for the 1,3,5-trimethylbenzene increases with increasing the SiO_2/Al_2O_3 ratio of the sample, that is with increasing the degree of dealumination. Similar results are obtained for the adsorption of 1,2,4-trimethylbenzene in the dealuminated mordenite samples. The sorption capacity for both the TMB isomers follows the sequence

DHM57 > DHM33 > DHM25 > HM10.

The equilibrium adsorption data illustrated in Table 4.7 shows that among the two trimethylbenzene isomers the uptake of 1,2,4-isomer is very much larger than 1,3,5-isomer The increasing uptake of trimethylbenzene isomers with increasing the degree of dealumination of the HM samples indicates the channels of mordenite becoming more accessible to TMB after acid treatment which removes the occluded amorphous material from the zeolite pores.

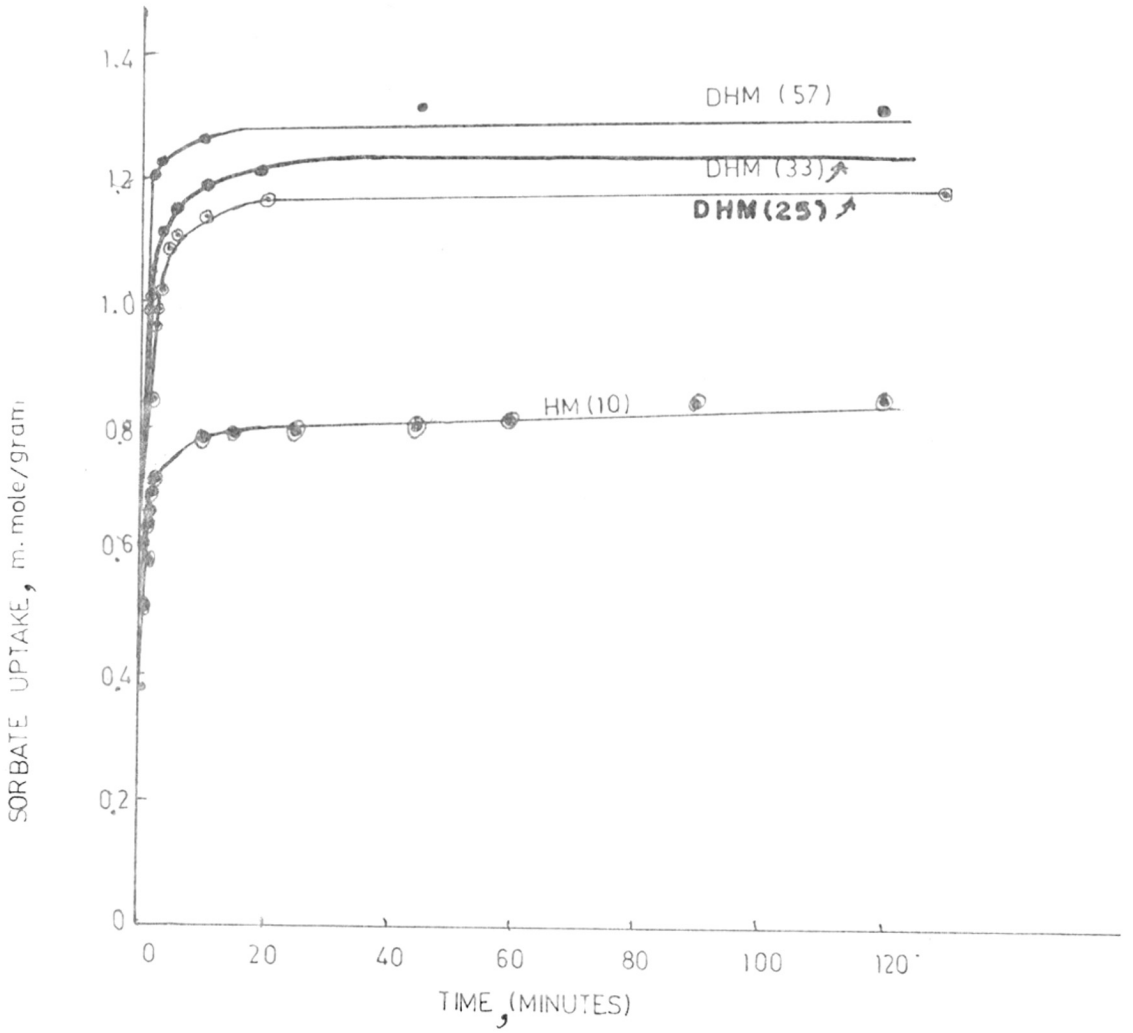

FIG. 4.4. ADSORPTION OF 1,2,4 TRIMETHYLBENZENE ON H-MORDENITE AND DEALUMINATED H-MORDENITES. THE NUMBERS IN BRACKETS REFER TO SiO_2/Al_2O_3.

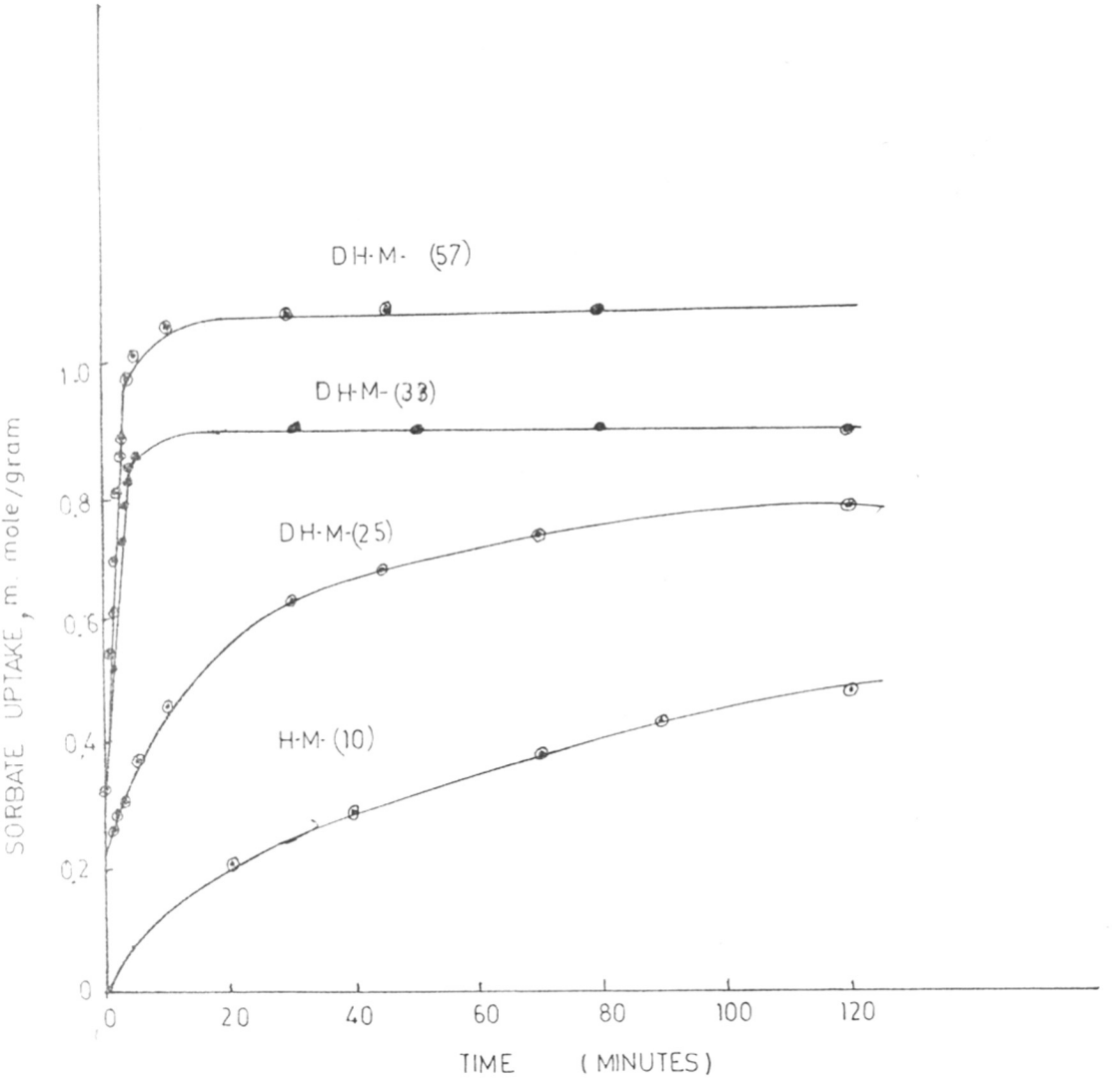

FIG. 4.5. ADSORPTION OF 1,3,5 TRIMETHYLBENZENE ON H – MORDENITE (H-M) AND DEALUMINATED H- MORDENITE (DHM). THE FIGURES IN BRACKETS REFER TO SiO_2/Al_2O_3 RATIO.

TABLE - 4.7

Sorption of trimethylbenzenes over mordenite and HZSM-5 blended with mordenite catalyst

Sample	SiO_2/Al_2O_3 ratio	Sorbate uptake mmoles/gram	
		1,2,4 TMB	1,3,5 TMB
1. HM	10	0.85	0.48
2. DHM	25	1.20	0.76
3. DHM	33	1.25	0.76
4. DHM	57	1.30	1.08
5. HZSM-5	36	0.35	-
7. HZSM-5 (80%)	36	0.82	-
7. HZSM-5 (50%)	36	1.0	-
8. HZSM-5 (25%)	36	1.08	-

Sample Nos. 6-8 refer to HZSM-5 blended with mordenite catalysts. Sample 2 has been used for blending.

Fig. 4.6 represents the uptake of 1.2.4 TMB in HZSM-5 and DHM-25 mixtures of various compositions with SiO_2/Al_2O_3 ratio 36 and 25 respectively. As expected, the rate as well as uptake increases with the increase of the DHM-33 content in the blend.

(B): Influence of SiO_2/Al_2O_3 ratio

The influence of SiO_2/Al_2O_3 ratio of dealuminated hydrogen mordenite for transalkylation reaction of toluene with C_9 aromatics, mainly trimethylbenzenes, is illustrated in Table 4.8. The detailed product distribution along with feed composition is also given. The B/X molar ratio in the product are lower than unity which indicates that the transalkylation has occured between toluene and trimethylbenzenes. Toluene conversion by disproportionation/transalkylation is found to decrease from 45 to 29 (% wt.) with increasing SiO_2/Al_2O_3 ratio. The lower activity of the high SiO_2/Al_2O_3 ratio mordenite compared to SiO_2/Al_2O_3 = 10 could be attributed to the decrease in the number of Brönsted acid sites which are directly related to the aluminium content in the zeolite framework, since these reactions (Fig. 4.2) are catalysed by Brönsted acid sites[11,133]. However, the selectivity (defined as B/X molar ratio in the product) increases with increasing SiO_2/Al_2O_3. This shows that the acid sites of the lower strength may be active for the disproportionation/transalkylation of toluene, since the strength of acid sites decreases with increasing SiO_2/Al_2O_3 ratio[134].

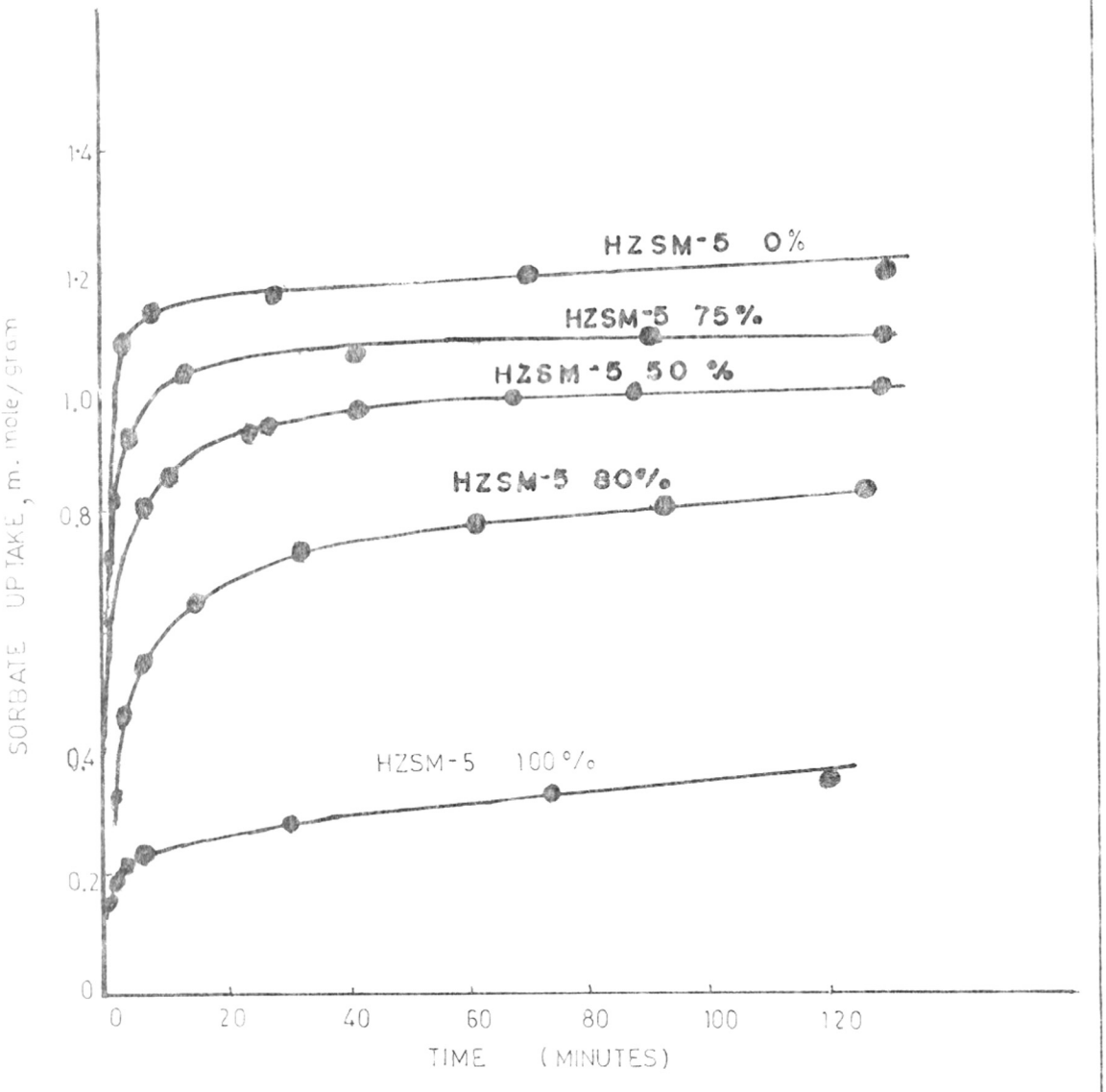

FIG. 4.6. ADSORPTION OF 1, 2, 4 TRIMETHYLBENZENE ON HZSM-5 & HZSM-5 BLEND WITH DEALUMINATED HYDROGEN MORDENITE .

TABLE - 4.8

Influence of SiO_2/Al_2O_3 ratio of H-mordenite on transalkylation of toluene with C_9 aromatics

Reaction conditions :

Temp. (K) - 673
Pressure (bar) - Atmospheric.
WHSV (hr-1) - 2
H_2/feed (mole) - 2

Sample		HM (10)	DHM (25)	DHM (33)	DHM (57)
Product distribution (% wt.)	Feed				
Aliphatics	0.32	2.63	2.33	1.66	1.57
Benzene	0.09	14.41	15.81	12.27	8.00
Toluene	76.06	41.82	44.59	48.68	53.84
E-Benzene	0.20	0.75	0.74	0.95	1.02
P-Benzene	0.16	7.16	6.55	6.56	5.92
M-Xylene	0.24	16.03	15.40	14.49	13.29
O-Xylene	0.73	7.14	6.58	6.50	5.80
1,4, E-Toluene	2.00	0.37	0.33	0.49	0.64
1,3, E-Toluene	3.35	0.79	0.70	1.03	1.34
1,2, E-Toluene	1.15	0.21	0.18	0.28	0.35
1,3,5 TMB	2.66	0.02	1.76	1.63	1.85
1,2,4 TMB	9.46	5.37	5.05	4.32	5.01
1,2,3 TMB	2.31	0.83	0.72	0.69	0.83
C_{10} aromatics	1.2	0.48	0.24	0.42	0.50
B/X mole	-	0.65	0.75	0.60	0.44
% Toluene conversion	-	45.0	41.37	35.99	29.21
% C_9 conversion	-	54.18	58.24	59.67	52.12

Note - The number in bracket below the code refers to SiO_2/Al_2O_3 ratio. DHM = Dealuminated mordenite.

It is interesting to note that by leaching out aluminium with HCl from the original mordenite (SiO_2/Al_2O_3 = 10), the diffusivity and sorption capacity for trimethylbenzenes increases. However, the present results show that toluene conversion decreases eventhough the diffusivity and sorption capacity increase indicating that the toluene disproportionation/transalkylation with 1,2,4-trimethylbenzene is independent of sorption and diffusion over these catalysts. The acidity seems to play a dominant role as in the n-pentane hydroisomerization[135] and hexanone cracking reactions[136]. In contrast, the conversion of 1.3.5-trimethylbenzene increases with increasing diffusion and sorption. Hence, pore accessibility seems to be a dominant factor for the occurrence of this latter reaction[137].

The influence of SiO_2/Al_2O_3 ratio on catalyst stability is shown in Fig. 4.7. To describe the rate of deactivation of the samples 1-4, (Table 4.9), in the toluene transalkylation, the activity of the catalyst was characterized by an apparent first order rate constant K, where

$$K = \frac{1}{W} \ln \frac{1}{1-x} \qquad \ldots\ (1)$$

where W = weight of catalyst in grams and X = fractional conversion. The values of K derived from the equation (1) above were fitted to the following equation

$$K = K_o\, e^{-\alpha Y}$$

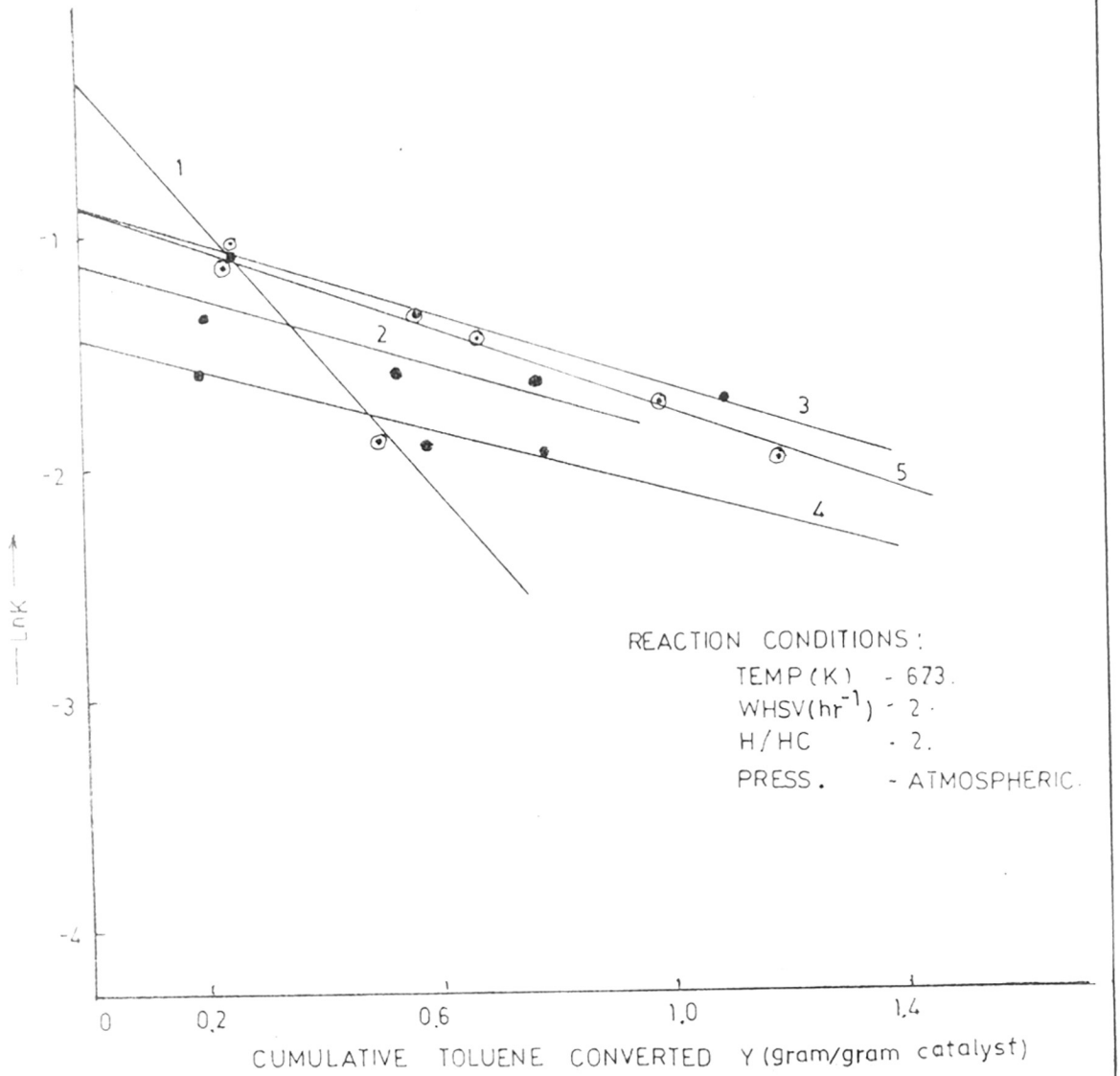

FIG. 4.7. INFLUENCE OF SiO_2/Al_2O_3 RATIO ON THE AGING OF MORDENITE CATALYST. NUMBERS 1-4 REFER TO SiO_2/Al_2O_3 RATIOS 10, 25, 33 AND 57 RESPECTIVELY. NUMBER 5 REFERS TO NiHM. (SiO_2/Al_2O_3 RATIO 10).

where Y is the cumulative amount of toluene that has been converted to products and K_o and α are constants which are the initial activity and aging rate of the catalyst respectively. The value of K_o and α for the samples 1-4 calculated by fitting experimental data to equation 2 are given in Table 4.9.

It can be seen that the sample with high aluminium content deactivates faster due to deposition of coke. It may be noted that the coke formation on zeolites takes place via polymerization of olefins that are formed in the cracking process[137,137]. The formation of gaseous aliphatic products in the samples increases with decreasing SiO_2/Al_2O_3 ratio (Table 4.8) indicating intensive cracking over H-mordenite (HM-10, SiO_2/Al_2O_3 = 10) and results in fast deactivation.

(C): Activity of HZSM-5-mordenite blends

The HZSM-5 mordonite blends[d] (HZSM-5, SiO_2/Al_2O_3 = 36) samples were prepared by mixing appropriate amounts of the two zeolites in distilled water. The well homogenized slurry was then filtered and dried at 395 K and calcined at 823 K in presence of air. The resulting mixture was tested for toluene transalkylation reaction. The results are given in Table 4.10. As expected, on mixing the mordenite with HZSM-5 zeolite the trimethylbenzene conversion and xylene selectivity increase. This is due to the fact that the channels of

TABLE - 4.9

Catalytic deactivation (α) and initial activity (K_o) parameter for the hydrogen mordenite, dealuminated hydrogen mordenite

Sample	SiO_2/Al_2O_3	$\alpha(g^{-1} sec^{-1})$	$K_o(sec^{-1})$
1 HM	10	2.93	0.72
2 DHM	25	0.77	0.42
3 DHM	33	0.74	0.32
4 DHM	57	0.63	0.24

TABLE - 4.10

Toluene transalkylation with C_9 aromatics over HZSM-5 blended with dealuminated mordenite catalysts

Reaction conditions
Temp. (K) - 673
Pressure (bar) - Atmospheric
WHSV (hr^{-1}) - 2
H_2/feed(mol) - 2

Sample		HZSM-5 (100%)	HZSM-5 (80%)	HZSM-5 (50%)	HZSM-5 (25%)	DHM (100%)
Product (% wt.)	Feed					
Aliphatics	0.32	1.31	1.95	2.49	3.48	2.33
Benzene	0.09	3.20	8.45	14.20	18.16	15.81
Toluene	76.06	70.28	51.44	43.29	42.36	44.59
E Benzene	0.20	0.33	0.80	0.77	0.61	0.74
P-Xylene	0.16	1.47	6.14	7.06	6.58	6.55
M-Xylene	0.24	3.25	13.84	15.92	14.83	15.40
O-Xylene	0.73	1.41	6.10	7.07	6.64	6.58
1,4 E-Toluene	2.0	1.02	0.62	0.37	0.25	0.33
1,3 E-Toluene	3.35	2.08	1.33	0.80	0.52	0.70
1,2 E-Toluene	1.15	0.48	0.36	0.22	0.15	0.18
1,3,5 TMB	2.66	2.77	2.04	1.79	1.51	1.76
1,2,4 TMB	9.46	9.82	5.42	4.75	4.26	5.05
1,2,3 TMB	2.31	1.78	0.87	0.89	0.66	0.72
% Aromatics	1.2	0.62	0.60	0.76	0.76	0.54
B/X mole ratio	-	0.71	0.44	0.64	0.88	0.75
% Toluene conversion	-	7.59	32.29	43.08	44.30	41.75
% C_9 conversion	-	14.23	49.16	57.85	64.88	58.39

Note - The number below the code refers to the wt. % of HZSM-5 zeolite in dealuminated mordenite.

of mordenite are more accessible than the channels of ZSM-5 for the trimethylbenzenes which, in turn, provides more transalkylating centres. Further increasing the amount of mordenite in the blend, the C_9 conversion increases but the selectivity for xylene decreases, due to cracking and dealkylation reactions of toluene. This may be due to strong acid sites of mordenite , which are active in cracking and dealkylation reactions.

CONCLUSIONS

(1) It was found that while ZSM-5 based catalysts are, in general, quite suitable for the transalkylation reaction, problem might arise if the C_9^+ aromatics fraction contains a significant concentration of 1,3,5-trimethylbenzene. Owing to its larger diameter, this compound is unable to enter into the pores of ZSM-5 zeolite and undergo reaction.

(2) The transalkylation of toluene with C_9 aromatics to yield xylenes occurs mainly on the external surface of ZSM-5 crystals. The disproportionation of toluene to yield benzene and xylenes, on the other hand, takes place predominantly in the pore system. Among the trimethylbenzenes, the bulky 1,3,5-isomer does not undergo transalkylation as readily as the 1,2,3 and 1,2,4-isomers. In this respect, ZSM-5 zeolites differ significantly from H-mordenite wherein

both the reactions occur mainly in the pore system. This difference is due to smaller diameter in the ZSM-5 zeolites.

(3) In contrast to HZSM-5 zeolites, the mordenites and HZSM-5 blended mordenites offer good performance for the trans-alkylation of toluene with the mixture of C_9 isomers.

SUMMARY

ZSM-5 zeolites offer high performance over the classical shape-selective zeolites for a variety of reactions like the conversion of alcohol and syngas (CO + H_2) to hydrocarbons, alkylation, isomerization, disproportionation, naptha reforming etc. The architecture and the size of the ZSM-5 channel systems which matches with the size of the benzene molecule is one of the factors responsible for their superior performance.

A series of ZSM-5 zeolites with varying SiO_2/Al_2O_3 mole ratios have been prepared and characterized by chemical analysis, X-ray diffraction, DTA/TG, scanning electron microscopy, infrared spectroscopy, adsorption of hydrocarbons, temperature programmed desorption of ammonia and x-ray photoelectron spectroscopy. These zeolites have been modified by ion-exchange, thermal activation and incorporation of suitable modifiers like phosphorous, boron, magnesium, nickel and platinum. The catalysts thus prepared, have been further characterized by employing the above physico-chemical methods and their catalytic properties have been evaluated for toluene disproportionation and transalkylation reactions.

The diffusion and sorption properties of these zeolites have been investigated by adsorption of benzene, toluene, para-xylene, cyclohexane, ortho-xylene and 1,2,4

trimethylbenzene which cover the entire range of products formed during toluene disproportionation. The sorption and diffusion in the case of catalysts modified with Ni, P, B and Mg is reduced as compared to HZSM-5. The reduction in the case of the last three is very much pronounced.

The sorption capacity and diffusivity of HZSM-5 zeolites are nearly constant for benzene, toluene and para-xylene irrespective of their SiO_2/Al_2O_3 ratio. However, for cyclohexane, ortho-xylene and 1,2,4 trimethylbenzene, the sorption capacity and diffusivity decrease with increasing SiO_2/Al_2O_3 ratio. It is suggested that at higher ratios a shrinking of the unit cell takes place. This, in turn, may impose diffusional restrictions on molecules like o-xylene, cyclohexane and 1,2,4 trimethylbenzene to cause reduction in the adsorbate uptake. This would result in enhanced selectivity for p-xylene, because its diffusivity is independent of SiO_2/Al_2O_3 ratio and disproportionation of o-xylene to trimethylbenzenes and toluene is marginally reduced. This is, in fact, observed.

For the evaluation of number, strength and the stability of Brönsted acid sites, systematic investigations have been carried out because of their vital role in

reactions and their stability, especially at higher temperatures. The techniques of thermogravimetry, temperature programmed desorption of ammonia and infrared spectroscopy have been used for this purpose. TG of TEPA-ZSM-5 (ZSM-5 synthesized using triethyl n-propyl ammonium bromide as the templating agent) shows the decomposition of approximately 4 occluded TEPA molecules per unit cell as expected. Two exotherms in DTA thermograms observed during the decomposition of the TEPA-ZSM-5 indicates that the TEPA ions occupy two different sites within the zeolite channels. One site would be at channel intersection with no acid sites nearby while other adjacent to the aluminium sites where TEPA ions act as counter ions. The second stage (at higher temperature) decomposition of TEPA ions is in good agreement with the number of aluminium atoms present in the zeolite indicating that the acid sites are located at channel intersections. However, in the TG thermograms, the two stages were not separated distinctly.

In the temperature programmed decomposition of NH_4ZSM-5, all the ammonia molecules liberated were titrated upto 823 K. The TG curve for decomposition of NH_4ZSM-5 wt. loss upto 823 K was associated with conversion to H form. Further gradual wt. loss due to dehydroxylation of Brönsted acid sites was observed in the temperature range

873 to 1273 K. This gradual conversion of Brönsted acid sites to Lewis acid sites was also confirmed by acidity measurements of the calcined sample at 923, 973 and 1273 K Absence of the weight loss in the temperature range 823-873 K shows that the Brönsted acid sites are stable in this range and further increase in temperature give rise to formation of Lewis sites via dehydroxylation. Amount of NH_3 liberated, when plotted against the number of aluminium atoms/unit cell, yielded a straight line. However, the slope of this straight line was less than unity indicating that all the aluminium atoms in the zeolite are not located in the framework. These results were confirmed by ir and TPD of the reconstructed NH_4ZSM-5. The latter was obtained by chemisorption of ammonia on HZSM-5. The ir bands observed at 3720 and 3650 cm^{-1} are attributed to the OH groups generated by extra framework aluminium atoms and the terminal silicon atoms. This corresponds to the TPD peaks observed in the temperature range (420-470 and 373-390) due to desorption of ammonia chemisorbed on these sites. The third ir band observed at 3600 cm^{-1} corresponds to the OH groups generated by the framework aluminium atoms. A TPD peak observed in the temperature range (620-675) is due to desorption of NH_3 chemisorbed at this site. It has been observed that the concentration of the acid sites generated by the extra framework aluminium atoms also increases with increase in aluminium content.

To investigate the relationship between the nature of acid sites and catalytic activity, the toluene disproportionation reaction has been studied as a function of calcination temperature of NH_4ZSM-5 using conditions parallel to those used for the decomposition of NH_4ZSM-5. Toluene conversion is highest in the case of catalysts calcined at 823 to 873K and decreases with increasing calcination temperature from 873 to 1273 K implying that the Brönsted rather than Lewis acid sites are the seats of catalytic activity. Keeping the calcination temperature constant (823 K), the catalytic activity for toluene disproportionation for the samples of different SiO_2/Al_2O_3 ratios was evaluated. It was found that the conversion increases with increasing aluminium which is in agreement with the acidity. However, the question arises here whether it is the effect of strong acid sites (generated by framework aluminium atoms) or a combined effect of weak, medium (generated by extra framework aluminium atoms) and strong acid sites. If one assumes it is the effect of three types of acid sites, then the activity per aluminium atom should be atleast equal to that per strong acid site. However, the activity per aluminium is found to be less than that per strong acid site which indicates that the acid sites generated by extra framework aluminium atoms or terminal silicons are inactive in the toluene disproportionation.

In the TPD results it is seen that the strength of strong acid sites decreases with increasing SiO_2/Al_2O_3 ratio and/or modification with nickel, boron, magnesium and phosphorous. The catalysts with SiO_2/Al_2O_3 ratios in the range 150 to 320 and modified with above elements convert toluene selectively into one mole of benzene and one mole of xylenes (toluene disproportionation) while the catalysts with SiO_2/Al_2O_3 ratios 36 and 86 convert significant amount of toluene into benzene and gaseous products like methane, ethylene, ethane and so on (toluene dealkylation/cracking) in addition to toluene disproportionation. This indicates that the strong acid sites of higher strength are not suitable for toluene disproportionation, but are suitable for toluene dealkylation and cracking reactions. However, the catalysts modified with boron, magnesium and phosphorous show a poor performance in respect to toluene conversion. On the other hand, the catalysts modified with nickel offer a high performance in respect to toluene conversion as well as selectivity.

In the catalytic deactivation of HZSM-5 zeolites, it has been suggested that the presence of $[Si(OAl_n)^{n-}...Al_{n/3}^{3+}$ types of centres which show the property of super acid, act as coke synthesizing centres. Then the rate of deactivation of the ZSM-5 zeolite should increase with increasing aluminium since these centres are the results of extra

framework aluminium atoms. In the present study the rate of deactivation of the HZSM-5 zeolites during toluene disproportionation showed that it is directly proportional to the number of aluminium atoms, consistent with the above model. The TPD, ir and toluene disproportionation studies have proved the presence of extra framework aluminium ions and support the present results and the concept of super acid. The rate of internal coking that has been observed on account of the above super acid in the ZSM-5 zeolites is much slower than external surface coking.

In contrast to HZSM-5 zeolite the NiHZSM-5 zeolite shows a stable activity over a prolonged period of time. The main role of nickel is in keeping the surface 'clean' by hydrogenating the coke precursors that are formed during the disproportionation/transalkylation reactions. This is confirmed by the data obtained in the absence of hydrogen. The presence of nickel in the ZSM-5 zeolite does not confer any additional stability if there is no hydrogen in the reactant stream.

Toluene transalkylation with a mixture of C_9 aromatics over a series of HZSM-5 zeolites, dealuminated mordenites and HZSM-5 blended with mordenites have been investigated. The influence of process parameters such as temperature, pressure, hydrogen to hydrocarbon ratio, have

also been investigated. In contrast to HZSM-5 zeolites, mordenites and HZSM-5 blended with mordenite transalkylate toluene more effectively. It is found that among the C_9 aromatics that are present in the feed, the ethyltoluenes are extensively deethylated to toluene. The transalkylation of toluene with C_9 aromatics to yield xylenes occurs mainly on the external surface of ZSM-5 crystals. The disproportionation of toluene to yield benzene and xylenes, on the other hand, takes place predominantly in the pore system. Among the trimethylbenzenes, the bulky 1,3,5-isomer does not undergo transalkylation as readily as the 1,2,3 and 1,2,4 isomers. In this respect, ZSM-5 zeolites differ significantly from H mordenites wherein both the reactions occur mainly in the pore system. This difference is due to the smaller pore diameter in the ZSM-5 zeolites.

REFERENCES

1. H. C. Brown and K. L. Nelson, J. Amer. Chem. Soc., 75, 6292 (1953).

2. H. C. Brown and J. K. Hans, J. Amer. Chem. Soc., 77, 3584 (1955).

3. H. C. Brown and H. W. Pearsall, J. Amer. Chem. Soc., 74, 191 (1952).

4. H. C. Brown and H. W. Pearsall, J. Amer. Chem. Soc., 73, 4681 (1951).

5. D. V. Nightingale, Chem. Rev., 25, 329 (1939).

6. W. L. Benedict and Wm. J. Matiox, U.S. Pat. 2418689, C.A. 41, 4512g (1947).

7. N.V. Satmicarbon, Dutch Pat. 80067, C.A. 50, 16847g (1955).

8. E. R. Boedeker, U.S. Pat. 2795629, C.A. 52, 1224F (1957).

9. R. N. Battacharya, . . A. N. Rao, H. L. Adinath, Indian Pat. 110604 (1969).

10. L. E. Aneke, L.A. Gerritsen, P. J. Van Den Berg and W. A. DeJong, J. Catal., 59, 26-36 (1979).

11. H. A. Benesi, J. Catal., 8, 368-374 (1967).

12. Kh. M. Minachev, Ya. I. Iasakov, V. P. Kalinin N. Ya Vasachev; Kinet. Katal. 14(2), 418-25 (1973).

13. V. Penchev, N. Peshev and N. Davidova, Dokl. Bolg. Akad. Nauk, 28(3), 347-50 (1975).

14. E. L. Pollitizer, U.S. Pat. 3417157 (1968).

15. I.V. Nicolescu, Serban Olga, I. Sandulescu L. Stoiclescu,Rev. Roun Chim. 22 (1), 97-102 (1977).

16. S.S. Bhavikatti and S.R. Patwardhan, Ind. Eng. Chem. Prod. Res. Dev. 20, 102-105 (1981).

17. S. Narayanan, J. Chem. Soc. Faraday Trans. I, 72 (2), 434-9, 1979.

18. B. Coughlan and S. Narayanan, Chem. and Ind. 765 (1977).

19. Y. Tatsuaki, M. Yoshinori, M. Tsugio, H. Nobuyoshi, Sekiya Gakkaishi, 15(6), 487-92 (1972).

20. N. Davidova, N. Peshev and D. Shopov, J. Catal., 58, 198-205 (1979).

21. R. J. Argauer and G. R. Landolt, U.S. Pat. 3702886 (1972).

22. S. L. Meisel, J. P. McCullough, C. H. Lechthaler and P. B.Weisz, Chemtech, 6, 86 (1976).

23. P. B. Weisz, Pure and Appl. Chem., 52, 2091 (1980).

24. S. L. Meisel, J. P. McCullough, C. H. Lechthaler, P. B. Weisz, Recent Advances in Production of Fuel and Chemicals over Zeolite Catalysts, Leo Friend Symp., 174, Am. Chem. Soc. Mtng. Chicago, Illinois, August(1977).

25. W. O. Haag, F. G. Dwyer, Aromatics Processing with Intermediate Pore Size Zeolites Catalysts, Am. Inst. Chem. Eng. Annual Meeting, Boston,Massachusetts, August 1979.

26. E.G. Derouane, B. Imelik et al (Editors), Catalysis by Zeolites, p. 5 (1980).

27. N. Y. Chen and W. E. Garwood, J. Catal., 52, 453 (1978).

28. W. W. Kaeding, C. Chu, L. B. Young and S.A. Butter, J. Catal., 69, 392-398 (1981).

29. Chu-Chin Chium, U.S. Pat. 4302622.
30. Chu-Chin Chium, U.S. Pat. 4302620.
31. Chu-Chin Chium, Europ. Pat. 40463.

32. Chu-Chin Chium, Europ. Pat. 35836.

33. N. Y. Chen, W. W. Kaeding, F. G. Dwyer, J. Amer. Chem. Soc., 101, 6783-84 (1979).

34. G. T. Kokotailo, S. L. Lawton, D. H. Olson and W. M. Meier, Nature, 272, 437-438 (1978).

35. E. M. Flanigen, J. M. Bennett, R.W. Grose, J. P. Cohen, R. L. Patton, R. M. Kirchner and J. V. Smith, Nature, 271, 512 (1978).

36. C. V. McDaniel and P. K. Maher, Zeolite Chemistry and Catalysis, J. A. Rabo, editor, ACS Monograph, 171, p. 285 (1976).

37. R. M. Barrer; D.A. Langley, J. Chem. Soc. 3804 (1958).

38. S. L.Meisel, J. P. McCullough, C. H. Lechthaler and P. B. Weisz, ACS Meeting, Chicago, Illinois (1977).

39. E. G. Derouane, Z. Gabelica, J. Catal., 65, 486-489 (1980).

40. J. R. Anderson, K. Foger, T. Mole, R.A. Rajadhyaksha and J. V. Sanders, J. Catal., 58, 114 (1979).

41. J. W. Ward, Zeolite Chemistry and Catalysis, J.A. Rabo (Editor), ACS Monograph, 171, p. 118 (1976).

42. A. K. Ghosh and G. Curthoys, J. Chem. Soc. Faraday Trans. I, 80, 99-109 (1984).

43. A Auroux, J. C. Vedrine and P. C. Gravelle, J. Rouquerol and K.S.W. Sing (Editors) "Adsorption at the gas-solid and liquid-solid interface" page 305 (1981).

44. N. Y. Topsóe, K. Pendersen and E. G. Derouane, J. Catal. 70, 41-52 (1981).

45. J. C. Post and J.H.C. Van Hoof, Zeolites, 4, 9-4 (1984).

46. J. Valyon, J. Muhalyfi, H. K. Beyer and P. A. Jacobs, Proc. Workshop on Adsorption, Berline (DDR) 1979.

47. E. G. Derouane and J. C. Vedrine, J. Molec. Catal., 8, 479 (1980).

48. I. Wang, T. J. Chen, K. J. Chao and T. e. Tsai, J. Catal., 60, 140 (1979).

49. P. A. Jacobs, J. B. Uytterhoeven, M. Steyns, G. Froment and J. Weitkamp, Proc. 5th Intern. Confer. Zeolites, Naples, June 1980.

50. N. Y. Chen, R. L. Gorring, H. R. Ireland and T. R. Stein, Oil Gas J., 75, 165 (1977).

51. J. C. Kuo, U.S. Pat. 4046830 (1977).

52. C. D. Chang and A. J. Silverstri, J. Catal., 47, 249 (1977).

53. D. E. Walsh and L. D. Rollmann, J. Catal., 56, 195 (1979).

54. P. Dejaifve, A. Auroux, P.C. Gravelle, J. C. Vedrine, Z. Gabelica and E.G. Derouane, J. Catal. 70, 123 (1981).

55. D. H. Olson, W. O. Haag and R. M. Lago, J. Catal. 61, 390-396 (1980).

56. E. G. Derouane, S. Detrennerie, Z. Gabelica and N. Blom, Applied Catalysis, 1, 201-224 (1981).

57. A. Erdem and L. B. Sand, J. Catal., 60, 241-256 (1979).

58. S. B. Kulkarni, V. P. Shiralkar, A. N. Kotasthane, R. B. Borade and P. Ratnasamy, Zeolites, 2, 313-318 (1982).

59. A. Erdem, M.Sc. Thesis submitted to Worcester Polytechnic Institute (1978).

60. Chin-Chium Chu, U.S. Pat. 4137195 (1979).

61. R.B. Borade, A. J. Chandwadkar, S.B. Kulkarni and P. Ratnasamy, Indian J. of Technology, 21, 358-362 (1983).

62. E. L. Wu, S.L. Lawton, D. H. Olson, A.C. Rohraman Jr. and G.T. Kokotailo, J. Phys.Chem., 83, 2777-2781 (1979).

63. Hiromi Naukamota and Hiroshi Takashi, Chemistry Letters, 1013-1016 (1981).

64. D. M. Bibby, L. P. Aldridge, M. B. Milestone, J. Catal., 72, 373-374 (1981).

65. E. M. Flanigen, Zeolite Chemistry and Catalysts, J. A. Rabo (Editor) ACS Monograph 171, 80 (1976).

66. S. P. Zhdanov, A.V. Kiselev, V. I. Lygin, T. I. Totova, Russ. J. Phys. Chem., 38, 1200 (1964).

67. K. J. Chao, T. C. Tasi, M.S. Chen and I. Wang, J. Chemical Soc. Faraday Trans. I, 77, 547 (1981).

68. P. A. Jacobs, E.G. Derouane and J. Weitkamp, J. Chem. Soc. Chem. Comm., 591-593 (1981).

69. P. A. Jacobs, H. K. Beyer and J. Valyon, Zeolites, 1, 161-168 (1981).

70. J. Valyon, J. Mikalyfi, H. K. Beyer and P. A. Jacobs, in Proc. Workshop on Adsorption, Berlin, DDR, 1, 134 (1979).

71. I. Suzuki, S. Namba and T. Yashima, J. Catal., 81, 485-488 (1983).

72. A. L. McClellan, H. F. Harisberger, J. Colloid Interface Sci., 23, 577 (1967).

73. S.Brunauer, P. H. Emmett and E. Teller, A. Amer. Chem. Soc., 60, 309 (1938).

74. M. M. Dubinin, J. Colloid Interface Sci., 23, 487 (1967).

75. N. Y. Chen, J. Phys. Chem., 80, 60-64 (1976).

76. Hiromi Nakamoto and Hiroshi Takahashi, Zeolites, 2, 67-68 (1982).

77. W. W. Kaeding and S. Butter, J. Catal., 61, 155-1964 (1980).

78. I. Balkrishnan - unpublished data.

79 a: R. L. Mao, O. Palapi , A. Mazi, G. L.Fanti, A. Villa and V. Ragaini, React. Kinet. Catal. Lett., 15(2), 293-302 (1980).

79 b: J. R. Anderson, T. Mole and V. Christov, J. Catal. 61, 477-484 (1980).

80. H. W. Haynes, Catal. Rev. Sci. Eng., 17, 273 (1978).

81. P. A. Jacobs and R. V. Ballmoos, J. Phys. Chem., 86, 3050 (1982).

82. J. C. Vedrine, A. Auroux, V. Balis, P. Djaifve, C. Naccache, P. Weirzchowski, E.G. Derouane, B. Nagy, J. P. Gilson, J. H. C. Van Hoof, J. P. Vandeberg and Wolthuizen, J. Catal., 59, 248 (1974).

83. G. P. Babu, S. G. Hegde, S.B. Kulkarni and P. Ratnasamy, J. Catal., 81, 471-477 (1983).

84. K. H. Chandawar, S.B. Kulkarni and P. Ratnasamy, Applied Catalysis, 4, 287-295 (1982).

85. J. B. Utterhoeven, L. B. Christner, W. K. Hall, J. Phys. Chem., 69, 2117 (1965).

86. J. W. Ward, J. Catal., 9,225 (1967).

87. A. Auroux, P.C. Gravelle, J.C. Vedrine and M. Rekas, in 5th Intern. Confer. on Zeolites, L. V. Rees (edited), Heyden, London, 433 (1980).

88. A. Auroux, V. Bolis, P. Weirzchowsk, P. C. Gravelle and J. C. Vedrine, J. Chem. Soc. Faraday Trans. I, 75, 2544 (1979).

89. J. C.Vedrine, A. Auroux, P. Dejaifve, V. Ducarone, H. Hoser and S. Zhous, J. Catal., 73, 147 (1982).

90. K. H. Rhee, V.V.S. Rao and J. M. Stencel, Zeolites, 3, 337-343 (1983).

91. K. H. Rhee, F. R. Brown, D. H. Finseth and J. M. Stencel, Zeolites, 3, 344-347 (1983).

92. J. M. Stencel, V. U.S. Rao, J. R. Diehl, K. H. Rhee, A.G. Dhere and R. J. Deangelis, J. Catal. 84, 109-118 (1983).

93. P. B. Weisz, Advan. Catal., 13, 137 (1962).

94. K. H. Minachev and Ya. I. Isakov, Zeolite Chemistry and Catalysis, J.A. Rabo (Ed.) ACS Monograph, 171, 552 (1976).

95. S. Badrinarayanan, R. I. Hegde, I. Balkrishnan, S. B. Kulkarni and P. Ratnasamy, J. Catal., 71, 439-442 (1981).

96. C.D. Wagner, Anal. Chem., 44, 1050 (1972).

97. K. S. Kim, W.E. Baitinger, J. W. Amy and N.Winograd, J. Elect. Spectrosc. Relat. Phenom., 5, 351 (1974).

98. G. Ertl, R. Hierl, H. Knözinger, N. Thiele and M. P. Urbach, Appl. Surface Sci.,5,49, (1980).

99. Defosse Camille, Thesis submitted to Universite Cathalique de Louvain, p. 35 (1976).

100. M. Wu, D. M. Hercules, J. Phys. Chem., 83, 2003 (1979).

101. L. M. Parker, D. M. Bibby and J. E. Patterson, Zeolites, 4, 168-174 (1984).

102. J. Crank, "The Mathematics of Diffusion" Clarendon Press, Oxford (1956).

103. R. Auschütz and H. Immendorff, Ber. Deut. Chem. Ges., 17, 2, 2816 (1984).

104. S. Otani, Chemical Engineering, 118 (1970).

105. S. Otani, Matswoka and M. Sato, Japan Chem. Quart. 4 (6), 16 (1968).

106. T. Ponder, Hydrocarbon Processing, Nov. 141 (1979).

107. M. J. S. Dewar, J. Chem. Soc., 406 (1946).

108. H. C. Brown, H. W. Pearsall and L. P. Eddy, J. Amer. Chem. Soc., 72, 5747 (1950).

109. H. C. Brown and W. J. Wallace, J. Amer. Chem. Soc. 75, 6279 (1953).

110. D. A. McCauley and A. P. Lien, J. Amer. Chem. Soc. 73, 6285 (1953).

111. W. L. Benedict and Wm. J. Mattox, U.S . Pat. 2418689 (1947).

112. E. R. Beedeker, U.S. Patent, 2795629 (1957).

113. K. M. Wang, J. M. Lunsford, J.Catal., 24,262 (1972).

114. T. Yashima, H. Moslchi and N. Haaag, Bulletin of the Japan Petroleum Institute, 12, 105-111 (1970).

115. M. R. Allan, Gen. Offen, 2460539 (1974).

116. a: S. A. Butter, U.S. Pat. 4007231 (1977).

116. b: J. H. Perry, Chemical Engineering Handbook, McGraw Hill, 3rd Edn. p, 237 (1959).

117. P. B. Weisz, V.J. Frilette, J. Phys. Chem., 64, 382 (1960).

118. a : Garbowski, C. Mirodatos and M. Primet, 'Metal Microstructure in Zeolites' Jacobs et al (editors) 235 (1982).

118. b : N. P. Davidova, M. L. Valchev and D. M. Shopov, Catalysis by Zeolites, B. Imelik et al (editors) 285 (1980).

119. P. B. Venuto, L.A. Hamilton, Ind. Eng. Chem. Prod. Res. Dev., 6, 190 (1967).

120. D. E. Walsh and L. D. Rollmann, J. Catal., 49, 369 (1977).

121. L. D. Rollmann and D. E. Walsh, J. Catal., 56, 139 (1979).

122. N. S. Gnep, and M. Guisnet, Applied Catalysis, 1, 329 (1981).

123. K. G. Ione, V.G. Stepanov, G.V. Echevskii, A. A. Shubin and E.A. Paukshtis, Zeolites, 4, 114-119

124. D. Eisenbach and E. Gallei, J. Catal., 56, 377-389 (1979).

125. W.W. Kaeding and L.B. Young, U.S. Pat. 4034053 (1977).

126. K.G. Ione, G.V. Echevskii, G. N. Nosyreva, J. Catal., 85, 287-294 (1984).

127. S. H. Hasting and D. E. Micholson, J. Chem. Eng. Data, 6, 1 (1961).

128. V. N. Romannikov, V. M. Mastikhin, S. Hocevar, and B. Drzaj, Zeolites, 3, 311 (1983).

129. S. Szakacs, J. Papp. J. Lejtouicz, D. Kallo, React. Kinet. Catal. Letts. 21, 365 (1982)

130. I. V. Mishin, G.A. Piloyan, A. L. Klychko-Gurvich and A. M. Rubinshtein, Bull. Akad. Sci. USSR, 22, 1298-1300 (1973).

131. I.V. Mishin, A. L. Klyachko-Gurvichi, B. I. Shikunov, G.A. Ashavaskaya, G.I. Kapustin and A. M. Rubinshtein, Bull. Akad. Sci. USSR, 22, 1301-1303 (1973).

132. S. Namba, O. Iwase, N. Takahashi, T. Yashima, and N. Hara, J. Catal., 56, 445-452 (1979).

133. M. A. Lanewala, A. P. Bolton, J. Org. Chem., 34, 3107 (1969).

134. P. E. Eberly, Jr., C. M. Kimberlin Jr., A. Voorhies, Jr., J.Catal., 22, 419-426 (1971).

135. D. K. Thakur, S.W. Weller, Molecular Sieves Adv. Chem.Ser., 121, 596 (1973).

136. R. Beecher, A. Voorhies Jr., P.E. Eberly Jr., Ind. Eng. Chem. Prod. Res. Dev., 7, 203 (1968).

137. D. J. Chick, Jr., Katzer and B.C. Gates, Molecular Sieves-II, ACS Symposium Series, 40, 515-527 (1977).

138. H. G. Karge and J. Ladebeck, B. Imelik, et al. (editors), Catalysis by Zeolites, 151-159 (1980).

139. W. J. Taylor, D.D. Wagman, M.G. Willian, K. S. Ditzer and R. D.. Rossini, J. Res. Natl. Bur., 37, 29 (1947).